HYDROLOGICAL IMPACTS OF CLIMATE CHANGE ON THE CASTLE RIVER WATERSHED, ALBERTA, CANADA

TIMOTHY S. ANDERSON
B.Sc., University of Lethbridge, 2012

A Thesis
Submitted to the School of Graduate Studies
of the University of Lethbridge
in Partial Fulfillment of the
Requirements for the Degree

[MASTER OF SCIENCE]

Department of Geography
University of Lethbridge
LETHBRIDGE, ALBERTA, CANADA

HYDROLOGICAL IMPACTS OF CLIMATE CHANGE ON THE CASTLE RIVER WATERSHED, ALBERTA, CANADA

TIMOTHY S. ANDERSON

Date of Defense: August 19, 2014

Dr. Stefan W. Kienzle Supervisor	Professor	Ph.D.
Dr. Hester Jiskoot Thesis Examination Committee Member	Associate Professor	Ph.D.
Dr. Joseph Rasmussen Thesis Examination Committee Member	Professor	Ph.D.
Dr. Craig Coburn Chair, Thesis Examination Committee	Associate Professor	Ph.D.

Abstract

The ACRU (Agricultural Catchments Research Unit) agro-hydrological model was used to estimate historical and future hydro-climatological variables including streamflow that have occurred during 1951-2010, and to simulate the impacts of climate change in the Castle River watershed (CRW) for the future period 2041-2070. ACRU is driven by a driver station(s) by extrapolating meteorological variables across the watershed, making corrections for differences between elevation, slope and aspect. Two driver station datasets, the Beaver Mines Climate Station (BMCS, 05AA022) and 10 km Grid (Hutchinson et al., 2009) are compared to determine whether impacts of climate change are best suited for simulation using single point locations or spatially interpolated grids. Model parameterization is based on the Hydrological Response Unit (HRU) concept. Verification of mean temperature, snow water equivalent (SWE) and streamflow is reported. Projected increases in air temperature and precipitation resulted in decreases of SWE and increases in streamflow during peak runoff season.

Acknowledgements

I would like to first thank my family; my wife Brittany, who has given me all the support I have needed to stay committed not only to this project, but to everything in life that I pursue; our four children, for often sacrificing time with their dad so that I could purse and education that I had left undone until now; my parents and parents-in-law, for their support and encouragement that came in times of need.

I owe much gratitude to my supervisor, Stefan Kienzle, he has been very kind and patient in his encouragement over the development of this Thesis. Stefan has created a great learning atmosphere where questions were always welcome, which encouraged an enthusiasm for learning. He also has a wealth and breadth of knowledge and experience that was invaluable to this research. I would like to thank my committee members; Dr. Hester Jiskoot, for all her time and guidance. Hester was very supportive and constructive with her suggestions which greatly enhanced this thesis; and Joe Rasmussen, who provided a unique perspective to aspects of the modelling analysis that had not been considered.

I would like to thank the Department of Geography and the School of Graduate Studies, for opportunities that I had as a graduate teaching assistant to teach and learn under the direction of Dr. Stefan Kienzle, Dr. Craig Coburn and Dr. Hester Jiskoot. I also owe a big thank-you for all the data support gained from the Kienzle Watershed Lab; Dr. Stefan Kienzle, Mark Mueller, Mike Nemeth, Martin Haüsser, Colin Langhorn, Charmaine Bonafacio and Jacob Palardy.

Table of Contents

List of Tables

List of Figures

List of Abbreviations

AAFC	Agriculture and Agri-Food Canada
AARD	Agriculture and Rural Development
ACRU	Agriculture Catchments Research Unit
AESRD	Alberta Environment and Sustainable Resource Development
AGRASID	Agricultural Regions of Alberta Soil Inventory Database
AR4	IPCC Fourth Assessment Report
AR5	IPCC Fifth Assessment Report
BMCS	Beaver Mines Climate Station
CanESM2	The second generation Canadian Earth System Model
CanRCM4	The fourth generation Canadian Regional Climate Model
CGCM3	The third generation coupled global climate model
CRCM	The Canadian Regional Climate Model
CRW	Castle River Watershed
DEM	Digital Elevation Model
EC	Environment Canada
ENSO	El Niño Southern Oscillation
EOSD	Earth Observation for the Sustainable Development of Forests
ET	Evapotranspiration
FAO	Food and Agriculture Organization of the United Nations
FC	Field Capacity
GCM	Global Circulation Model
GFDL	Geophysical Fluid Dynamics Laboratory
GHG	Greenhouse Gas
GIS	Geographic Information System
HRM3	Hadley Regional Model 3
HRU	Hydrological Response Unit
HYDAT	Hydrometric Data
IPCC	Intergovernmental Panel on Climate Change
LAI	Leaf Area Index
LiDAR	Light Detection And Ranging
MODIS	Moderate-Resolution Imaging Spectroradiometer
MSC	Meteorological Service of Canada
NLWIS	National Land and Water Information Service
NOAA	National Oceanic and Atmospheric Administration
NRCS	Natural Resource Conservation Service
NSE	Nash-Sutcliffe Coefficient of Efficiency
NSIDC	National Snow and Ice Data Center
ORB	Oldman River Basin
P	Precipitation
P_{ds}	mean monthly precipitation for each driver station
P_{HRU}	mean monthly precipitation for each 100 m HRU
PARC	Prairie Adaptation Research Collaborative
PDO	Pacific Decadal Oscillation
PO	Soil Porosity
PRISM	Parameter-Elevation Regressions on Independent Slopes Model
PTC	Plant Transpiration Coefficient
RCM	Regional Climate Model
RCM3	The third generation Regional Climate Model
RH	Relative Humidity

SCCW	Swift Current Creek Watershed
SCS	Soil Conservation Service
SMRW	St. Mary River Watershed
SSRB	South Saskatchewan River Basin
SWE	Snow Water Equivalent
TGICA	Task Group on data and scenario support for Impact and Climate Analysis
Tmax	maximum temperature
Tmin	minimum temperature
U	wind speed
UNSRB	Upper North Saskatchewan River Basin
USGS	United States Geological Survey
VACEA	Vulnerability and Adaptation to Climate Extremes in the Americas
WP	Wilting Point
X	Variable of interest (wind speed or relative humidity)
X_{ds}	mean monthly wind speed or relative humidity for each driver station
X_{HRU}	mean monthly wind speed or relative humidity for each 100 m HRU

ACRU Variables

COFRU	Coefficient of base flow response.
COIAM	Coefficient of initial abstraction
CORPPT	Rainfall adjustment factor
ICC	Monthly values for canopy coverage (for forested catchments only)
QFRESP	Stormflow response fraction for the catchment/subcatchments
RHUCOR	Relative humidity adjustment factors
SNCAPI	Canopy interception for snow for forested HRUs only
TMaxLR	Mean regional lapse rate (+/-°C. 1000 m^{-1}) for maximum temperature.
TMinLR	Mean regional lapse rate (+/-°C. 1000 m^{-1}) for minimum temperature.
WINCOR	Wind speed adjustment factors

Chapter 1: Thesis Introduction

1.1 Introduction

By the end of this century in many mid-latitude and sub-tropical dry regions, mean precipitation is expected to decrease, while in many mid-latitude wet regions, mean precipitation is likely to increase (IPCC, 2013). Additionally, as global mean surface temperature increases, extreme precipitation events over most of these areas are likely to become more intense and more frequent (IPCC, 2013). In the summer of 2013, a manifestation of our changing climate created perfect conditions for massive flooding destroying several southern Alberta communities. These flood events were most likely a manifestation of our changing climate. Even though the 2013 flood event was marked as an extreme wet year, extreme dry years are also likely to take place in the future. In fact, according to (Xu, 1999a), one of the most important impacts that future societies will have to deal with in relation to climate change is the regional availability of water. Vulnerability and Adaptation to Climate Extremes in the Americas (VACEA) is a project that will help address the gap in the current understanding of consequences associated with global climate change and vulnerability that rural populations and indigenous communities experience. One of the key objectives of the VACEA project is to provide new information on the impact of climate change, and the associated increase in both frequency and duration of extreme weather events, on the availability of water resources in various study watersheds.

1.2 Research Objectives

The primary objective of this research is to estimate critical historical and future hydro-climatological variables that have occurred between 1951 and 2010 and are projected to occur between 2041 and 2070 in the Castle River Watershed (CRW) in southern Alberta. In order to achieve this goal, a number of secondary objectives need to be achieved. The secondary objectives are (a) to simulate daily streamflow using the ACRU agro-hydrological modelling system, and (b) to compare two different methods of feeding climate data into the model.

The CRW is a headwater region of the Oldman River Basin (ORB) and larger South Saskatchewan River system which supplies freshwater to the semi-arid Canadian Prairie Provinces of Alberta, Saskatchewan and Manitoba. Meteorological observations from climate stations are crucial to successfully modelling the hydrology within any basin, but spatial models can be increasingly more valuable in that they typically provide complete spatial coverage for many study locations, but especially in mountain regions like the Castle where climate stations are sparsely located.

Two datasets will be applied to estimate hydro-climatological variables in the CRW. First, a dataset containing observed meteorological records from the Beaver Mines Climate Station (BMCS, A3050600), and second, a spatially gridded climate dataset with 10 x 10 km grid spacing (here after referred to 10 km Grid). The dataset proving to be the most reliable in estimating hydro-climatological variables including, inter alia, streamflow, will be applied to simulate future (2041-2070) streamflow conditions for the CRW. Not only will future hydrological processes be predicted, but a case will be made for the preference of model input and methodology in which datasets such as these are applied in future watershed studies. Other sub-objectives include the calculation of a range of important hydro-climatological indices, where percent change comparisons can be made between historic and future years. For example, predicted changes in mean temperatures, precipitation amounts including rainfall, snowfall and total precipitation, snow water equivalent (SWE) depths and streamflow.

1.3 Thesis Structure

This thesis is divided into six chapters, beginning with this chapter which describes the thesis topic and main objectives. Chapter 2 is comprised of a literature review of climate change in Southern Alberta and background information on the various types of hydrological models, focusing on the ACRU agro-hydrological model that has been used in climate change studies. The chapter finishes off summarizing spatial climatic datasets and the different methods used in applying them in hydrological modelling. In Chapter 3 the key concepts of the ACRU model and detailed parameterization of ACRU for the CRW are presented. Chapter 4 focuses on the verification of ACRU output for the hydrological

variables of temperature, snowpack (represented by SWE) and streamflow, providing justification regarding the most reliable dataset for simulating these variables for this project. Chapter 5 provides information on the simulated impacts of climate change for the CRW, including statistical analysis based on probability plots and changes in a range of hydro-climatological variables. Chapter 6 provides the summary and conclusions of this research as well as recommendations for future research in this area.

Chapter 2: Literature Review

2.1 Introduction

Water supply in Alberta must meet water demands of various industrial, agricultural, aquatic, domestic and recreational uses. However, recent population growth and increasing developments in the agriculture and industrial sectors have caused increased demand and pressures on Provincial water resources. These pressures, coupled with the highly allocated (by the end of 2005, more than 9.5 billion m^3 of water had been allocated throughout the province, where the South Saskatchewan River Basin (SSRB) accounts for 58%, and the North Saskatchewan River Basin (NSRB), 29% (Alberta Environment)) status of water and resultant new moratorium (initiated in 2006) (Alberta Environment, 2013) restricting the approval of new water licenses in the South Saskatchewan River Basin have caused governments, water managers and others to become aware of and address the problems associated with the quantity and quality of water resources. The Province of Alberta is a region that experiences a very diverse climate which affects the natural diversity of water availability on an increasing population. Adding the uncertainties associated with climate change establishes the need of an inventory of the current and future water resources to be made (Kienzle and Mueller, 2013).

This literature review serves as an introduction to climatic change research in Southern Alberta and the resulting impact on water resources in headwater regions typically found in mountainous areas. Context will be provided to explain the need for physically-based hydrological models to predict climate change impacts in watersheds. Finally, spatial climatic datasets, which are typically used to drive hydrological models, coupled with various methodologies in how they are applied will be explored.

2.2 Global Climate Change

According to the 2007 Synthesis Report by the Intergovernmental Panel on Climate Change (IPCC), Climatic change refers to a change in the state of the climate that can be identified (e.g. using statistical tests) by changes in the mean and/or the variability of its properties, and that persists for an extended period, typically decades or longer. It refers to any change in climate over time, whether due to

natural variability or as a result of human activity (IPCC, 2007). The most common projections of future climatic change are from Global Circulation Model (GCM) outputs averaged over several decades and applicable to large continental areas (Sauchyn and St. Jacques, 2009). For example, the IPCC (2007) reported that projected global surface temperatures will increase by 0.2°C per decade throughout the 21st century. Climate change takes place as a result of a perturbation of the energy balance in the atmosphere and or land surface of the earth. The resulting positive or negative changes are expressed as radiative forcing, which is used to compare warming or cooling influences on global climate (IPCC, 2007). GCMs are used to simulate climatic sensitivity to increased carbon dioxide concentrations and other green house gases (GHGs) (Loaiciga et al., 1996) and have spatial scales ranging from approximately 200 x 600 km. As such, they are unable to simulate meaningful output for local or regional scales.

2.3 Climate Change in Southern Alberta

Southern Alberta is situated in a unique region of the North American continent. The landscape is characterized by a flat prairie landscape in the east that transitions into the Rocky Mountains in the west. Regional precipitation originates as evaporation from land and the oceans. As the region receives precipitation, moisture is absorbed in the soil, used by plants and returned to the atmosphere. Water that does not evaporate or transpire or seep into groundwater aquifers runs off to form the Province's rivers and streams. The Rocky Mountains act as a reservoir by storing water in the form of snow, which is released during a short melt period during the spring and early summer months. As a result, the Rocky Mountains have been referred to as "continental water towers" (Rood et al., 2005). With an increased awareness of a warming global climate, concerns in Southern Alberta will continue to grow regarding climate change impacts and their effects on the region. According to the Canadian Disaster Database, some of the most costly natural disasters in Canadian history have been the culmination of droughts and floods in the Prairie Provinces (Public Safety Canada, 2013). According to De Loë (2001), agriculture in southern Alberta is particularly vulnerable to climate change. For example, some suggest that within the Oldman River basin climate change will cause a decline in soil moisture and a reduction of streamflow

runoff (Byrne et al., 1989; Nkemdirim and Purves, 1994). The intensity and frequency of these disasters are increasing and are causing many questions to be asked such as: “How will water resources be affected?”, or “What will this mean for the agricultural industry that is so heavily dependent on water?” Since many downstream communities of this continental hydrographic apex are dependent on water, an accounting of the current and future natural water resources under a changing climate is needed, especially when cumulative effects of climatic warming are taking place in the form of an increased frequency of extreme events such as droughts and floods.

2.4 Observations of Climate Change in Southern Alberta

2.4.1 Temperature

Greenhouse gases have had a profound effect on Earth’s temperature by trapping heat in the atmosphere and causing global temperatures to rise (Alberta Environment, 2013). If greenhouse gases continue to increase in concentration, air temperatures will increase over time (Gleick, 1999). Reconstructed temperatures from dendroclimatic records in the Canadian Rocky Mountains spanning the last millennium show that the period of greatest warming took place from the mid-1800s onwards (Luckman and Wilson, 2005). In the Prairies, temperatures have shown a 1 to 4°C increase over the last century (Schindler and Donahue, 2006), with the most pronounced warming in winter and spring occurring since the 1940s (Cayan et al., 2001). Projections of future climates suggest that under a doubling of CO_2, temperature increases could be as much as 8°C during winter months (Barnett et al., 2005; Gan, 2000). Warming temperatures will affect the regional hydrological cycle. For example, the higher the temperature, the more water is evaporated and less water runs off as streamflow. According to the IPCC (2007), impacts of projected warming will be greatest over land and at the most northern latitudes. An example of this can be seen in a study conducted by MacDonald et al. (2012) in the Upper North Saskatchewan River Basin (UNSRB), located in the central Rocky Mountain region of Alberta, Canada. MacDonald et al. (2012) concluded that air temperature increases due to climate change have resulted in substantial spatial changes in the date of maximum and minimum SWE, with subsequent

changes in the proportion of precipitation falling as snow and shorter melt rate seasons. In the prairies, this projected warming has the potential to create longer growing seasons, enhancing the productivity of forests, crops and grasslands while also exacerbating the effects of drought (Schindler and Donahue, 2006).

2.4.2 Precipitation

There are two main weather systems that bring the majority of precipitation to southern Alberta. Autumn and winter precipitation is predominantly produced from westerly winds, while spring and summer precipitation is caused by winds that swing north around a high pressure system in Idaho (Al-Rawas and Valeo, 2009). During the winter, a strong rain shadow effect takes place in the lee of the Rocky Mountains (Reinelt, 1970), creating increasingly drier conditions from west to east. During the spring and summer, this effect is reversed, creating drier conditions from east to west (Al-Rawas and Valeo, 2009). Statistical characteristics of precipitation in the Canadian Prairies showed that for the last 75 years of the 20^{th} century, 70% of the mean annual precipitation fell as rain and 30% as snow (Akinremi et al., 1999). Moving west towards the Rocky Mountains this ratio changes, for example, Kienzle (2008) verified that the proportion of precipitation falling as snow for 15 climate stations located in south-western Alberta ranged from 20% in the northern Prairies to 66% at a high-elevation site in the Rocky Mountains. Precipitation generally increases with elevation (Basist et al., 1994; Daly et al., 1994; Johnson and Hanson, 1995). In snow dominated regions such as southern Alberta and the western United States., most mountain based precipitation during the winter falls as snow and melts in the spring and summer (Barnett et al., 2005). However, under future higher temperatures, Schindler and Donahue (2006) expect winter precipitation that normally falls as snow to increasingly fall as rain. In a study assessing future climate scenarios under climatic warming, MacDonald et al. (2011) found that changes in the proportion of snow as a percentage of the total precipitation in the St. Mary River watershed (a major contributing mountainous headwater region of southern Alberta) will steadily decrease anywhere from approximately 70% to 40% (depending on the GCM scenario used). These conclusions are consistent with other findings

for alpine regions (Groisman et al., 1999; Lapp et al., 2005; Leung and Ghan, 1999; MacDonald et al., 2012) and prairie regions (Lemmen et al., 2008). Summer precipitation amounts (May to Aug) have decreased over the 20th century in southern Alberta (Shen et al., 2005), and projections based off a warmer/drier future scenario assert the largest decreases will occur during the summer season (Barrow and Yu, 2005). In future years, major water shortages are expected in southern Alberta generally due to warming that is taking place across the globe (Schindler and Donahue, 2006). Potential impacts will affect southern Alberta's agricultural region, as changes in the timing and intensity of precipitation events are expected to take place (Sauchyn and Kulshreshtha, 2008).

2.4.3 Snowpack

Mountain snowpack plays a crucial role in freshwater availability (IPCC, 2007). It determines the timing of peak river discharge, and in many instances, maintains river flows even during warm and dry summer periods (Beniston et al., 2003). Any changes in the amount, duration and timing of the snowpack can have long-lasting environmental consequences (Beniston et al., 2003), such as intensifying the effects of drought (Schindler and Donahue, 2006) and declines in spring runoff volumes (Lapp et al., 2005). For example, Schindler and Donahue (2006) claimed winter snowpacks in Alberta that are subjected to periodic melting during warmer winter conditions will diminish high river flows in May and June, while only supplying little more than half of current flow volumes. Winter warming promotes the conversion of winter precipitation to rain (Lapp et al., 2005; MacDonald et al., 2012; MacDonald et al., 2011; Merritt et al., 2006), reduces snow accumulation across the prairies (Sauchyn and Kulshreshtha, 2008) and alpine areas (Lapp et al., 2005; Leung and Ghan, 1999), where a general upward movement of 150 m of the snowline can result from an average rise of 1°C (Beniston et al., 2011), which is in line with the general lapse rate. The greatest reductions of overall SWE are predicted to occur at lower elevations, where critical temperature thresholds are likely to be exceeded in the future (MacDonald et al., 2011). For example, Lapp et al. (2005) stated snowpacks at low elevations (1400-1600 m) will decline by about two thirds on average relative to historical conditions and by one third on snowpacks at higher elevations

(2000-2200 m). Additionally, significant decreasing trends in maximum SWE over the St. Mary River watershed have been observed (MacDonald et al., 2011). According to Barnett and Lettenmaier (2005), the most significant impacts of a general warming was found to be a large reduction in mountain snowpack and a substantial shift in streamflow seasonality, so that by 2050 the spring streamflow maximum will come about one month earlier in the year. This one-month advance in timing of snowmelt runoff could threaten storage efficiencies for many reservoirs as they are often operated for flood protection (Stewart et al., 2004). In western North America, this earlier onset of melt has already been observed (Burn, 1994; Cayan et al., 2001; Clow, 2010; Stewart et al., 2004).

2.4.4 Streamflow

In snow dominated basins, spring snowmelt and precipitation during colder months are the major contributors to streamflow. This is especially true in high altitude mountain basins located in Alberta's south-west corner of the Rocky Mountains, where, for instance, more than 100,000 m^3 km^{-2} of water yield is produced annually (Kienzle and Mueller, 2013). The St. Mary River Basin (SMRW), part of the south-west headwater region, originates in Montana and contributes a high mean annual water yield of 649,000 m^3 km^{-2} $year^{-1}$ (Kienzle and Mueller, 2013). The lowest water yields in the province are produced in the prairies and portions of central Alberta where the combined effects of low annual precipitation and high evaporation losses result in water yields under 11,000 m^3 km^{-2} and occasionally negative water yields (Kienzle and Mueller, 2013). The CRW produces, for the period 1971 to 2000, approximately 15 percent of the total water contribution in the ORB (Kienzle and Mueller, 2013). Combining the CRW with other headwater watersheds such as the St. Mary, Belly, Waterton and Crowsnest, together produce 74 percent of the annual water yield contribution for the greater ORB (Kienzle and Mueller, 2013). High water yields such as these attest that streamflow originating from southern Alberta's eastern slopes of the Rockies is critical and should be protected in order to secure high quality water supplies in the future (Kienzle and Mueller, 2013).

Since human activities and regional ecosystems are usually well adapted to current climate conditions, and current water management strategies assume that runoff will continue to follow historical patterns (Gleick, 1999), changes in the hydrological regime as a result of large or rapid changes in the climate will cause these systems to become increasingly vulnerable. The most serious risk from recent and projected climate warming in western Canada is a shift in the amount and timing of streamflow (Axelson et al., 2009). Potential implications resulting from these changes in surface hydrology for human populations and regional scale physical and ecological processes are far reaching (Nijssen et al., 2001). For example, earlier snowmelt runoff events could threaten storage efficiencies of reservoirs (Barnett et al., 2005; Stewart et al., 2004) and cause decreased streamflow during periods of peak demand (Barnett et al., 2005; Gleick, 1999). Instream flow needs to maintain aquatic and ecological habitats will be threatened (Barnett et al., 2005; IPCC, 2007; Rood et al., 2008; Schindler and Donahue, 2006). Increased flooding early in the year will take place (Gleick, 1999), and agriculture productivity in the Canadian Prairies will be more at risk (Barnett et al., 2005; Rood et al., 2005). It has been stated that snowpack is more effective at creating runoff than rainfall (Dingman, 2002). This is because a rainfall amount has to create saturated soil conditions before runoff begins, where during the snowmelt season, soils are often still frozen or saturated from winter conditions thus allowing runoff to take place more effectively. As a consequence, annual runoff volumes will decrease as a result of the conversion of snowfall to liquid precipitation in the mountains (Lapp et al., 2005; Gleick, 1999). However, where more winter precipitation falls as rain, winter runoff has the potential will increase.

2.4.5 Evapotranspiration and Soil Moisture

Evapotranspiration (ET) rates are expected to change as a result of climatic warming. According to the IPCC, (2007) semi-arid regions such as the prairies in southern Alberta will suffer a decrease in water resources. These expectations are partially based on scientific theory that ET rates will increase with higher temperatures, reducing the amount of water available for streamflow runoff. Barnett et al (2005) stated pan evaporation has been steadily decreasing for the past fifty years contrary to the

expectation that warming would cause increased evaporation. These findings are important because pan evaporation data have shown to be highly correlated with ET from surrounding vegetation under conditions of full cover and good water supply. According to Schindler and Donahue (2006), ET rates have already increased in many places across Canada. A recent study on climate change impacts on the Crowsnest River, Alberta, identified that rates of ET are increasing in spring and decreasing in summer (Mahat and Anderson, 2013). The summer decrease can be explained by natural feedbacks, such as increased cloudiness, higher relative humidity (RH), or a decrease in soil moisture availability.

ET is the dominant hydrological process in terms of volume or water balance in many watersheds and a variety of climatic zones (Beven, 1979). However, climate change studies tend to give less attention to ET as an important climatic factor controlling energy and mass exchange between terrestrial ecosystems and the atmosphere. ET is often estimated from theoretical predictive equations requiring meteorological data (Grismer et al, 2002). About 50 methods are available for estimating ET, often yielding inconsistent results as their assumptions and meteorological data requirements differ (Grismer et al, 2002). The most reliable ET method under various climates is the Penman-Monteith equation (Chen et al., 2005).

The Penman-Monteith equation is physically based, and explicitly incorporates both physiological and aerodynamic parameters , reflecting changes in all meteorological factors affecting evaporation and plant transpiration (Shenbin et al., 2006). It is also extensively used throughout the world, including Southern Alberta (Gobena and Gan, 2013). For example, it is considered the standard reference evaporation method recommended for use by the American Society of Civil Engineers (Allen et al., 1995) and the Food and Agriculture Organization of the United Nations (FAO). ET rates differ across climatic and topographic zones and more specifically vegetation types. According to Gurtz et al. (1999) the amount of energy available for ET is strongly controlled by elevation, aspect, exposure and slope and actual ET rates rely to a great extent soil moisture storage capacity.

2.5 Hydrological Models

Hydrological models provide a framework in which to conceptualize and investigate the relationships between climate and water resources (Leavesley, 1994), potentially including ground-water levels, streamflow variability and the water quality of regions ranging from hillslopes to river basins to entire continents (Dingman, 2002). Coupled with climate change predictions, hydrological models are used to estimate regional climate change (Gleick, 1999) and provide a framework whereby the relationships between climate and the hydrological processes of a watershed can be conceptualized (Leavesley, 1994; Xu, 1999b). Modelling the hydrology of river basins had its start in the late 1950s, when Dooge (1959) suggested that the response of a watershed could be modelled. Linear models were first developed which simply described the rapid surface flow and slower interflow as components of the storm hydrograph (Diskin, 1964). Non-linear relationships in hydrology that were recognized as being more realistic of catchment behavior were soon discovered (Chow, 1964), and implemented to produce runoff-routing models that were primarily initiated by Laurenson in 1964 (Shaw et al., 2010) and others in following years. Today, hydrological models in watershed science are based on well-known small-scale theories built into coupled balance equations for mass and momentum (McDonnell et al., 2007). According to Singh and Frevert (2002), a large number of highly sophisticated models have been developed due to increased understanding of hydrological processes, digital terrain attributes and increased computing power. Accordingly, Xu (1999b) suggested that, because of the success claimed by climate change studies, it is likely that the computer simulation of catchments will be increasingly used by decision makers that manage water resources. Regionally, various hydrological models are currently being used for water resource assessment and management decisions. The proceeding sections will briefly review the classification of hydrological models, and specific focus will be given to the ACRU Agro-hydrological model and its application throughout the world. ACRU is the model that will be used in this study.

2.5.1 Classification of Hydrological Models

All hydrological models are simplified representations of a portion of the natural or human-constructed world (Dingman, 2002; Refsgaard, 1996). In his review of hydrological concepts, Dingman (2002) compared a hydrological model to a map. He states, "A model is to hydrologic reality as a map is to the actual landscape". This map metaphor makes clear two essential characteristics of models: (1) a model, like a map, is designed for a specific purpose, and (2) is constructed at a particular scale (Dingman, 2002). Both map and model omit features that may not be needed for a specific purpose or scale. Considering purpose and scale to be a basis for model development and classification one can see why many varying types of models exist. Leavesley (1994) suggested that the purpose of the model application along with model structure, spatial partitioning of units, as well as spatial and temporal scale can all be used as criteria to classify different types of hydrological models. Many classification schemes involving hydrological models have been proposed over time, which, as mentioned by Todini (1988), is a result of the plethora of different rainfall-runoff mathematical models being available. Hydrological models have been evolving since first being used in the late 19th century (Todini, 1988). In 1965, Dawdy and O'Donnell proposed that the field of mathematical modelling (hydrology) could be divided by at least two methods of classification: (1) stochastic-deterministic; and (2) analytic-synthetic classification. Most classification schemes from the 1980s to the present day divide hydrological models into at least a physical/deterministic and or stochastic/empirical category (Kampf and Burges, 2007; Leavesley, 1994; Refsgaard, 1996; Shaw et al., 2010; Todini, 1998; Xu and Singh, 1998), where the deterministic models seek to simulate the physical processes in the watershed, and stochastic (empirical) models describe the hydrological variables such as rainfall, evaporation and streamflow involving distributions in probability (Shaw et al., 2010).

2.5.1.1 Empirical (Stochastic) Models

In his comprehensive theory of rainfall-runoff modelling, Beven (2011) suggests that empirical models dating back nearly 150 years were the first widely used and oldest approach to hydrological

modelling. For example, the first hydrologists attempting to predict the flows that could be expected from a rainfall event had insights into hydrological processes but were limited by the data and computational techniques available to them (Beven, 2011). Today, empirical models use experimentally determined relationships such as linear regressions to simulate water flow processes and storages (Dingman, 2002; Kampf and Burges, 2007). Their system operation is usually described by a set of equations linking the input and output variables through the use of probability distributions (Te Chow et al., 1988) without considering the governing physical laws of the processes involved (Leavesly, 1994). Compared to physically based models, empirical models typically (but not always) have relatively low data requirements, but may also be less accurate when applied outside conditions for which the empirical relationships were determined. Beven (2001) suggested that regression relationships should always be associated with an estimate of the uncertainty associated with the predictions of the dependent variables in empirical modelling. Arnell (1992) proposed that estimates based on empirical modelling should be treated with extreme caution. This opinion resulted from a study where he investigated the effects of climate change on river flow regimes in 15 basins in the United Kingdom. He compared the simulated output from a simple three parameter monthly water balance model with four different empirical models and found that not one empirical formulation gave a consistently closer match and that the differences among empirical models for the same scenario were large. Although empirical models function differently than physically based models, they nonetheless have their place in hydrological modelling. For example, they have been used for determining peak flow and the time-to-peak of a unit hydrograph (Beven, 2011), and are often used in water quality impact assessments for urban development (Praskievicz and Chang, 2009).

2.5.1.2 Physically Based Models (Distributed)

Physical models in hydrology are firmly based in understanding the physical processes that control basin response. They are typically derived from equations using basic physics such as the conservation of mass, energy, or momentum (Beven, 1989; Dingman, 2002; Leavesley, 1994). Generally,

physically based models are characterized by higher accuracy for predicting the effects of land use disturbance or climate change, but they also suffer from high data requirements (Beckers et al., 2009; Beven 2001). The availability, quality and scale of data for these models can often impede accurate estimations of model parameters as well as model validation (Leavesley, 1994). Some discredit physically based distributed models in that they are heavily over-parameterized (McDonnell et al., 2007), can be extremely time consuming to setup, and be difficult to calibrate (Bormann et al., 2009).

Distributed hydrological modelling describes spatial discretization by considering the spatial heterogeneity of hydrological characteristics of a catchment (Schumann, 1993). To develop a hydrological model for a river basin it has to be decided which sub-basins should be modelled separately and which could be lumped together (Schumann, 1993). Although this decision is usually based on hydro-meteorological data, the spatial heterogeneity of the hydrological characteristics within the river basin should be considered (Schumann, 1993). According to Schulze (1995) this delineation process is largely subjective and dependent on the purpose of the modelling exercise. Advantages in the application of distributed physically-based hydrological models include, inter alia, that they provide a detailed and potentially more correct description of hydrological processes in the catchment than other model types (Refsgaard, 1996), their ability to couple hydrological processes with a variety of physically based models of biological and chemical processes (Leavesley, 1994) provides a connection between scientific disciplines, and their ability to assess the impacts of climate change has been recognized (Barnett et al., 2005; Barrow and Yu, 2005; Bathurst and O'Connell, 1992).

2.5.2 ACRU Agro-hydrological Model

The ACRU agro-hydrological modelling system has been developed at the School of Bioresources Engineering and Environmental Hydrology (formerly the Department of Agricultural Engineering) at the University of KwaZulu-Natal, Pietermaritzburg, Republic of South Africa, since the late 1970s (Kienzle et al., 2012). Model updates have taken place over the years with major additions improving the model's ability to simulate physically based processes associated with cold environments and terrain dependent

hydrological variables. For example, these updates include the addition of snowpack and snow/glacial melt routines as well as temperature corrections based on differences of incoming net radiation as a function of exposition and slope.

ACRU requires considerable spatial information, inter alia, on topography, a wide range of climatic parameters, soils, land cover, reservoirs and streams. The spatial organization of sub-units in ACRU is flexible, and includes sub-watersheds, square grid cells and HRUs. As ACRU is land cover sensitive, the parameterization of land cover dependent variables is important (Kienzle, 1993; 1996; 2011; Schulze, 1995). The ACRU model is further described by Schulze (1995), Smithers and Schulze (1995),Kiker et at., (2006) and Kienzle (2011). Kienzle (1993) described the link between ACRU, Geographic Information Systems (GIS) and decision support systems.

2.5.3 Physical Processes of the ACRU Model

ACRU is a multi-purpose, multi-level, integrated physical model that is designed to simulate total evaporation, soil water and reservoir storages, land cover and abstraction impacts, snow water dynamics and streamflow at a daily time step (Schulze, 1995). ACRU revolves around multi-layer soil water budgeting with specific variables governing the atmosphere-plant-soil water interfaces. Surface runoff and infiltration are simulated using a modified Soil Conservation Service (SCS) equation (Schmidt and Schulze, 1987), where the daily runoff depth is proportional to the antecedent soil moisture content. ACRU is not a parameter fitting or optimizing model, as all variables are estimated from the physical characteristics of the watershed. When not all required variables are available, they are estimated within physically meaningful ranges based either on available literature or complex GIS analysis, local expert knowledge, or calibration against observed data, such as the slope of the groundwater recession. The output of the ACRU model consists of daily time series of 52 variables for each spatial modelling unit, including streamflow, groundwater flow, groundwater recharge, soil water deficit and surplus, irrigation requirements, water use by vegetation and evaporation from wet surfaces. From the time series, risk analyses on any variable can be carried out using exceedance probability plots, which provide information

on the percentage of time a certain value, e.g. flood, soil moisture, or low flow is exceeded. A typical application of the ACRU model requires the set-up and verification analysis for historical periods, typically for a 30-year time period (e.g. 1971-2000), and then the set-up for changed environmental conditions, such as land cover change, urbanization, or climate change.

2.5.4 ACRU around the world

ACRU has been applied around the world for a variety of different climates, landscapes and situations. For example, ACRU has been used extensively for water resource assessments (Everson, 2001) flood estimation, land use impacts (Kienzle and Schulze, 1992; Tarboton and Schulze, 1993), forest hydrology applications (Jewitt and Schulze, 1999), nutrient loading, climate change impacts (Kienzle et al., 2012; New, 2002; New and Schulze, 1996; Schulze, 2000; Schulze et al., 2004; Schulze and Perks, 2003; Warburton et al., 2010), irrigation supply, irrigation impacts (Kienzle and Schmidt, 2008) and requires extensive GIS pre-processing (Kienzle, 1993, 1996).

2.5.5 ACRU and Climate Change

An assessment of the complex interactions between the hydrological processes associated with climate change can be accomplished through the use of a hydrological model. Schulze (2005) and Warburton et al. (2002), both suggest that the ACRU agro-hydrological model is one such model that is suitable for such studies. ACRU has been applied in a variety of diverse climates to simulate, inter alia, how future streamflow volumes will be impacted as a result of global climate change. Application of the ACRU model in climate change studies include, the identification of areas in South Africa that are vulnerable to climate change (Schulze and Perks, 2003), the analysis of impacts of climate change on the hydrological response in the mixed underdeveloped/developed Mgeni catchment in South Africa (Schulze et al., 2004), the assessment of hydrological responses to climate change for three catchments with diverse climate (Warburton et al., 2010), the first application of ACRU on a watershed in southern Alberta, Canada (Forbes et al., 2011), and the assessment of the UNSRB (Nemeth et al., 2012; Kienzle et al., 2012).

2.6 Spatially Gridded Climatic Datasets

Meteorological data such as precipitation and temperature are required for many hydrological analyses and are often used as key drivers of computer models which, according to Daly (2006) and Wang et al (2012), form the basis for scientific conclusions, management decisions and policy making. Problems fundamentally associated with hydrological analysis or modelling, however, are typically attributed to the estimation of hydrological variables at unmonitored sites (Hevesi et al., 1992; Running et al., 1987). These problems result from the lack of areal coverage of climate stations, especially in regions dominated by mountainous terrain where orographic effects can be large (Hevesi et al., 1992). Additional to the lack of climate stations in mountainous basins is another problem with the temporal scale at which meteorological data are observed and made available. For example, data in mountainous regions are often seasonal. These problems can often times become compounded in scientific analysis creating obstacles in various hydrological studies.

In recent years, spatial databases of historical climate have become important and are in high demand (Hutchinson et al., 2009; Perry and Hollis, 2005; Wang et al., 2012), the demand for historical climate datasets are fueled in part by the widespread adoption of computer technology that enables a variety of hydrological, ecological, natural resource and other models and decision support tools to be linked to GIS. These spatial datasets are produced using a number of varying statistical procedures and interpolation techniques, which weight irregularly spaced point data to estimate regularly spaced prediction grids. Historically, they were produced with incomplete spatial coverage resulting in coarse resolution (New et al., 2002). At regional or country scales high resolution data (<25 km grid spacing) tend to be required; however, in many regions of the world, such data have not been available. Today, computing capabilities allow very fine-resolution climate grids (1 km) to be created over most of the world (Daly, 2006) offering the potential for deriving a range of surface conditions that have not been directly observed. Including, for example, soil moisture, SWE, ET, runoff and subsurface soil moisture transport (Hamlet and Lettenmaier, 2005).

2.6.1 PRISM

PRISM (Parameter-elevation Regressions on Independent Slopes Model) (Daly, 2006; Daly et al., 2002; Daly et al., 1994) surfaces are created by the PRISM climate group based at Oregon State University. According to their website http://prism.oregonstate.edu/ (2014), they gather climate observations from a wide range of monitoring networks and develop spatial climate datasets which reveal short- and long-term climate patterns. These peer-reviewed mapping efforts have produced official precipitation and temperature maps for the United States, Canada, China and Mongolia as well as other regions (Daly et al., 2007). Estimations of annual, monthly, daily and event-based climatic events are created using point data, a Digital Elevation Model (DEM), spatial datasets and knowledge based computer algorithms based on geospatial climatology, which are then interpolated to a regular grid (Daly et al., 2002; Daly et al., 2007). Geospatial climatology is described by (Daly et al., 2002) as the study of the spatial patterns of climate and their relationships with geographic features, such as for example, elevational influence on climate, terrain-induced climate transitions, coastal effects, two-layer atmosphere and orographic effectiveness of terrain. PRISM surfaces are used extensively in many scientific analyses which are dependent on meteorological variables of temperature and precipitation and provide, in many instances, a first approximation of these variables in regions that lack observational monitoring systems.

2.6.2 Canada-wide 10 km Gridded Climate series

Through a concerted modelling effort, the 10 km Grid, which consists of daily estimations minimum and maximum temperature (Tmin and Tmax) and precipitation has been produced for Canada for the period 1961–2003 (Hutchinson et al., 2009). According to Natural Resources Canada (2014), recent updates on the daily grids have been made available for the years 1950-2010 and will continue to be updated as new data become available and resources allow. Relatively few studies have generated historical daily climate grids of the spatial coverage and resolution presented in Hutchinson et al (2009), where the complex spatial patterns associated with daily data across Canada as spatially continuous functions of longitude, latitude and elevation are considered (Hutchinson et al., 2009). The gridded

dataset was produced as a requirement of agricultural and forestry applications in the southern half of Canada, as this is where most agricultural and forestry activity occurs and where the overwhelming majority of Canadian meteorological stations are located (Hutchinson et al., 2009). As they are made available, the daily grids will also become a source of great value to scientists in a variety of scientific disciplines, including, inter alia, those in the physical and earth sciences. A methodology describing the generation of the gridded dataset can be found in Hutchinson et al (2009) and recent updates including the impact of aligning climatological day can be found in Hopkinson et al (2011).

Chapter 3: Model Parameterization

3.1 Study Area

The area selected for this study is the Castle River Watershed (CRW), which is a sub watershed of the ORB, located in the southern Alberta Rocky Mountains (Fig. 1). A large percentage of the population in southern Alberta lives within the ORB where water is considered an extremely valuable commodity. The CRW borders the north-west portion of the Waterton Glacier International Peace Park and extends northwest along the continental divide to the Crowsnest Pass (Fig. 1). The basin's physical extent is bounded between 49° 9' 15.8" to 49° 34' 11.7"N and -114° 7' 40.7" to -114° 36' 18.0" W.

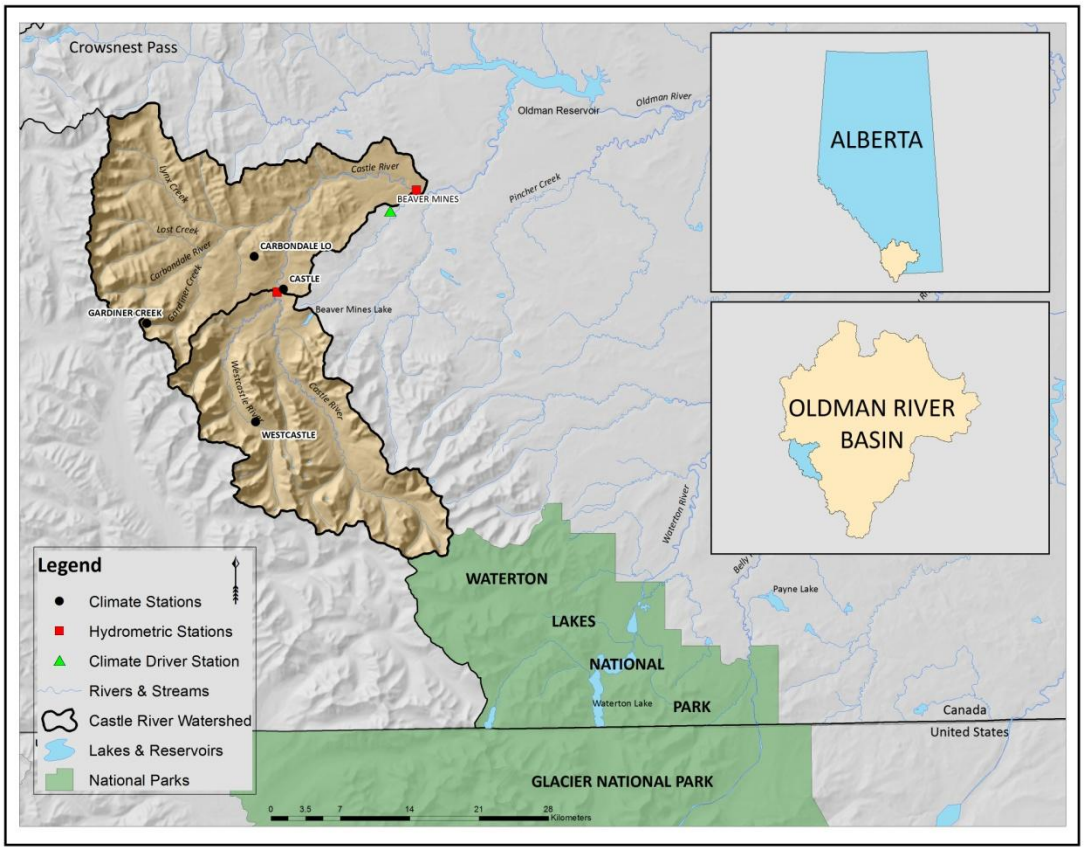

Figure 3.1 A map showing the physical extent of the Castle River Watershed and its situation within Southern Alberta

The watershed, defined by its outlet at the water survey of Canada gauging station (05AA022), has an area of 825 km^2 and consists of alpine, sub-alpine, montane and foothills landscapes in the eastern

slopes of Rocky Mountains. The watershed has been identified as a pristine wilderness area, although it has been subjected to minor industrial activity such as natural gas extraction and logging. There is a ski resort located in the Westcastle River valley which attracts more than 60,000 people annually to its slopes and backcountry (Castle Mountain Resort, 2009). The Castle River is the main water course in the watershed, with a mean annual discharge rate of 15 $m^3 s^{-1}$ and contributes, on average, 15% of the annual flows of the Oldman River. The range in elevation from the hydrometric outlet station at Beaver Mines moving westward to the continental divide increases from 1188–2677 m and is predominantly covered by broadleaf and coniferous forest (64%), while herb and grassland (16%), shrub (11%) and non-vegetated land (9%) account for the rest of the land cover. The CRW is characterized by a continental climate with annual temperature variations ranging from over 30°C in the summer to -30°C in the winter. Based on available PRISM surfaces (Daly et al., 2008) the mean annual precipitation (1971-2000) for the CRW is 925 mm.

3.2 The ACRU agro-hydrological modelling system

When applied to simulate hydrological responses in large and heterogeneous watersheds, ACRU requires substantial spatial information, inter alia, on topography, a wide range of climatic parameters, soils, land cover, reservoirs and streams (Figure 3.2). The spatial organization of sub-units in ACRU is flexible, and includes sub-watersheds, square grid cells and HRUs, which are user defined areas consisting of relatively homogeneous bio-physical characteristics that produce a specific hydrological response in relation to a precipitation event. For example, the 20,000 km^2 UNSRB was subdivided into 1528 HRUs, each having a unique combination of elevation, land cover and climate (Nemeth et al., 2012). As ACRU is land cover sensitive, the parameterization of land cover dependent variables is important (Kienzle, 1993, 1996, 2011). The ACRU model is further described by Schulze (1995), Smithers and Schulze (1995), Kiker et at., (2006) and Kienzle (2011). A typical application of the ACRU model requires the set-up and verification analysis for historical periods, typically for the time period 1961-1990 or 1971-2000 and then the set-up for changed environmental conditions, such as land cover change, urbanization or climate change.

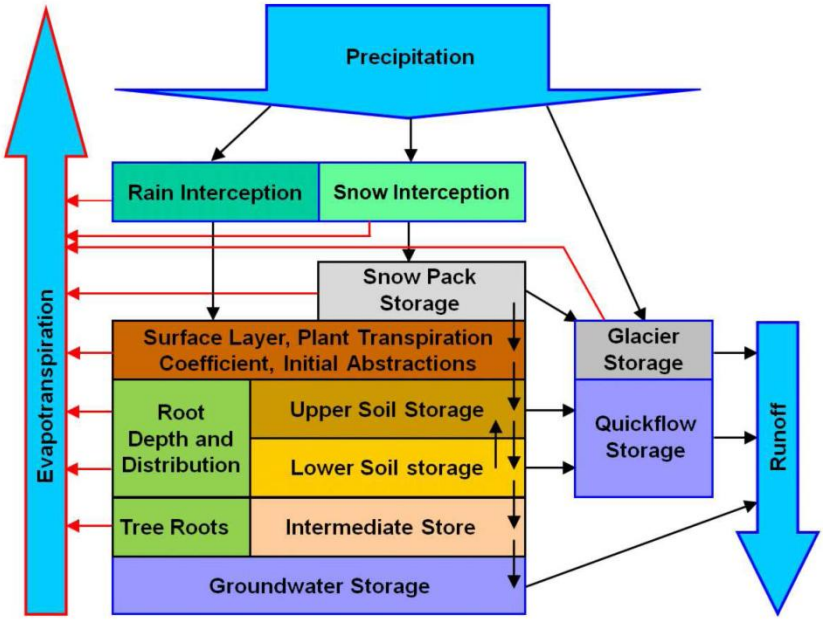

Figure 3.2 The ACRU agro-hydrological modelling system (taken with permission from Kienzle and Schmidt, 2008)

3.3 Hydrological Response Units

HRUs are user defined entities representing specific dynamics unique to the system response of the hydrological interactions within the areal unit. The watershed is delineated into individual HRUs, ideally not exceeding 30 km^2 (Schulze, 1995).

The delineation of HRUs for the CRW was based on elevation, land cover, mean annual radiation and the watershed boundary. A 100 m DEM was classified into 14 elevation bands using 100 m intervals ranging from 1200 m to 2600 m. Land cover data produced by the National Land and Water Information Service (NLWIS) were downloaded from the GeoBase portal (GeoBase, 2011) at 30 m resolution and generalized to 100 m to match the DEM. Of the 36 different land cover classes found in the province of Alberta only 13 were represented in the CRW. Mean annual radiation was calculated in ArcGIS using the Area Solar Radiation tool using half hour intervals every three days throughout the year. To account for the fraction of radiation that passes through the atmosphere, monthly transmittivity values ranging from 0.53 – 0.65 were also implemented, which were based on observations of the three nearest climate

stations which recorded solar radiation. The radiation output was then classified into four quartiles. The CRW was sub-divided into upper and lower watersheds corresponding to the two streamflow gauging stations. The spatial boundaries of the four input variables (15 elevation bands, 13 land cover classes, four mean annual radiation classes and two watershed boundaries) were overlaid in ArcGIS, creating 230 HRUs for the entire CRW, where 98 HRUs constitute the upper sub-watershed, and 132 HRUs make up the lower sub-watershed.

3.4 Data Requirements

Regardless of the spatial complexity of a watershed, a minimum amount of information is required to enable the simulation of hydrological processes. Geographic information such as location, area and elevation is required at the HRU level. Climatic information including daily observations of precipitation and minimum and maximum air temperature are required. ACRU also requires the input of reference evaporation data. Since it is difficult to accurately measure evaporation directly, the physically based Penman-Monteith method using meteorological data are used. The Penman-Monteith method requires inputs such as daily mean air temperature (°C), wind speed (U, m s^{-1}), relative humidity (RH, %) and net radiation at the earth's surface (MJ m^{-2} day^{-1}). Other essential data requirements include soil and land cover information. The soil data requirements include, for both A- and B-horizons, soil depth, soil porosity (PO), field capacity (FC), wilting point (WP) and soil water redistribution variables. Land cover classes, such as coniferous forest or shrubland, must be translated into hydrologically meaningful variables, such as monthly interception rates or leaf area index (LAI), plant transpiration coefficient and rooting depths. In order to enable validation of simulated output, observed data should include at a minimum daily streamflow time series, but ideally also independently recorded temperature time series and snow pillow or snow course data.

3.5 Model Parameterization

Once the physical characteristics and climatic information of the watershed are obtained, they are parameterized into the model. In ACRU, parameterization refers to the assignment of relevant hydrological variables to HRUs which are distributed throughout the watershed.

For climate input, ACRU was parameterized following the so-called driver station approach. This approach is based on a "base station" method as described by Hungerford et al. (1989), which is the extrapolation of meteorological variables from a point of measurement (referred to as a "base" station) to the study "site" of interest, making corrections for differences in elevation, slope and aspect between the base station and the site. The base station method is applied to provide climatological input into the spatially distributed hydrological model using two different climatic datasets. The first dataset represents the long continuous climate record observed at the BMCS (A3050600), and the second dataset represents a spatially continuous 10 km Grid, wherein each grid cell contains estimates of daily weather variables for its particular area.

3.5.1 Climate Data

A number of datasets were used to parameterize the ACRU agro-hydrological model. Details summarizing the major datasets that were used are outlined in Table 3.1. Two different climate datasets are applied to "drive" ACRU as a spatially distributed model. The first dataset, comprised of daily observations of Tmin, Tmax and precipitation, were made available by Environment Canada (EC) (2012a) http://climate.weather.gc.ca/index_e.html#access. These data were observed and recorded at the BMCS (05AA022) which captures 100 years (1912-2012) of daily observations. From this dataset the 1971-2000 historical record was chosen as a baseline period. Days with missing observations accounted for less than 1% of the entire 30 yr daily time series and were infilled using an infilling procedure based on the following methodology:

1. Select climate stations in close proximity to the driver station (Beaver Mines). If possible, climate stations that share similarities in topography such as mountains, foothills, or plains landscapes are given highest priority for patching/infilling.
2. Divide data into 12 monthly series (Jan to Dec) for all station records so that each month contains observations for the whole historical time period (e.g. Jan. 1971-2000, Feb. 1971-2000, etc..).
3. Run linear regressions for each month between the driver station and all infilling stations.
4. Order in-filling stations from highest to lowest according to the coefficient of determination (r^2) derived in Step 3.
5. The station with the highest r^2 value is used to infill missing days in the driver station record. If missing data are encountered at that station, the station with the next best r^2 - is selected and used. This process is repeated until all missing days in the driver station climate record are infilled.

Table 3.1 Meteorological and terrestrial based data used to model the CRW

Data Description	Temporal Resolution	Spatial Resolution	Variables of Interest	Source
Observed time series data from stations of varying length	Daily	Point data	Tmin (°C), Tmax (°C), Tmean (°C), Precipitation (mm/day), Net Radiation (MJ m^2/day)	Environment Canada (EC)
Observed time series data from stations of varying length	Daily	Point data	Wind speed (m/s), Relative Humidity (%)	National Oceanic and Atmospheric Administration (NOAA)
Spatially continuous gridded dataset (1951-2010)	Daily	10 x 10 km grids (100 km^2)	Tmin (°C), Tmax (°C), Precipitation (mm/day)	National Land and Water Information Service (NLWIS), Agriculture and Agri - Foods Canada (AAFC)
Interpolated time series	Monthly normals 1971-2000	2 km	Tmin (°C), Tmax (°C), Precipitation (mean monthly)	Parameter-elevation Regressions on Independent Slopes Model (PRISM)
Snow Survey Data	Seasonal	Point data	Snow Water Equivalent (SWE)	Alberta Environment and Sustainable Resource Development (AESRD)
Hydrometric Data	Daily	Point data	Streamflow discharge (m^3 s^{-1})	Environment Canada HYDAT
Soil Data (polygon shapefiles and databases)	Published online in 2003	Polygons at scale 1:50,000	Soil Texture and Hydrological Soil Properties	Alberta Agriculture and Rural Development (AARD)
Land cover	2007-2008	30 m Resolution	Land Use	NLWIS, Geobase
Leaf Area Index (LAI)	2004	1000 m Resolution	Leaf Area Index	MODIS satellite images from the National Snow and Ice Data Center (NSIDC)
Plant Transpiration Coefficients (PTCs)	2004	Point data	Water Vapor and Energy Fluxes	Environment Canada (Fluxnet-Canada) and the U.S. Department of Energy (AmeriFlux)
Albedo	Monthly	Point data	Albedo	From Literature

The second dataset, a Canada-wide daily 10 km Grid was made available by Agriculture and Agri-Food Canada (2013). It was originally released in 2007 by the National Land and Water Information Service and provides coverage south of 60°N across the landmass of Canada. The dataset consists of daily estimations of Tmin, Tmax and precipitation for the 1950-2010 period of record. These grids were

spatially interpolated from 7514 climate stations from the Canadian Climate Data Archives of Environment Canada. Detailed information regarding the grid creation including error analysis associated with the interpolation of the climate data with can be found in Hutchinson et al. (2009). Parameterization using the 10 km Grid required an overlay of the grid with the CRW by partitioning the basin across 20 separate 10 x 10 km grid cells. In order to minimize the number of daily climate time series, climate grid cells that were either covering a small portion of the CRW, or that were very similar to a neighbouring climate grid cell, were aggregated into larger, non-square, climate grid cells. As a result of differences or similarities in topography, geographic boundaries and HRU representation, nine polygons were delineated from the 20 grid cells, each containing estimates of daily Tmin, Tmax and precipitation (Figure 3).

In mountain environments data are often sparse or unavailable; therefore, having spatially continuous estimations for areas where observations are normally not measured can be invaluable when simulating hydrological processes. Similar to the Beaver Mines dataset, the estimated spatially gridded data are applied to “drive” ACRU as a distributed hydrological model. The following sub-sections provide a more in-depth description of hydro-climatological variables that were parameterized in ACRU for the CRW.

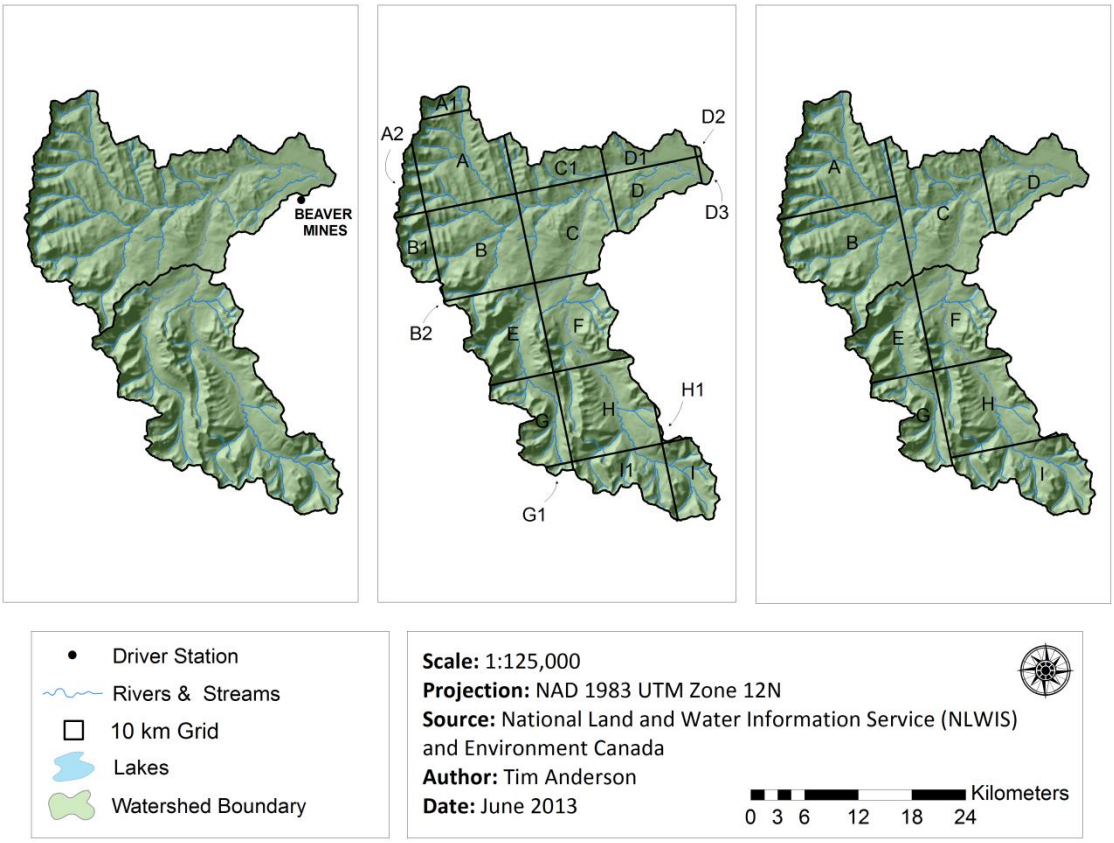

Figure 3.3 Driver station parameterization "base" station method using the BMCS (left) and the 10 km gridded daily models (middle and right).

3.5.1.1 Temperature

Average temperature decreases with elevation in the free atmosphere according to an environmental lapse rate approximation of 6°C km^{-1} (Barry, 2008). Due to a number of influences common in mountain environments such as temperature inversions, katabatic winds and diurnal temperature fluctuations, temperature lapse rates derivation can be highly complex, and, due to the scarcity of temperature measurements, is extremely difficult to estimate for all locations across an entire watershed. As air temperatures are also influenced by slope, exposition and land cover (e.g. north- vs. south-facing slopes, valleys that receive little or no direct incoming radiation and forested vs. open areas), temperature measurements derived at the base station are adjusted internally within ACRU according to user defined lapse rates, solar radiation and land cover (Kienzle, 2011). Temperature adjustments using lapse rates are

made from the location of the base station(s) for both climate datasets. For example, when the Beaver Mines data are applied to run the ACRU model, temperature values are adjusted daily by calculating the difference in elevation between the BMCS (1257 m.a.s.l.) and the individual HRU. The same approach is applied for the 10 km gridded data, where the mean elevation of each gridded area "A" to "I" is used.

Monthly lapse rates can be estimated by using the PRISM climate normals and calculating the monthly PRISM temperature values at the driver station as well as mean monthly temperatures for each elevation band and applying linear regression analysis. The slope of the monthly regression line is equivalent to the monthly lapse rate. However, when this method was applied, the resulting lapse rates were unrealistic. For instance, calculated Tmax lapse rate (TMaxLR) and Tmin lapse rate (TMinLR) gradients exceeded -10°C km^{-1} for most months and at times reached and exceeded -20°C km^{-1} on a monthly basis. Therefore, regional lapse rates were derived through the application of a weighted distance calculation to PRISM based lapse rates previously determined for the UNSRB (Kienzle et al., 2012) and SMRW (Kienzle, 2011), and are listed in Table 3.2. Lapse rates calculated for the CRW are in line with those calculated by Blandford et al. (2008) for a Rocky Mountain area in south-central Idaho, where steeper lapse rates occur during summer months and shallower lapse rates occur in winter months. For example, Blandford et al. (2008) reports (TMaxLR) in December to January to be -4.3°C km^{-1}, gradually steepening through February and March (-5.1 to -5.3°C), followed by a sharp increase during spring and summer where TMaxLR reaches as large as -7.0°C km^{-1}, and then decreasing again during the fall and winter. TMinLR are quite shallow during December to January (-0.12 to -0.16°C km^{-1}), gradually steepening in February to March (-0.21 to -0.33°C km^{-1}), and dropping significantly to 0.03 during August to September, followed by an increase again during fall and winter.

Table 3.2 Regionally derived lapse rates of Tmax (top) and Tmin (bottom) for the headwater regions of the UNSRB, CRW and SMRW in the Rocky Mountains. Regional lapse rates for the UNSRB and SMRW were derived from 1970-2000 PRISM surfaces. Lapse rates for the CRW were derived by applying a weighted distance ratio of 2/3 towards the SMRW and the UNSRB.

Mean Monthly Temperature Maximum (Tmax) Lapse Rate												
Headwater Region	Jan	Feb	Mar	Apr	May	Jun	Jul	Aug	Sep	Oct	Nov	Dec
North Saskatchewan, AB, Canada	-5.2	-5.23	-4.94	-7.42	-8.04	-8.45	-8.37	-8.3	-8.15	-8.25	-7.06	-6.05
Castle, AB, Canada	-5.73	-5.74	-5.75	-6.56	-6.85	-7.16	-7.09	-6.9	-6.72	-6.9	-6.48	-6.14
St. Mary, MT, USA	-5.99	-6.00	-6.15	-6.13	-6.26	-6.51	-6.45	-6.2	-6.00	-6.23	-6.19	-6.18

Mean Monthly Temperature Minimum (Tmin) Lapse Rate												
Headwater Region	Jan	Feb	Mar	Apr	May	Jun	Jul	Aug	Sep	Oct	Nov	Dec
North Saskatchewan, AB, Canada	-1.17	-2.03	-3.56	-4.33	-4.38	-5.16	-4.23	-3.49	-3.42	-4.15	-4.03	-2.9
Castle, AB, Canada	-0.56	-0.75	-2.39	-4.05	-3.83	-4.2	-3.7	-2.95	-2.89	-3.38	-2.38	-1.35
St. Mary, MT, USA	-0.26	-0.11	-1.8	-3.91	-3.56	-3.72	-3.43	-2.68	-2.62	-2.99	-1.56	-0.58

3.5.1.2 Precipitation

The spatial and temporal variability of precipitation has led many researchers to examine precipitation lapse rates in mountainous terrain. This is a result of the fact that precipitation generally increases with altitude, at least up to the highest point of measurement (Shea et al., 2004). In ACRU, this variability is expressed as a precipitation adjustment factor where daily rainfall values are converted by a precipitation correction factor (CORPPT), which can vary month by month (Schulze 1995). CORPPT is determined by:

$$\text{CORPPT} = \frac{P_{HRU}}{P_{ds}} \qquad \text{[Eq. 3.1]}$$

where, the P_{HRU} is the mean monthly PRISM precipitation for each HRU and P_{ds} denotes the mean monthly precipitation for each respective driver station (Beaver Mines or 10 km Grids "A to I"). PRISM precipitation is based on the 1971-2000 normals. When applying the BMCS, precipitation is extrapolated from the station elevation of 1257 m.a.s.l., and adjusted according to changes in the elevation of each HRU across the watershed. Adjustments using the 10 km Grids "A" to "I" are extrapolated to HRUs above and below

the mean elevation of each grid. The adjustment factors for the BMCS are applied to the catchment as a whole, while those calculated from the nine gridded areas are subject to their respective spatial extents and when combined, provide spatial coverage for the entire watershed (Figure 3.4).

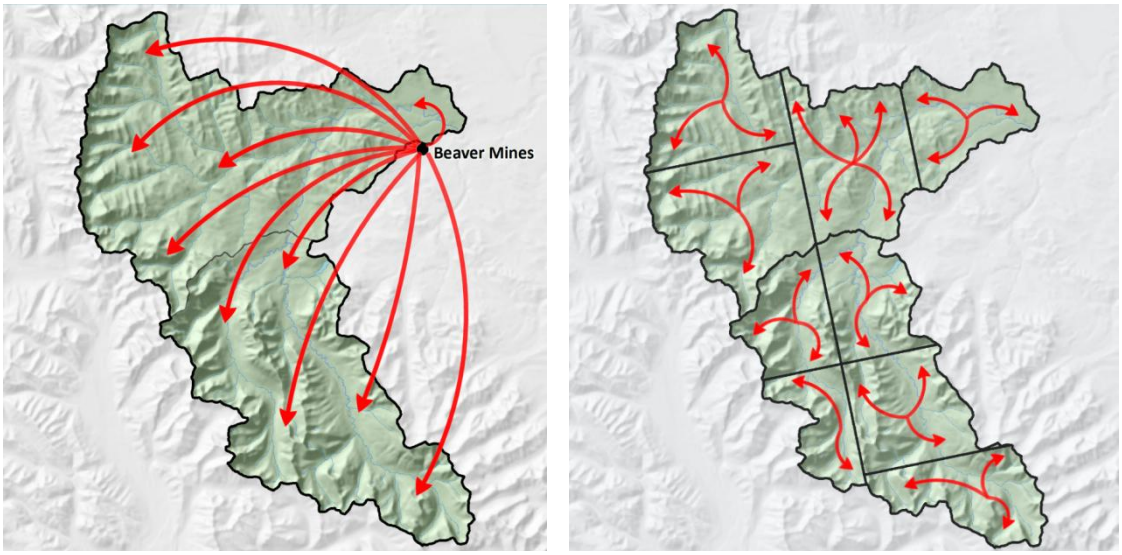

Figure 3.4 Correction factors are applied to extrapolate meteorological variables from a driver station to unmonitored sites in the watershed. Extrapolation occurs from a point measurement e.g. Beaver Mines (left) or from the mean elevation of a spatially gridded dataset such as the 10 km Grid (right).

3.5.1.3 Evapotranspiration

In ACRU, ET takes place from water storages in the soil-plant interface and is separated into evaporation and transpiration (Schulze, 1995) relative to energy balance and atmospheric demand. Daily potential ET is derived from the reference evaporation calculated using the Penman-Monteith equation, and monthly plant transpiration coefficients which are based on land cover type. The reference evaporation selected for use in this study is the FAO Penman-Monteith method (Allen et al., 1998) as it has been considered a universal standard for ET estimation for more than a decade (Sentelhas et al., 2010). The estimation of daily ET requires for each HRU daily minimum and maximum air temperatures, solar radiation at the earth's surface [MJ m^{-2} day^{-1}], the number of sunshine hours [hr day^{-1}], RH [%] and U [m s^{-1}]. The parameterization of each of these variables will be discussed in more detail below, excluding that of air temperature as it has already been discussed previously.

3.5.1.3.1 Relative Humidity and Wind Speed

Canadian climate normals for RH and U (1971-2000) were made available by Environment Canada (2012b) http://climate.weather.gc.ca/climate_normals/index_e.html#1981 for 17 RH and 26 U stations located in Alberta, 29 RH and 48 U stations in British Columbia (B.C) and 15 RH and 25 U stations in Saskatchewan. Additional measures of RH and U were also made available by the National Atmospheric and Oceanic Administration (NOAA) for 6 RH and 7 U stations located in the State of Montana of the United States. Climate normals consist of mean monthly climatic conditions at station locations established during a 30yr period throughout Canada and the United States. Minor adjustments were made on each set of climate normals, for example, conversion from miles per hour (mph) to kilometers per hour (km/h) for Montana U data were performed. Additionally, U data, which were measured at 10 m height from the ground surface, was converted to 2 m height.

To adjust and extrapolate RH and U throughout the watershed, each RH and U climate station is mapped in ArcGIS and spatially interpolated using spline to a 100 m grid across Alberta. Monthly means are calculated using statistical spatial analysis on the 10 km Grids and BMCS. Monthly means are then downscaled to daily values using a Fourier Transformation. Once daily values are obtained, the process is repeated for the 61-year climate time series and inserted for use in a climate input file (composite file) based on local hydrometeorological variables. Mean monthly estimates of RH and U are also converted by factors of WINCOR (wind correction factor) and RHUCOR (relative humidity correction factor) across the watershed. These calculations are described by:

$$\text{Correction Factor} = \frac{X_{HRU}}{X_{ds}} \qquad \text{[Eq 3.2]}$$

where, X denotes the variable of interest (U or RH), X_{HRU} is the mean monthly U or RH for each 100 m HRU and X_{ds} signifies the mean monthly U or RH for each respective driver station (Beaver Mines or 10 km Grid).

3.5.1.3.2 Sunshine Hours and Solar Radiation

Hours of bright sunshine and incoming solar radiation were calculated by way of extensive data processing in ArcGIS, using the Area Solar Radiation tool. The Area Solar Radiation tool is only applicable for maximum 1 degree latitude (approximately 111 km) because it only allows the input of a single latitude value for the computation of solar radiation over an entire study area. To account for increasing over estimation of solar radiation towards 60° N and increasing under-estimation of solar radiation towards 49° N, correction surfaces were created at 49° N and at 60° N. Combining the two resulting correction rasters provided the surface upon which simulated values of sunshine hours and net radiation could be made.

Observations of bright sunshine hours and net radiation were made available in the form of Canadian climate normals by Environment Canada (2012b) for 21 stations across the Province of Alberta. Points for each station location were imported into ArcGIS and mapped. A ratio of simulated and observed sunshine hours at the climate station point locations provided the basis for creating an interpolated raster surface and was used to divide the surface of simulated sunshine hours into a final sunshine map for the province of Alberta. Sunshine hours were corrected for each HRU in the CRW from the Beaver Mines base station as well as each gridded station "A" to "I". For each HRU, correction factors were calculated for both sunshine hours and radiation and for both the climate station point location and 10K climate grids.

3.5.1.4 Land cover

Land cover data were downloaded from the GeoBase portal (GeoBase, 2011) http://www.geobase.ca/geobase/en/data/land cover/csc2000v/description.html at 30 m resolution and generalised to 100 m. It was originally produced from raster thematic data from classified Landsat 5 and Landsat 7 ortho-images for the agricultural and forested areas of Canada. The agricultural product was produced by the National Land and Water Information Service (NLWIS) of Agriculture and Agri-Food Canada (AAFC), while the forest cover product was produced by the Earth Observation for the Sustainable

Development of Forests (EOSD) of the Canadian Forest Service. Together, through collaborative measures of each of the aforementioned mapping agencies, the land cover extent of Canada was made publicly available. The original land cover product is made up of a series of 34 groups and sub-groups of land cover classes, of which only 13 are present in the CRW. These 13 land cover classes are as follows: Water, Rock, Barren Land, Developed, Shrub Tall, Wetland-Shrub, Herb, Grassland, Agricultural-Annual Cropland, Agricultural-Perennial Crops and Pasture, Coniferous Dense, Coniferous Open and Broadleaf Dense. For purposes of modelling efficiency, two land cover sub-groups were generalized to their hierarchical group head. For example, the "Shrub-Tall" sub-group was re-classified as "Shrubland" and "Wetland-Shrub" was re-classified to "Wetland". In addition, the sub-groups "Exposed Barren Land" and "Developed" were re-classified as "Rock".

Table 3.3 Percent coverage of Land cover classes in the CRW

Land cover	Water	Rock	Shrubland	Wetland	Herb	Grassland	Annual Cropland	Perennial Crops and Pasture	Coniferous Dense	Coniferous Open	Broadleaf Dense
[%] coverage of total watershed area	0.2	9.5	10.6	0.1	6.4	6.7	0.4	2.9	57.2	1.7	4.3

3.5.1.5 Soils

Hydrological soil properties for each HRU in the CRW were estimated based on a method developed and described by Kienzle et al. (2012), which relies on the association between soil depth and soil texture, with associated water holding parameters (PO, WP, and FC). This association was based on available literature involving land classification and soils in the Rocky Mountains (Pettapiece, 1971). Additionally, soil data were obtained from the Agricultural Region of Alberta Soil Inventory Database (AGRASID) (Alberta Agriculture and Rural Development, 2012a) http://www1.agric.gov.ab.ca/$Department/deptdocs.nsf/All/sag14652 which originates from soil surveys and soil maps created by different mappers since 1920 (Brierley et al., 2001). Since AGRASID was developed only for the agricultural region of Alberta, little soil information exists for the Alberta Rocky

Mountains. The CRW is no exception, but due to the location of the outlet occupying a transitional zone between the foothills and mountain landscape, it was observed that AGRASID's data coverage extended into and provided data for approximately 10% of the low lying agricultural area of the CRW. Understanding that there is considerable uncertainty associated with generalizing soil information in mountainous terrain, soil properties based on attributes of known land cover were extrapolated to the remaining portion of the watershed where AGRASID's spatial coverage did not extend. Parameterized soil depth information for the A and B soil horizons for each land cover type in the CRW is reported in Table 3.3

Table 3.4 Soil depths and water holding parameters for corresponding land cover classes found in the CRW. For agricultural land, soil depth information was derived from AGRASID.

Land cover	Rock	Shrubland	Wetland Shrub	Herb	Grassland	Annual Cropland	Perennial Crops and Pasture	Coniferous Dense	Coniferous Open	Broadleaf Dense
Depth of A Horizon [m]	0.01	0.06	0.20	0.04	0.04	0.18	0.16	0.05	0.05	0.13
PO in A Horizon [%]	0.900	0.402	0.408	0.421	0.421	0.394	0.394	0.402	0.402	0.394
WP in A Horizon [%]	0.162	0.162	0.215	0.103	0.103	0.109	0.109	0.162	0.162	0.109
FC in A Horizon [%]	0.285	0.285	0.332	0.231	0.231	0.213	0.213	0.285	0.285	0.213
Depth of B Horizon [m]	0.00	0.33	0.40	0.24	0.24	0.48	0.47	0.29	0.27	0.53
PO in B Horizon [%]	0.900	0.402	0.408	0.402	0.402	0.394	0.394	0.402	0.402	0.394
WP in B Horizon [%]	0.162	0.162	0.215	0.162	0.162	0.109	0.109	0.162	0.162	0.109
FC in B Horizon [%]	0.285	0.285	0.332	0.285	0.285	0.213	0.213	0.285	0.285	0.213

3.5.1.6 Albedo and Rooting Depth

Surface albedo determines the proportion of incident solar radiation reflected by the Earth's surface and, thus, the amount of energy available for heating the ground and lower atmosphere as well as for evaporating water (Rowe, 1991). ACRU accounts for seasonal variations using mean monthly Albedo

values for each land cover class. Monthly albedo values were obtained from literature (Ahrens, 2007; Brutsaert, 1988; Gerrard, 1990; Pomeroy and Dion, 1996) and parameterized in the ACRU model (Table 3.4). In order account for the changes of albedo during periods of snow cover, albedo values are modified daily. Following a day of snowfall over 1 cm, albedo values are increased to 0.80, and during days without snowfall but with remaining snow cover, values are decreased by 1.5% d^{-1} to simulate the accumulation of dust and the metamorphosis of snow, until values reach a minimum snow albedo value of 0.60. Once the snow depth declines to 75 mm, albedo is set to decrease based on a dynamic degree-day factor, as it is assumed that an increasing proportion of the land surface is snow free (Nemeth et al., 2012).

Table 3.5 Monthly albedos corresponding to land cover classes found in the CRW were parameterized in ACRU.

	Monthly Albedo											
Land cover	Jan	Feb	Mar	Apr	May	Jun	Jul	Aug	Sep	Oct	Nov	Dec
Water	0.15	0.15	0.15	0.15	0.15	0.15	0.15	0.15	0.15	0.15	0.15	0.15
Rock	0.10	0.10	0.10	0.10	0.10	0.10	0.10	0.10	0.10	0.10	0.10	0.10
Shrubland	0.19	0.19	0.19	0.20	0.21	0.22	0.24	0.24	0.24	0.19	0.19	0.19
Wetland	0.16	0.16	0.16	0.16	0.17	0.17	0.17	0.17	0.17	0.17	0.16	0.16
Herb	0.16	0.16	0.16	0.17	0.20	0.22	0.26	0.26	0.26	0.16	0.16	0.16
Grassland	0.16	0.16	0.16	0.17	0.20	0.22	0.26	0.26	0.26	0.16	0.16	0.16
Cropland Annual	0.20	0.20	0.20	0.20	0.18	0.18	0.16	0.16	0.16	0.18	0.20	0.20
Pasture, Perennial Crops	0.20	0.20	0.20	0.20	0.20	0.25	0.25	0.25	0.25	0.20	0.20	0.25
Coniferous Dense	0.20	0.20	0.20	0.19	0.18	0.16	0.15	0.15	0.16	0.16	0.18	0.20
Coniferous Open	0.18	0.18	0.18	0.18	0.19	0.19	0.21	0.21	0.21	0.16	0.17	0.18
Broadleaf Dense	0.12	0.12	0.12	0.12	0.14	0.16	0.16	0.16	0.16	0.14	0.12	0.12

The rooting characteristics of plants determine the amount of water that can be accessed for plant growth and development. In ACRU, the effective rooting depth is a function of the overall depth of the A and B horizons. It also considers the proportion of the active root mass distribution within each horizon that extracts water from the soil (Schulze, 1995). Model inputs for rooting depths for each land cover type are taken from the literature (Canadell et al., 1996; Jackson et al., 1996; Strong and Roi, 1983) and applied to the CRW.

3.5.1.7 Plant Transpiration Coefficients

Currently, estimates of plant water use for vegetation in the CRW have not been made available in the literature and it is assumed that none exist. Consequently, plant transpiration coefficients (PTCs) applied in the CRW were taken from a study performed by Nemeth (2010), which focused on the verification of the ACRU model in a multi variable analysis of hydrological processes in the UNSRB in Alberta, Canada. Nemeth (2010) calculated PTC values, the equivalent to crop coefficients, corresponding to the most prevalent land cover classes found in the UNSRB using observed meteorological and flux net data from locations in Alberta and Saskatchewan, Canada and the State of Colorado in the United States. A minor correction factor (0.15) was applied as a result of an increase in soil moisture between the semi-arid southern Albertan climate and the UNSRB mountain region. Where observations for certain vegetated land covers did not exist (e.g. Shrubland, Annual Cropland, Perennial Cropland and Pasture and Wetland) monthly averages of available PTCs from Nemeth (2010) were combined. For example, Shrubland PTCs were calculated using a weighted percentage of grassland (60%) and broadleaf stands (40%), cropland was calculated following the method described in Hobbs and Krogman (1983), where for annual cropland monthly averages of prevalent Alberta crop types (wheat, barley and alfalfa) were used. A combination of alfalfa and grassland were used for perennial crops and pasture. Wetland PTCs were calculated from wetland and grassland values derived from Read et al (2008). Since the UNSRB and CRW are both Rocky Mountain headwater regions exhibiting general similarities in land cover, topography and climate, PTC values were kept relatively the same between study areas. Among the few minor changes made to PTCs between the UNSRB and the CRW include the assignment of a PTC value of zero to all vegetated land cover classes for the months Dec-Mar. This was done primarily as a result of a generally cold winter period where plant-water use is either negligibly minimal or non-existent. Aside from transpiration from plants, any evaporation that may take place during cold winter months is accounted for in ACRU through the application of the Penman-Monteith evaporation method. A methodology containing the calculation of PTCs used in this study can be found in Nemeth et al (2012). A list of PTC values as parameterized in the ACRU model and applied to the CRW can be seen in Table 3.5.

Table 3.6 Plant Transpiration Coefficients used in ACRU for vegetated land covers in the CRW

	Monthly Plant Transpiration Coefficients											
Land cover	Jan	Feb	Mar	Apr	May	Jun	Jul	Aug	Sep	Oct	Nov	Dec
Shrubland	0.00	0.00	0.00	0.09	0.29	0.50	0.51	0.43	0.28	0.08	0.06	0.00
Wetland	0.00	0.00	0.00	0.23	0.39	0.55	0.47	0.46	0.31	0.20	0.17	0.00
Herb	0.00	0.00	0.00	0.08	0.32	0.40	0.28	0.21	0.07	0.04	0.02	0.00
Grassland	0.00	0.00	0.00	0.08	0.32	0.40	0.28	0.21	0.07	0.04	0.02	0.00
Cropland - Annual	0.00	0.00	0.00	0.34	0.44	0.97	1.14	0.53	0.31	0.07	0.04	0.00
Pasture, Perennial Crops	0.00	0.00	0.00	0.10	0.59	0.81	0.76	0.64	0.58	0.06	0.01	0.00
Coniferous Dense	0.00	0.00	0.00	0.30	0.51	0.63	0.69	0.68	0.35	0.29	0.20	0.00
Coniferous Open	0.00	0.00	0.00	0.23	0.38	0.47	0.52	0.51	0.26	0.22	0.15	0.00
Broadleaf Dense	0.00	0.00	0.00	0.11	0.23	0.64	0.86	0.76	0.59	0.14	0.12	0.00

3.5.1.8 Forest Canopy Coverage and Leaf Area Index

Vegetation plays a dynamic role in the plant soil water evaporation process (Schulze, 1995). In ACRU, vegetation and land use processes are grouped into three classes: above-ground factors, surface factors and below-ground factors. Canopy interception losses are categorized as an above-ground factor. Interception is the process by which precipitation is caught by the vegetation canopy, stored on the canopy surface as interception storage and then evaporated, thus being effectively excluded from precipitation input into the watershed. Interception loss is used to calculate the difference between gross and net precipitation.

In ACRU, intercepted water stored on the plant canopy from a previous day's rainfall is evaporated back to the atmosphere using up the energy available from the reference potential evaporation. This is done before the remaining evaporation is used in ET processes (Schulze, 1995). Evaporation rates of stored water in wet forest canopies have been found to increase because of advection (Calder, 1982) and low aerodynamic resistances (Rutter, 1967). Evaporation rates applied in ACRU are found in the literature (Calder, 1982; Holmes and Wronski, 1981).

ACRU simulates wet canopy evaporation at an enhanced rate for forested HRUs. An HRU is classified as forested only when the forested area of the HRU is greater than 50%. In the CRW, forested HRUs exhibiting >50% forest cover were identified through the use of GIS. The forested HRUs are also

parameterized by way of an additional variable that accounts for interception on the canopy (ICC). These variables are based on available mean monthly LAI data which defines the planimetric area of the plant (forest canopy) to the soil surface area. Recent model development, as mentioned in section 2.4, adds a snow interception routine which accounts for the capacity of snow volume that is intercepted (SNCAPI) and is assumed to be sublimated back into the atmosphere. In the CRW, the forested areas are made up of several dominant conifer and broadleaf species. These are mentioned in more detail in section 4.2.4. Values for snow interception capacity were taken from the literature (Bunnell et al., 1985; Hedstrom and Pomeroy, 1998; Pomeroy et al., 1998; Schmidt and Gluns, 1991); for sites in British Columbia and Saskatchewan, Canada, as well as for locations in the State of Colorado, in the United States.

ACRU uses LAI to simulate changes in plant evaporation, soil water evaporation and canopy interception. The latter is estimated using the Von Hoyningen-Huene method (Schulze, 1995). LAI data were obtained from MODIS (Moderate Resolution Imaging Spectroradiometer) satellite images, downloaded from the National Snow and Ice Data Center (NSIDC) for the year 2004 (NSIDC, 2009). The data are originally based on the UNSRB study area but due to similarities between the land cover in the UNSRB and CRW, derived LAI values were translated across river basins. Since the land cover class “Herb” was not present in the UNSRB, and Herb canopy cover was reported to be 20% of grassland land cover, Herb LAI values were derived from grassland land cover values divided by 5.

The 2004-year was chosen as a suitable year for LAI data because the 2004 mean annual temperature was almost identical to the mean annual temperature of the baseline period 1961–1990 used by Nemeth et al. (2012). When prepared for the UNSRB study area, mean monthly LAI values were calculated in a GIS using a generalized land cover file. Values for December and January were adjusted to create a smooth distribution to better reflect plant phenology during winter months. Mean monthly LAI values as parameterized in ACRU and applied to the CRW are presented in Figure 3.4.

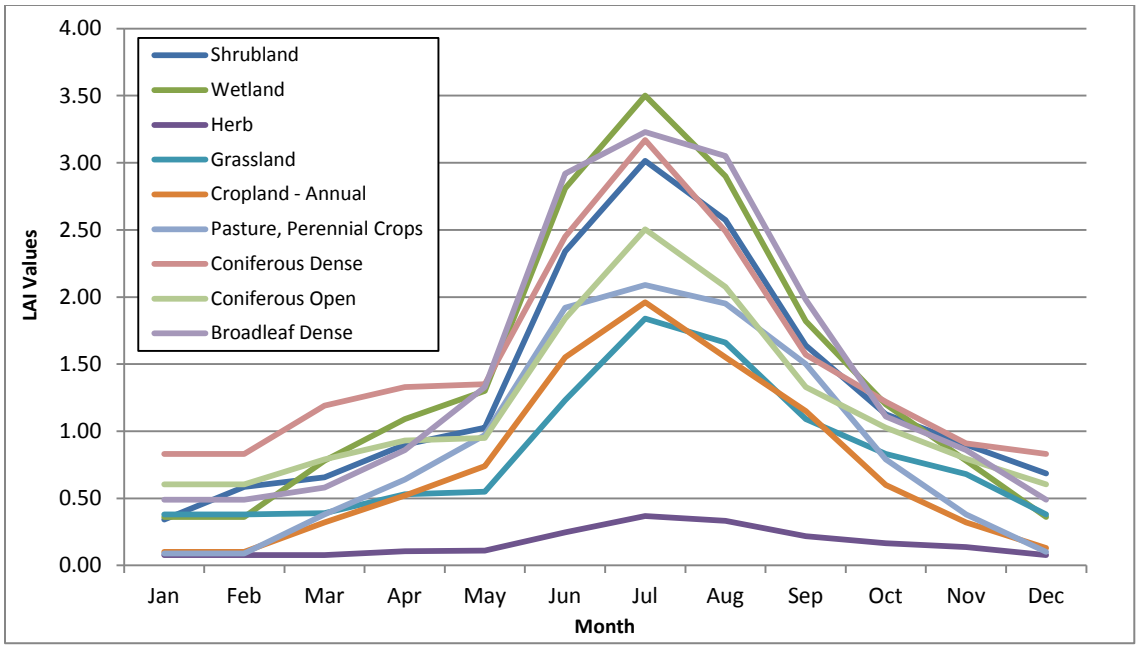

Figure 3.5 Adjusted LAI values according to land cover classes found in the CRW. LAI values were derived from monthly MODIS images (data taken with permission from Nemeth, 2010).

3.5.1.9 Streamflow

The simulation of streamflow in ACRU is accomplished through the parameterization of several streamflow related variables and by linking principles of the modified Soil Conservation Service (SCS) technique with a two-layer soil water budget to generate stormflow (Schulze, 1995). Streamflow is simulated as a summation of stormflow and baseflow. Stormflow consists of a quickflow response (QFRESP) comprised of both same day and delayed quickflow, while baseflow, expressed as a coefficient of baseflow response (COFRU), consists of delayed flows that have percolated through the various soil horizons into the intermediate or groundwater zones eventually being released into the streams or rivers in a watershed (Schulze, 1995). These parameters are dependent on the mean slope of an HRU, as it is hypothesized that a steep slope is associated with higher quickflow and baseflow responses than a HRU characterized by a flat slope.

Daily streamflow data from two hydrometric gauges within the CRW were obtained Environment Canada (2012c) http://wateroffice.ec.gc.ca/search/search_e.html?sType=h2oArc and used to validate the

simulated streamflows at the two corresponding HRUs. When a precipitation event takes place in the CRW a coefficient of initial abstraction (COIAM) accounts for initial infiltration, interception, or surface storage in hollows before stormflow begins (Schulze, 1995). Values used for COIAM depend largely on land cover. For instance, a value of 0.2 (20%) will typically be used for urban/semi-urban areas, 0.05 for arid areas or in conditions of frozen soils and 0.3 for afforested conditions or when the ploughing of lands take place (Schulze, 1995). The coefficients of initial abstraction parameterized in the CRW are shown in Table 3.6. ACRU also accounts for antecedent soil water conditions during the generation of stormflow processes. The effective soil depth at which this takes place is specified depending on the basin climate, soil condition, or land cover. In the CRW, these values were set to the depth of the A horizon.

Table 3.7 Monthly coefficients of initial abstraction pertaining to land cover in the CRW

	Monthly Coefficients of Initial Abstraction											
Land cover	Jan	Feb	Mar	Apr	May	Jun	Jul	Aug	Sep	Oct	Nov	Dec
Shrubland	0.00	0.00	0.00	0.00	0.00	0.00	0.00	0.00	0.00	0.00	0.00	0.00
Wetland	0.00	0.00	0.00	0.00	0.00	0.00	0.00	0.00	0.00	0.00	0.00	0.00
Herb	0.05	0.05	0.06	0.07	0.08	0.08	0.08	0.08	0.08	0.08	0.08	0.06
Grassland	0.05	0.05	0.08	0.15	0.20	0.20	0.20	0.20	0.20	0.20	0.20	0.08
Cropland - Annual	0.05	0.05	0.08	0.15	0.20	0.20	0.20	0.20	0.20	0.20	0.20	0.08
Pasture, Perennial Crops	0.05	0.05	0.08	0.15	0.20	0.20	0.20	0.20	0.20	0.20	0.20	0.08
Coniferous Dense	0.05	0.05	0.08	0.20	0.30	0.30	0.30	0.30	0.30	0.30	0.30	0.08
Coniferous Open	0.05	0.05	0.08	0.18	0.25	0.25	0.25	0.25	0.25	0.25	0.25	0.08
Broadleaf Dense	0.05	0.05	0.08	0.20	0.30	0.30	0.30	0.30	0.30	0.30	0.30	0.08

Chapter 4: Model Verification

4.1 Verification of Hydrological Processes

Simulation models provide us with the ability to make predictions about reality (Kleijnen, 1995; Robinson, 1997; Sargent, 2005). In hydrological modelling, these predictions affect the decisions end users make based on a number of water management planning issues (Klemeš , 1986), including, inter alia, streamflow runoff potential, timing and magnitude of runoff events, flood estimation, reservoir operation, agriculture, fisheries management and various human water needs throughout each year (Dettinger and Cayan, 1995). ACRU has been verified extensively for use in a number of different applications in many climates throughout the world (Jewitt and Schulze, 1999; Jewitt et al., 2004; Kienzle et al., 1997; Kienzle et al., 2012; Kienzle and Schmidt, 2008; Martinez et al., 2008). For example, ACRU was recently used in a multi-variable analysis where all elements of the hydrological cycle were simulated and variables such as temperature, SWE, glacier mass balance, potential evapotranspiration and streamflow were verified for the purpose of predicting the impacts of climate change in the headwaters of the UNSRB (Nemeth et al., 2012).

In the CRW, simulation results were compared with observed time series of temperature, snowpack and streamflow. Since streamflow is derived by regional precipitation patterns, it is important to verify hydrological variables in an order that makes sense from a hydrological standpoint. As such, temperature is verified first as it influences, inter alia, the separation of precipitation into rain and snow, the timing of snowmelt processes, and rates of sublimation and ET (Kienzle, 2013, 2011). Since the development of snowpack and timing of snowmelt processes are largely dependent on near surface temperatures, SWE will become the second element of the modelling process that is verified. In Alberta, snowpack is known to be the major source of a large quantity of fresh water to downstream communities. For example, Balk and Elder (2000) and Mote et al.(2008), report snowmelt runoff from mountainous regions in the western United States accounts for approximately 70-75% of the annual streamflow that maintains flow volumes throughout warm summer periods. As such, streamflow will be verified last and will include the comparison of observed and simulated streamflow using various model evaluation

statistics including linear regression, Nash-Sutcliffe coefficient of efficiency (NSE) (Nash and Sutcliffe, 1970) and various graphical techniques as explained by Legates and McCabe (1999) and Moriasi et al. (2007) including hydrographs. In general, these statistical and graphical techniques provide an evaluation of certain aspects of model simulation, including how well simulated data match measured data in terms of, inter alia, the timing and magnitude of peak flows and shape of the recession curve.

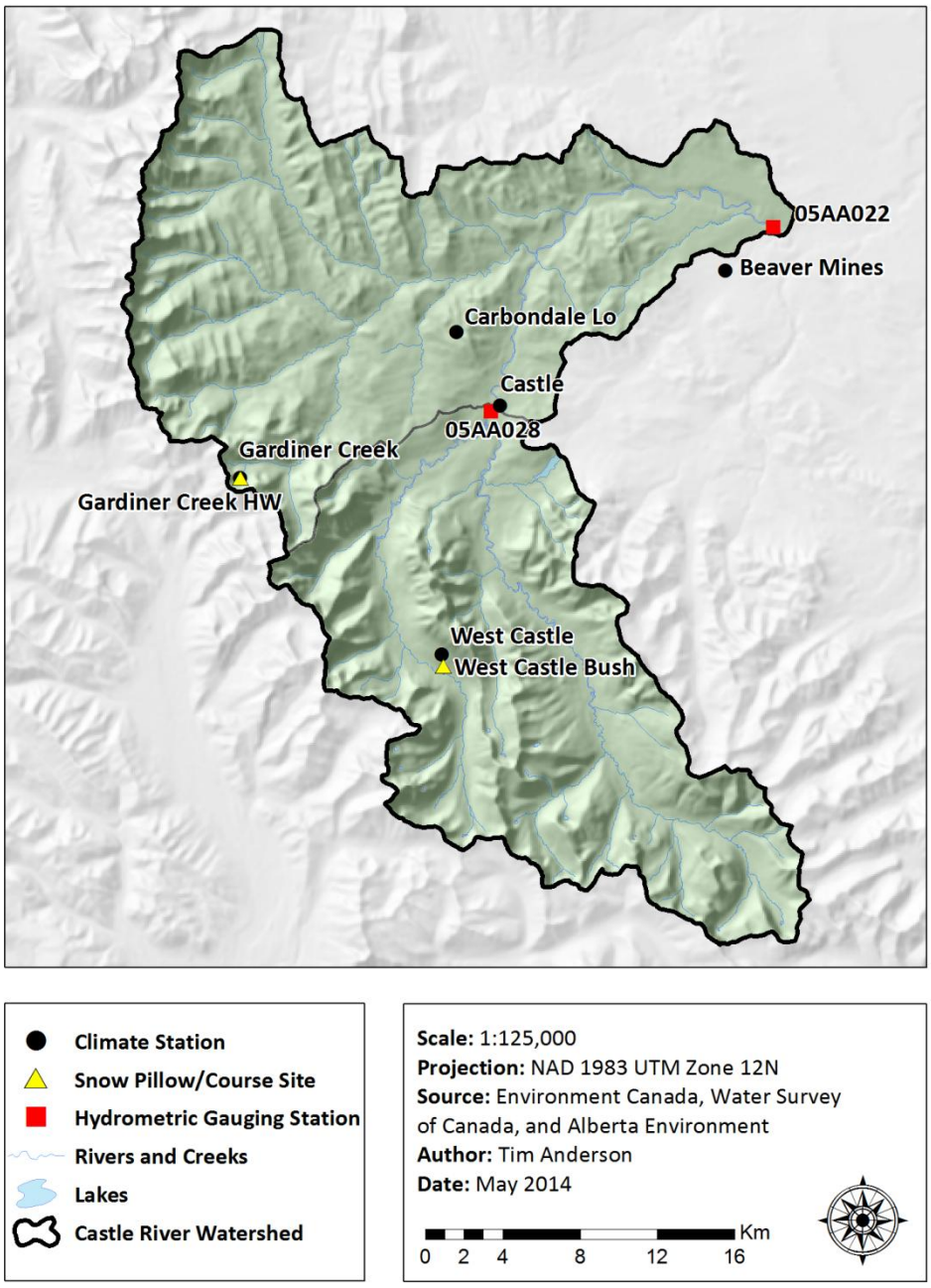

Figure 4.1 A map of the study area showing the location of climate stations, streamflow gauge stations and snowpack measuring sites. The climate station identifiers correspond to Table 4.1, the snowpack identifiers correspond to Table 4.3 and the streamflow gauge

4.1.1 Verification of Temperature

Daily observations of mean temperature from four Environment Canada climate stations were collected and used for temperature verification of the ACRU model in the CRW (see Table 4.1). Table 4.2

lists the original twenty 10 x 10 km grids that were merged together to create the nine areal features labelled “A” to “I”. An illustration of the merged grids is depicted in Figure 3.3. The seasonality of the Environment Canada and 10 km Grid stations is plotted in Figure 4.2. Temperature calibration requires an analysis of comparing simulated and observed monthly Tmin and Tmax where adiabatic lapse rates are adjusted to correct for temperature change with increasing altitude. Adiabatic lapse rates were kept within meaningful ranges for mountain environments, following ranges reported in the literature (Blandford et al., 2008; Bolstad et al., 1998; Pielke and Mehring, 1977; Pigeon and Jiskoot, 2008; Rolland, 2003), until the line of best fit between simulated and observed temperature is achieved. Lapse rates used in the CRW are shown in Figure 4.3. Photographs of two out of the four Environment Canada stations are shown in Figure 4.4. The four climate stations listed in Figure 4.1 are seasonal in that they record temperature during the spring through autumn seasons. Given the seasonal nature of an inhomogeneous record of observations, these climate stations are not suited for use as base stations but work well in verification analysis such as is required here.

Table 4.1 Climate stations used for hydrological simulation and temperature [°C] verification in the CRW

Station Name	Station ID	Latitude	Longitude	Elevation (m.a.s.l.)	Observed Time Period	N (days)
Carbondale Lo	3051310	49.4300	-114.3700	1798	1965-1990, 2001-2003	3427
Castle	3051430	49.4000	-114.3400	1360	1962-1976, 1989-2003	6784
Gardiner Creek	305B769	49.3611	-114.5158	1920	1998-2003	1730
West Castle	3057K55	49.2833	-114.3667	1524	1999-2003	1382

Table 4.2. A list of the interpolated climate stations of daily Tmax [°C], Tmin [°C] and precipitation [mm]. Twenty 10 km Grids were merged into nine, each being assigned a letter “A” to “I”. Climate data are available for the period 1950-2010, which equates to 16,071 days.

Station Name	Station ID	Latitude	Longitude	Mean Elevation [m.a.s.l.]
A	47559	49.5000	-114.5085	1728
A1*	47162	49.5867	-114.5429	1739
A2*	47558	49.4779	-114.6429	1942
B	47949	49.4133	-114.4743	1648
B1*	47948	49.3912	-114.6085	1870
B2*	48340	49.3045	-114.5741	1736
C	47950	49.4353	-114.3400	1466
C1*	47560	49.5221	-114.3740	1587
D	47951	49.4572	-114.2056	1377
D1*	47561	49.5439	-114.2394	1308
D2*	47562	49.5656	-114.1047	1192
D3*	47952	49.4788	-114.0711	1237
E	48341	49.3266	-114.4402	1862
F	48342	49.3486	-114.3062	1671
G	48736	49.2399	-114.4062	1895
G1*	49128	49.1531	-114.3724	1825
H	48737	49.2618	-114.2724	1878
H1*	48738	49.2836	-114.1385	1937
I	49130	49.1967	-114.1051	2053
I1*	49129	49.1750	-114.2388	1885

* Indicates a grid that was merged into grids A-I

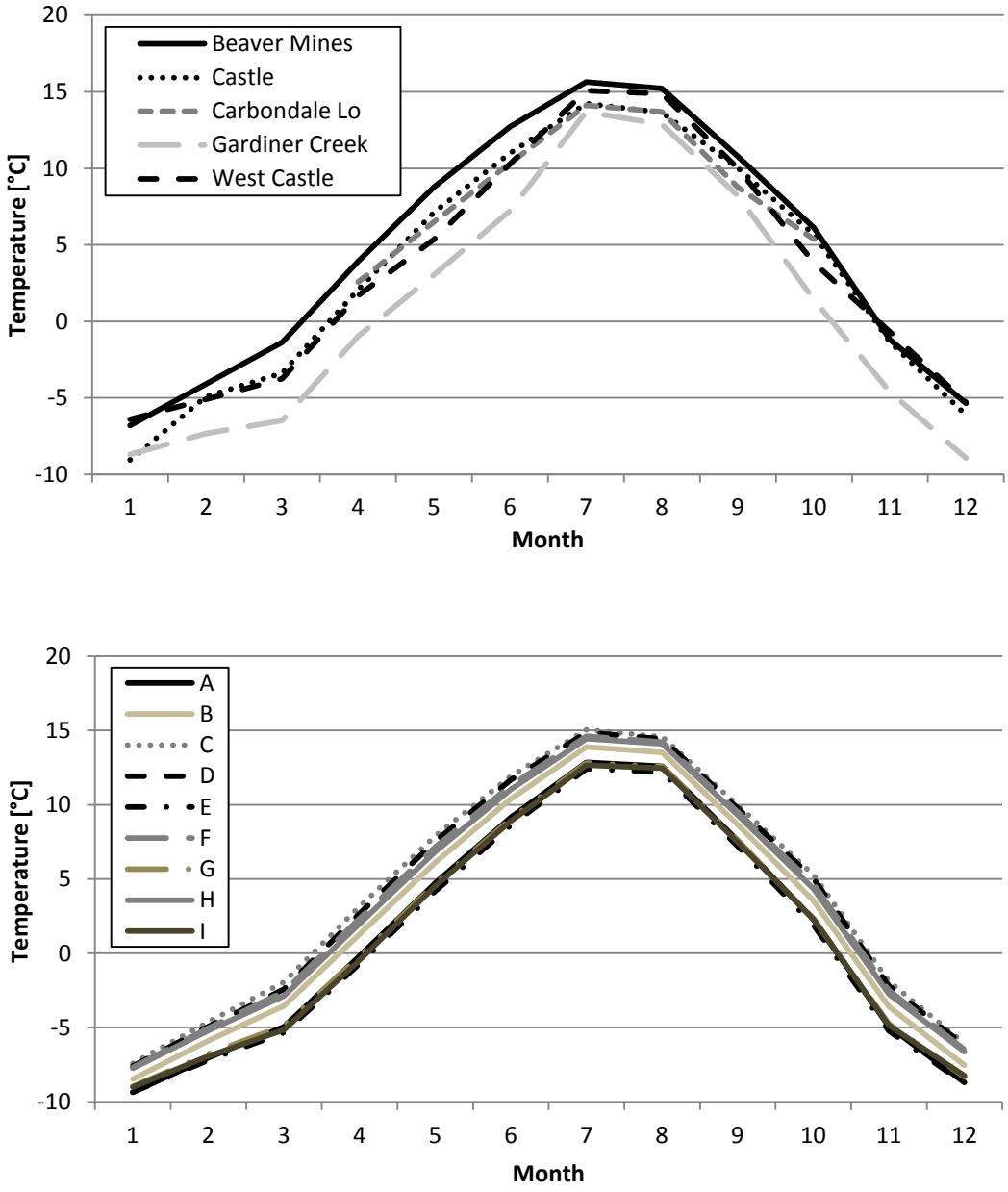

Figure 4.2 Mean monthly temperature [°C] from climate stations used for temperature simulation and verification in the CRW from 1960-2009. Environment Canada stations (top) and stations "A" to "I" from the 10 km gridded dataset (bottom) respectively.

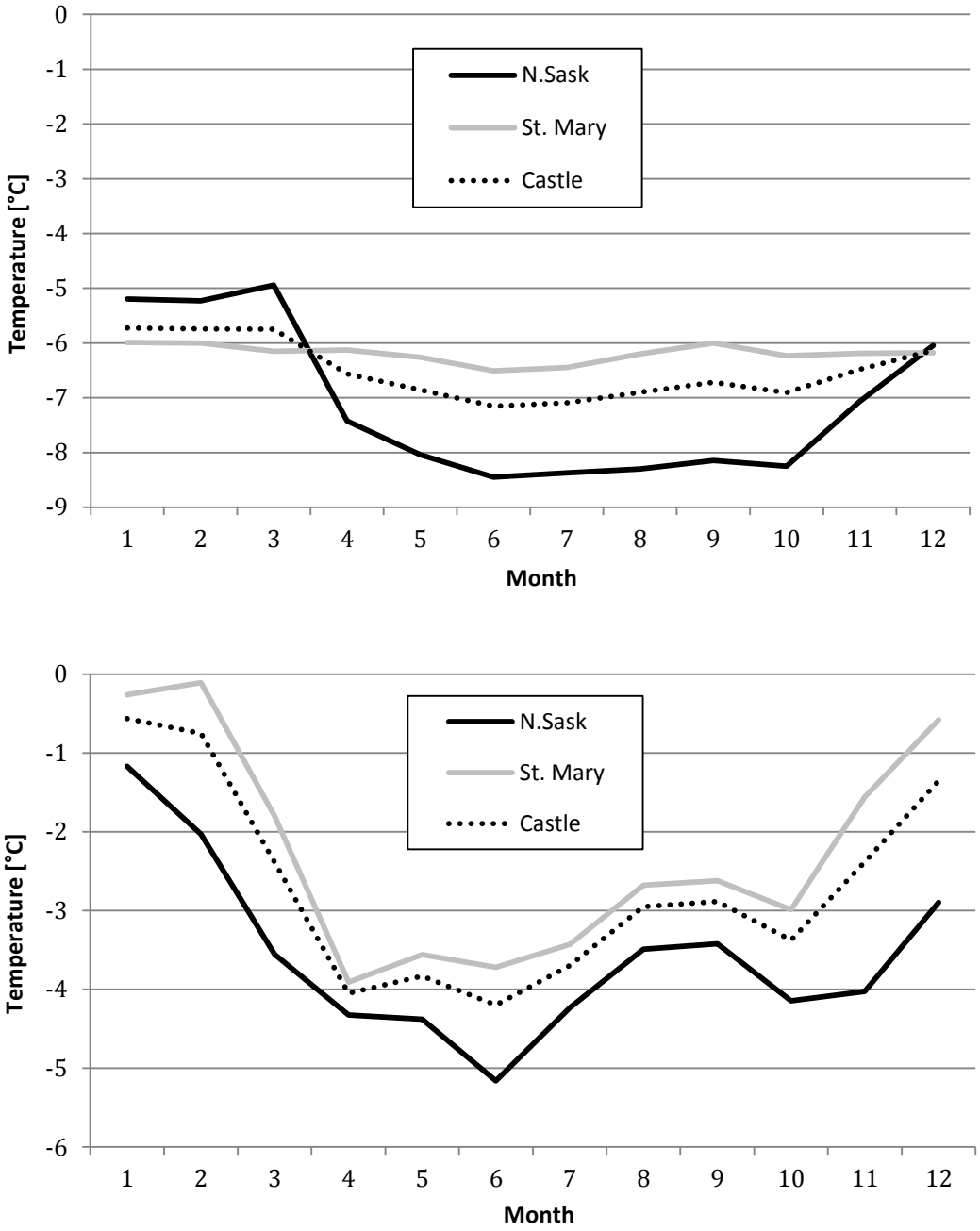

Figure 4.3 Regional mean monthly lapse rates of Tmax [°C] (top) and Tmin [°C] (bottom) for the UNSRB, SMRW, and CRW.

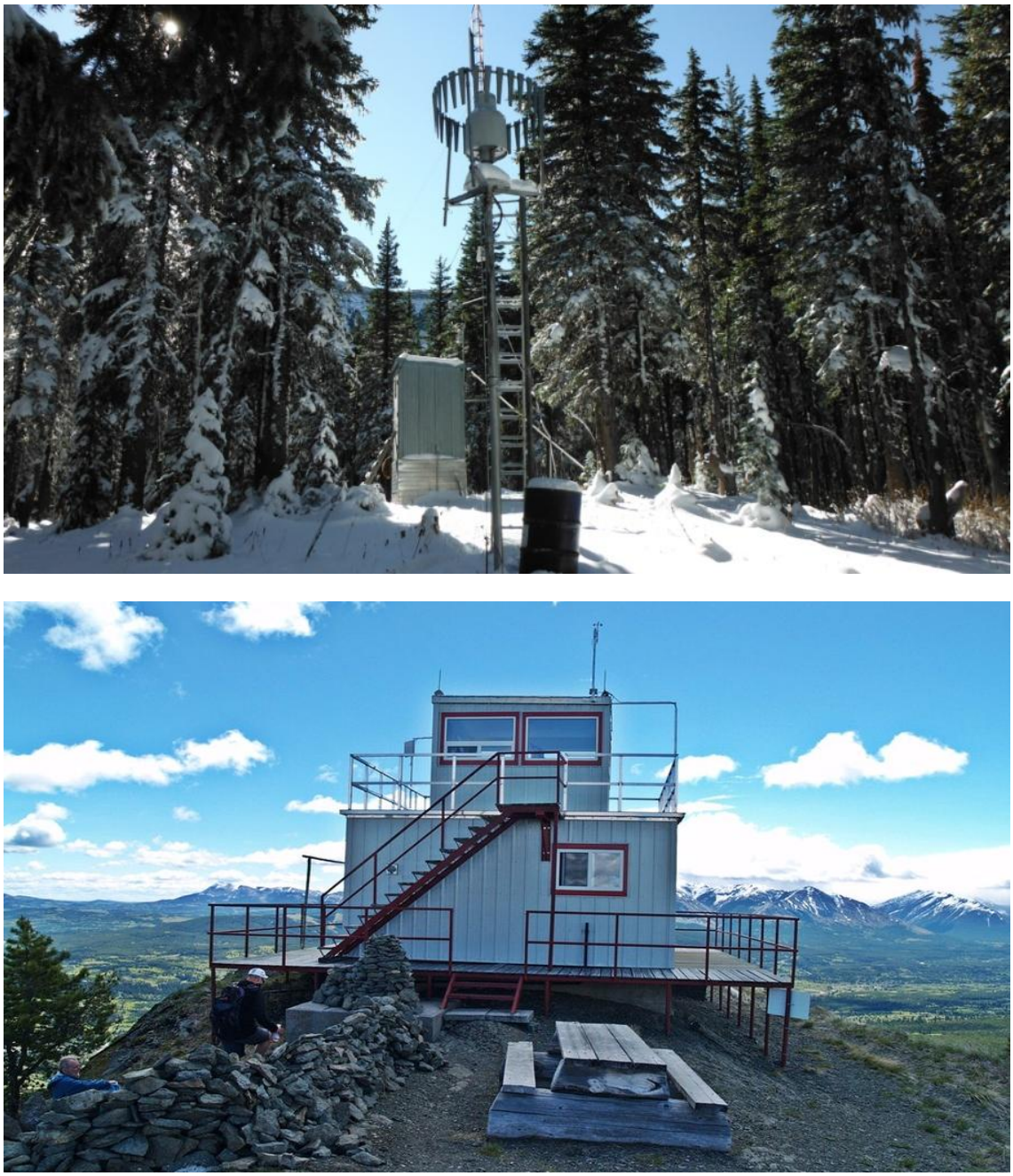

Figure 4.4 Climate stations in the CRW. Gardiner Creek Climate Station (top) Carbondale Lookout Station situated on Carbondale Hill (bottom). Photographs by Alberta Agriculture and Rural Development (2012b) (top) and courtesy of John Reid (bottom).

4.1.2 Verification of SWE

In Alberta, snow data collection combines both manual (snow course survey) and automated (snow pillow) methods following standards set by the Meteorological Service of Canada (MSC) and the

United States Geological Survey (USGS). This includes the standard practices of equipment installation and configuration (Minke, 2014, personal communication). Snow pillows are installed similar to the SnoTel sites operated by Natural Resource Conservation Service (NRCS) in the United States (Minke, 2014, personal communication). Some monitoring stations use both manual and automated data collection methods which helps ensure the data are verifiable (Alberta Environment, 2009). Snow data for two sites in the CRW were made available by Alberta Environment and Sustainable Resource Development (AESRD) and are listed in Table 4.3.

Table 4.3 Snowpack stations used for SWE [mm] verification in the CRW

Station Name	Station ID	Latitude	Longitude	Elevation [m.a.s.l.]	Observed Time Period	n
Gardiner Creek HW (snow pillow)	05AA809	49.3611	-114.5158	1920	1984-2010	6564
Gardiner Creek HW (snow course)	05AA809	49.3611	-114.5158	1920	1983-2003	133
West Castle Bush (snow course)	05AA801	49.2781	-114.3656	1524	1970-2010	126

Snow pillows measure SWE by use of circular or octagonal membranes filled with liquid that has a low freezing point. The weight of snow on the pillow controls the pressure of the liquid, which is recorded or measured via a manometer or pressure transducer (Dingman, 2002). Often times a pressure sensor can produce errors due to the difference between thermal properties of the sensor, the ground under the sensor and of the surrounding ground around the sensor (Johnson and Marks, 2004). Thus, melting and freezing of the snowpack resulting from these thermal inconsistencies can cause snow shear to either bridge the sensor causing under-measurement, or to transfer the snow load from the surrounding snow cover to the sensor causing over-measurement (Johnson and Marks, 2004). Snow pillow and snow course data were plotted in Figure 4.5 to potentially identify years where errors may exist.

The Gardiner Creek HW snow pillow and snow course measurements are made on a daily (snow pillow) and monthly (snow course) basis. The snow pillow site has been built in a location of partial forest cover of alpine fir and has been set up in direct proximity to the Gardiner Creek Climate Station (305B769) (Campbell, 2014, personal communication) (See Figure 4.2). The snow course is located in an adjacent forest clearing measuring approximately 20 m x 50 m with SWE survey points following the perimeter of the clearing (Campbell, 2014, personal communication). The second snowpack site is at West Castle Bush and is located in close but not direct proximity to the West Castle Climate Station (3057K55) maintained by Environment Canada. The snow course follows a linear (~200 m) path where the first 100 m consists of partial forest cover (~50%) and the last 100 m consists of open area (Campbell, 2014, personal communication).

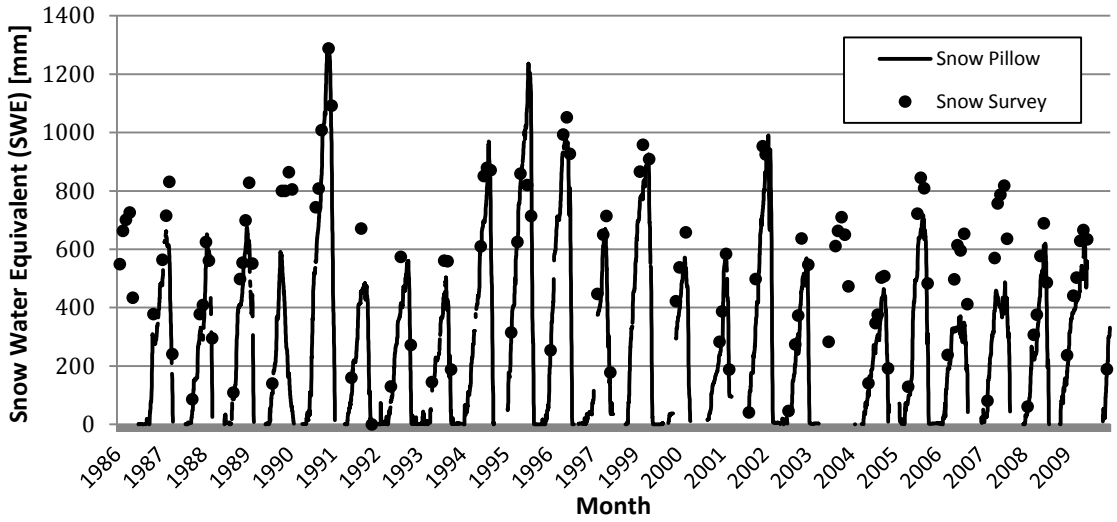

Figure 4.5 Gardiner Creek HW snow data representing the manual and automated methods of measurement for the years 1986-2010.

Figure 4.6 Gardiner Creek Climate Station and site for snow pillow and nearby snow course. Photograph by Alberta Agriculture and Rural Development (2012b).

4.1.3 Verification of Streamflow

In the CRW, hydrometric gauges are maintained by Environment Canada through the Water Survey of Canada monitoring agency measuring daily discharge ($m^3 s^{-1}$) at two locations along the Castle River (Figure 4.1, Table 4.4). Observations of historical streamflow are available in near real-time or in an archived format and can be downloaded from Environment Canada (2014).

Table 4.4 Hydrometric gauge stations used in streamflow verification in the CRW

Station Name	Station ID	Latitude	Longitude	Elevation [m.a.s.l.]	Observed Time Period	Number of Observations	Drainage Area [km^2]	Operational Schedule
Castle River at Ranger Station	05AA028	49.3992	-114.3388	1339	1967-2010	10994	375	Seasonal
Castle River near Beaver Mines	05AA022	49.4886	-114.1442	1191	1961-2010	18262	821	Continuous

The Castle River and its tributaries are all natural rivers (rivers with no upstream dams or diversions) so that the flow volumes observed can be used directly in the model. Hydrographs depicting the mean annual and monthly flows of the Castle River at the two gauge locations are depicted in Figure 4.7. Photographs showing the gauges are shown in Figure 4.8.

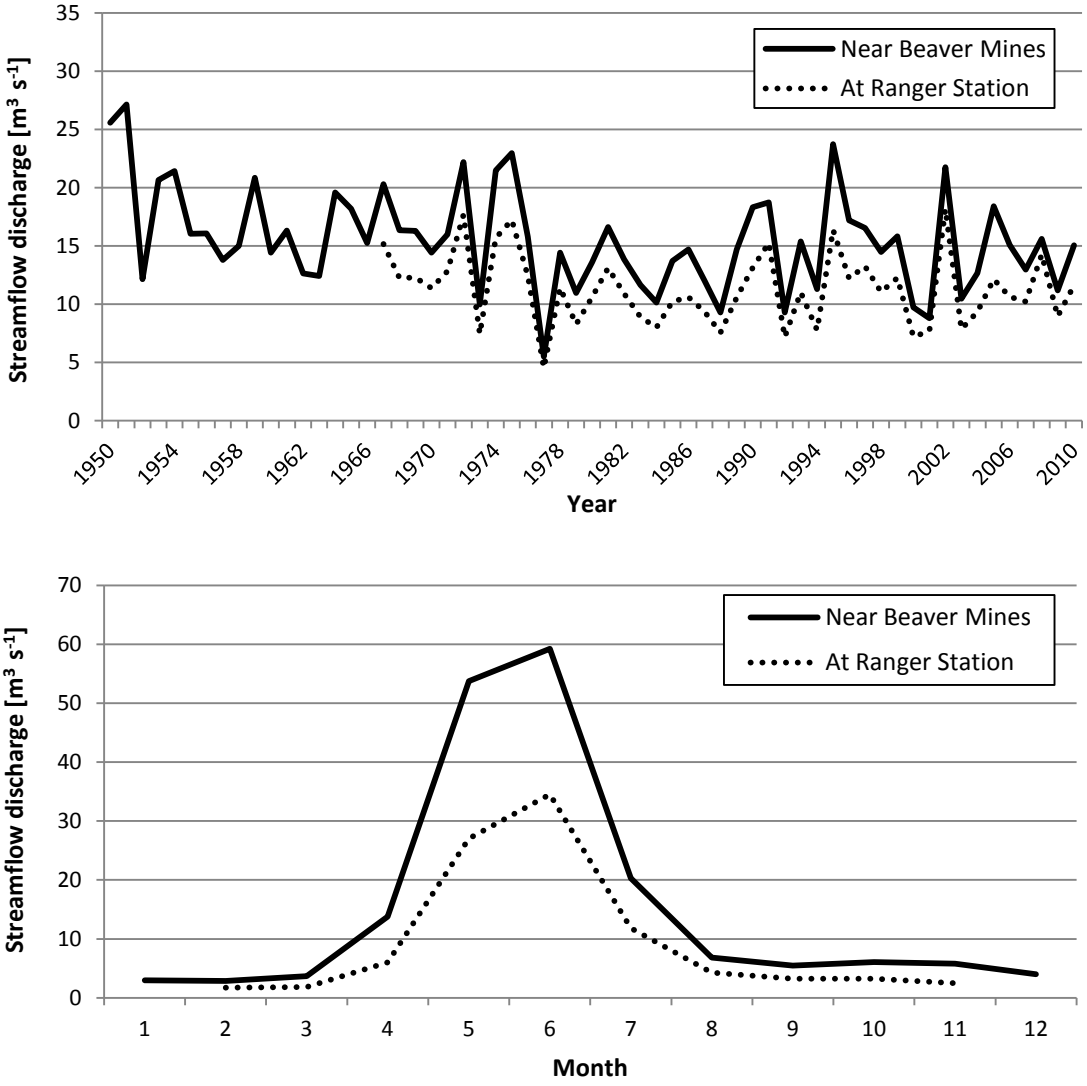

Figure 4.7 Mean (top) annual (bottom) monthly hydrographs of the Castle River measured near Beaver Mines (05AA022) and at Ranger Station (05AA028).

Figure 4.8 Hydrometric Gauges on the Castle River at Ranger Station (top) and near Beaver Mines (bottom), where streamflow conditions resemble high flow associated with the spring freshet (taken on May 28, 2008). Photographs courtesy of Environment Canada.

4.2 Verification Results: Beaver Mines Climate Station

4.2.1 Temperature

The initial run using Beaver Mines as a base station (1961-2003) yielded good results (r^2 =0.921, n=13323, y=0.9209x + 1.1079) and are shown in Figure 4.9. Results of simulated and observed mean monthly air temperature are reported in Table 4.5. As the elevation difference between the BMCS and the four temperature stations (Table 4.1) is small (103 m for the Castle, 267 m for West Castle, 541 m for Carbondale Lo and 663 m for Gardiner Creek) an adjustment of the lapse rate has only minor effect on the temperature at the verification station. If major changes were to be made to mean temperature simulations, unrealistic lapse rates would have had to been used. As a result, initial lapse rates (see Table 3.2) were used. Although over-simulation occurs during colder months, comparison of the daily (p=0.00) and monthly (p=0.00) means using a t-test reveals both are statistically the same (Table 4.5). Simulated and observed variances show a percent difference of 7.88% for daily and 9.03% for monthly means. Temperatures during warm summer months were simulated well, while temperatures during the spring and autumn seasons and into the winter months were increasingly over-simulated. Over-simulation of temperature below the freezing point is insignificant, as all precipitation falls as snow, and no snow melt occurs.

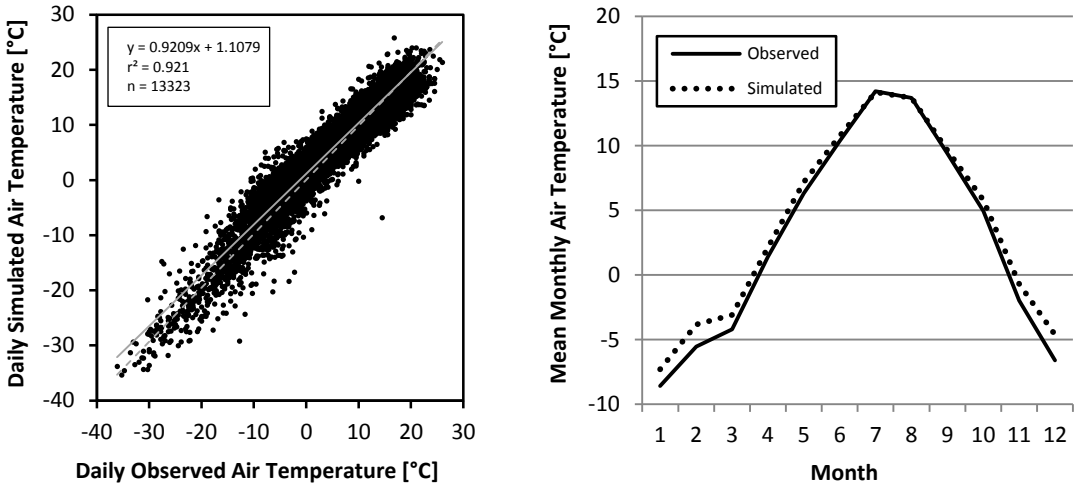

Figure 4.9 Results of model output for the BMCS. Linear regression scatterplot of daily simulated and observed air temperature [°C] (left). Mean monthly simulated and observed air temperature [°C] for four climate stations (right).

Table 4.5 Model performance for daily and monthly temperature [°C], SWE [mm] and streamflow [$m^3 s^{-1}$] data in the CRW using the Beaver Mines Base Station. Daily and monthly streamflow [$m^3 s^{-1}$] are separated into three decadal periods: 1971-1980 calibration period, 1981-1990 validation period and 1951-2010 total period.

	Temperature		SWE		Daily Streamflow			Monthly Streamflow		
	Daily	Monthly	Snow Course	Snow Pillow	1971-1980	1981-1990	1961-2010	1971-1980	1981-1990	1961-2010
Sample Size (n)	13323	331	259	6564	3653	3652	18262	120	120	600
[%] Difference of the Mean	n/a	n/a	-19.83	3.26	3.46	-9.14	5.52	3.52	-9.19	5.53
P(T<=t) two tail	0.00	0.00	0.00	0.00	0.01	0.00	0.00	0.38	0.10	0.01
[%] Difference of Variance	7.88	9.03	-8.92	3.64	-37.4	-75.61	-42.59	-24.66	-75.49	-25.23
Coefficient of Determination (r^2)	0.921	0.978	0.622	0.755	0.802	0.766	0.736	0.910	0.809	0.830
Regression Coefficient (Slope)	0.92	0.94	0.76	0.89	0.76	0.66	0.72	0.86	0.68	0.81
Regression Intercept	1.11	0.86	32.99	44.31	0.44	0.36	0.53	0.29	0.33	0.38
Nash Sutcliffe Coefficient of Efficiency	n/a	n/a	n/a	n/a	0.80	0.75	0.73	0.91	0.78	0.83
Standard Deviation	n/a	n/a	n/a	n/a	2.40	1.48	2.17	1.81	1.63	1.62

4.2.2 SWE

Modelled output was verified against data measured from one snow pillow and two snow courses from the Gardiner Creek HW and West Castle Monitoring Stations. Statistical comparisons between these observations and simulated outputs are reported in Table 4.5. Figure 4.10 shows under-estimation of SWE at Gardiner Creek HW during the 1987-1988 and 1990-1992 winter seasons. In 1988-1989, SWE is slightly under-simulated to the snow pillow while the following year (1989-1990) the under-simulation follows more closely to the snow course measurements. Simulating closer to the snow course SWE in contrast to the snow pillow also occurred from 1992-1994. In 1990-1991, the snow course and pillow are more consistent with each other verifying it as a year of higher than normal SWE, while the model significantly under estimates this year by approximately 33%.

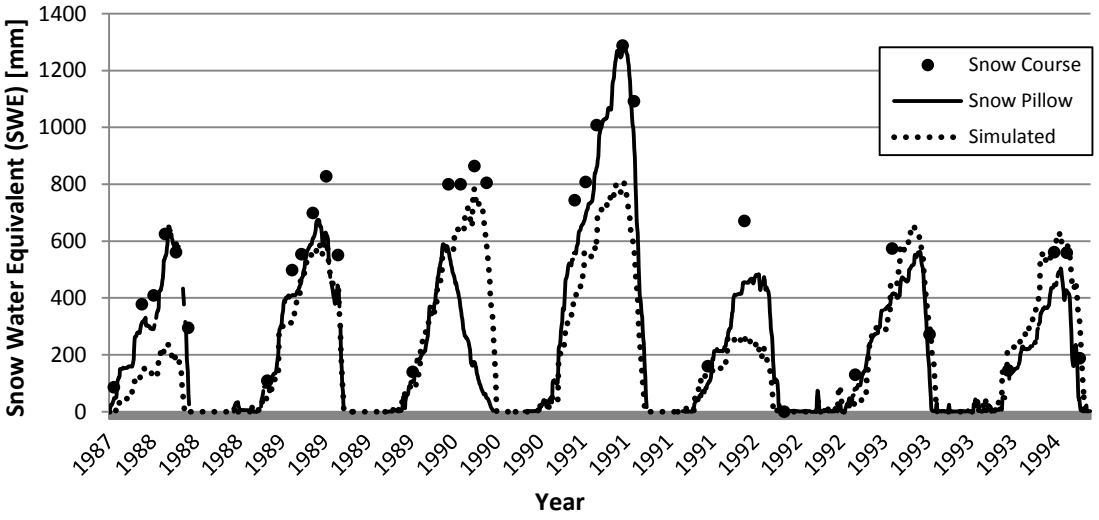

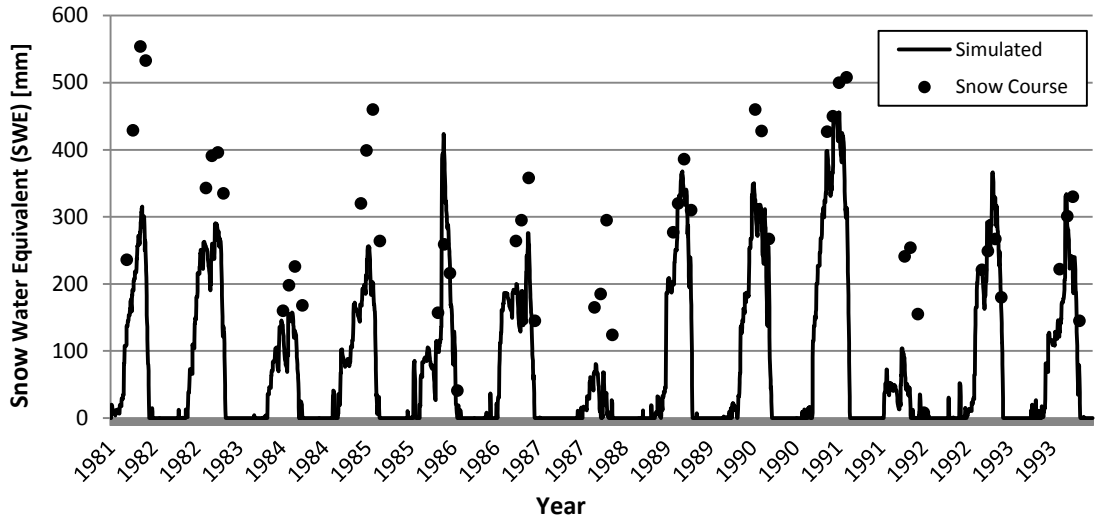

Figure 4.10 Simulated and observed SWE [mm] from snow course and pillow measurements at Gardiner Creek Monitoring Station (top) and simulated and observed SWE [mm] measured at the West Castle snow course (bottom). The BMCS was used in the production of these simulated time series.

Based on visual comparison, at West Castle Bush, two years are over-simulated (1985-1986 and 1992-1993), two years are simulated very well (1988-1989 and 1993-1994) and nine years are under simulated. Based on snow pillow measurements (daily) at Gardiner Creek HW, the model slightly over-simulates SWE over the entire historical period by approximately 3%. A comparison between all snow course measurements (monthly based data from both sites) to the simulated SWE reveals an increased difference of the means to approximately 16%, but this time as an under-simulation of overall SWE. The difference between variances is low for snow pillow (3.64%), and higher for snow course (8.92%) measurements. The coefficient of determination for snow pillow is 0.755 (n = 6564) while for the snow course it is 0.622 (n = 259).

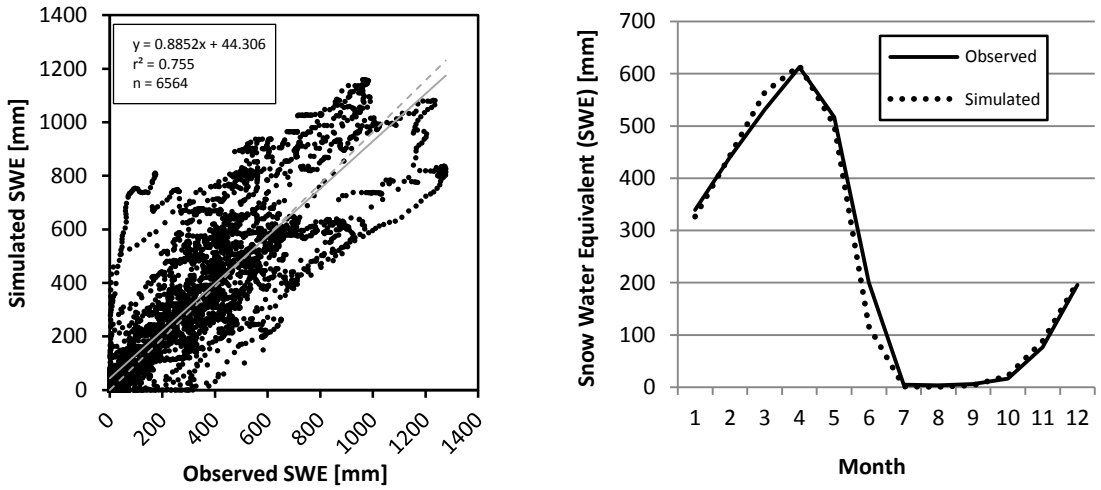

Figure 4.11 Scatter plot of daily simulated and observed SWE [mm] (left) and seasonal plot of mean monthly SWE [mm] at the Gardiner Creek HW (right).

4.2.3 Streamflow

Results comparing observed and simulated streamflow using model runs from the BMCS on daily and monthly time steps are reported in Table 4.5. Daily and mean monthly flows during the 1971-1980 calibration periods are both slightly over-simulated by approximately 3.5%. During the 1981-1990 validation period, simulated flows decrease to an under-estimated discharge of 9.14% (daily) and 9.19% (monthly). Finally, daily and monthly mean comparisons from the total simulation period of 1961-2010 revert back to an over-estimation, this time an increased result, of approximately 5.5%. P-values from two-tailed t-tests reveal that during the calibration (1971-1980), validation (1981-1990) and total simulation (1961-2010) periods, significant differences between simulated and observed means were apparent. However, a comparison of monthly means revealed no distinct difference between simulated and observed flow data except for the total simulation period (1961-2010). The use of the Beaver Mines dataset also resulted in a large spread of the data distribution where variances ranged between a 37-76% difference for daily flows and 24-76% differences for monthly flows. Other model evaluation methods included the calculation of coefficients of determination and efficiency (Nash-Sutcliffe coefficient) and standard deviation plots. Reported r^2 values for both the calibration and validation periods of daily

streamflow are 0.802 (1971-1980) and 0.766 (1981-1990). These values both increased to 0.910 and 0.809 on monthly time scales. Daily and monthly r^2 values during the total simulation period of 1961-2010 are reported at 0.736 and 0.830 respectively. The NSE for both daily (0.80) and monthly (0.91) calibrated values are measures of good fit, but decrease for the 1981-1990 validation period to 0.75 (daily) and 0.78 (monthly). The NSEs for the 1961-2010 period of record are 0.73 (daily) and 0.83 (monthly). Overall, the slope of the 1:1 line reveals a relatively similar relationship between the simulated and observed time series. Annual comparisons for the 1961-2010 period in Figure 4.12 shows the comparison of simulated and observed streamflow. During the calibration period (1971-1980), streamflow is modelled well, whereas in subsequent years, flow is generally over-simulated. A comparison of worst and best simulation years (1961-2010) including plots of standard deviation is shown in Figure 4.13. Lastly, the comparison of mean monthly simulated and observed streamflow for the 1961-2010 period is shown in Figure 4.14.

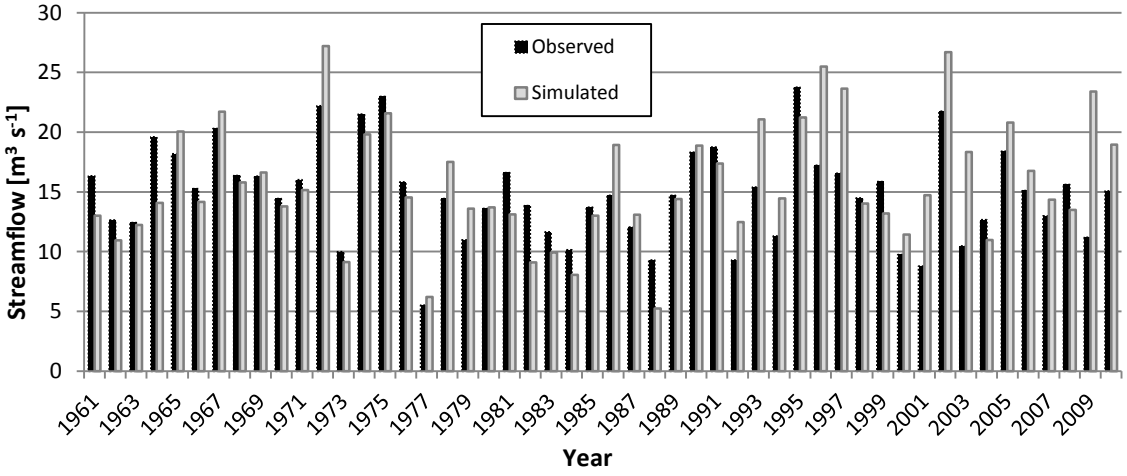

Figure 4.12 Annual hydrograph of simulated and observed streamflow [$m^3 s^{-1}$] (1961-2010) from model runs using the BMCS.

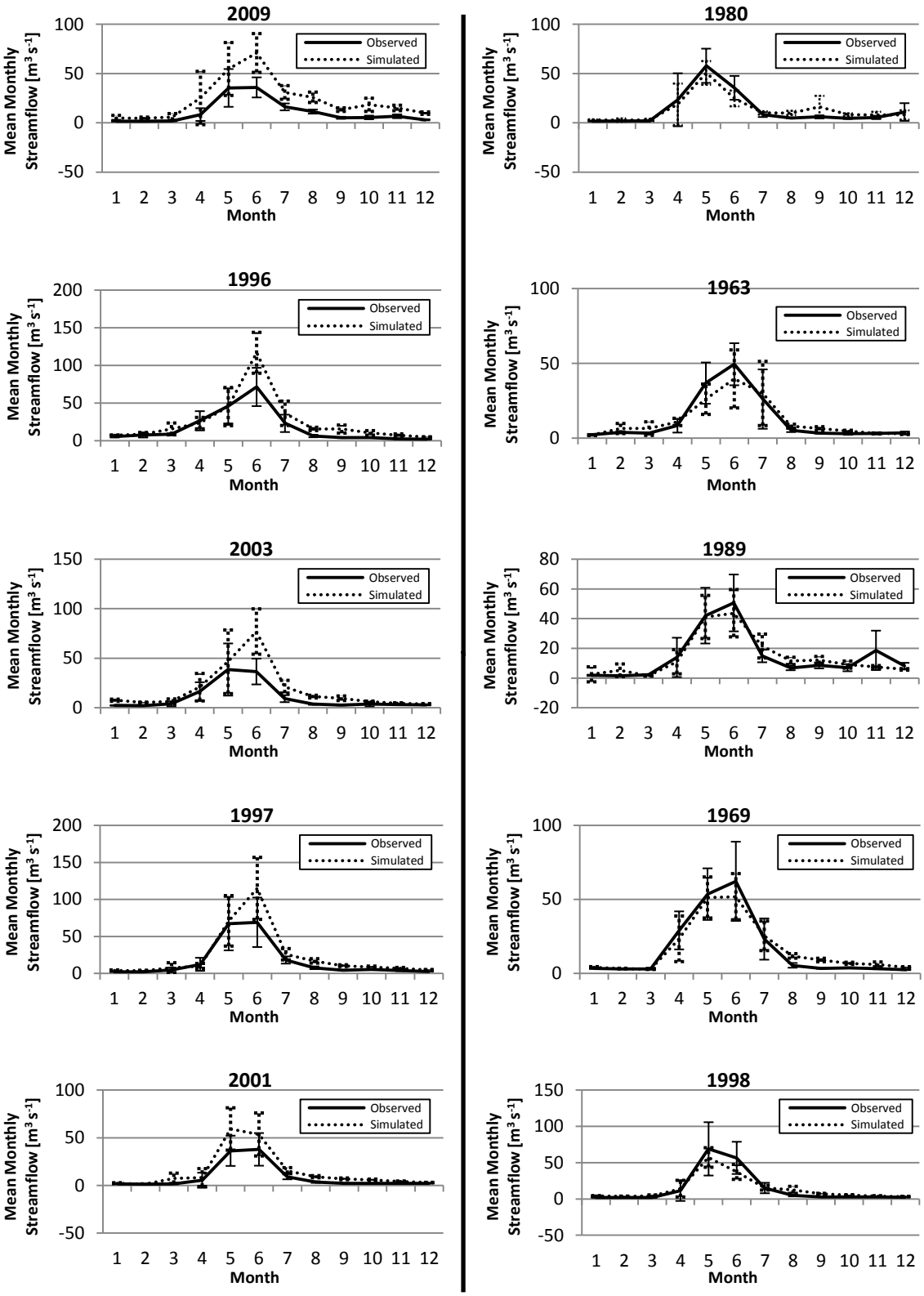

Figure 4.13 Standard deviation plots of observed and simulated streamflow [$m^3 s^{-1}$] using the BMCS model runs. Plotted are the five worst (left column) and best (right column) years in descending order.

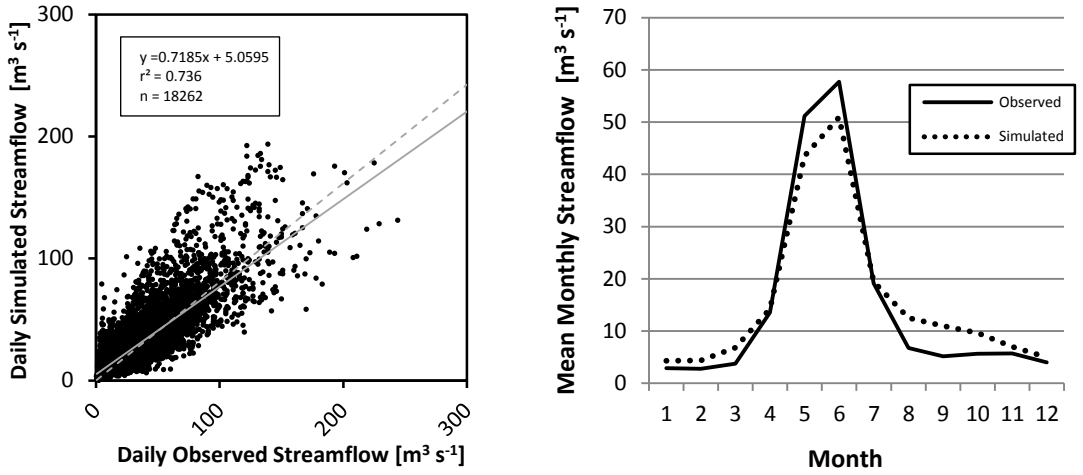

Figure 4.14 Results from Beaver Mines model output (1961-2010). Linear regression scatterplot of daily simulated and observed streamflow [$m^3 s^{-1}$] (left). Mean monthly simulated and observed streamflow [$m^3 s^{-1}$] (right).

4.3 Verification Results: 10 km Grid

4.3.1 Temperature

The first model run using this multiple station approach (1961-2003) produced excellent results (r^2 = 0.978, n=13323, y=0.9613x + 1.1035). Figure 4.15 shows a comparison of mean monthly simulated and observed temperature and a linear regression scatterplot comparing daily simulated and observed output. Lapse rates used for the 10 km Grid were the same as those used for the Beaver Mines simulation (Table 3.2 and Figure 4.3). Due to the high coefficient of determination and slope near the 1:1 line, being close to unity, further calibration was not performed. Inferential statistics for this model run are reported in Table 4.6. The Student's t-statistic for daily (p=0.00) and monthly (p=0.00) means shows confidence that, statistically speaking, the means for simulated and observed temperatures are the same. The percent difference between simulated and observed variances of daily (5.87%) and monthly (5.14%) air temperature show a high degree of efficiency in model simulation.

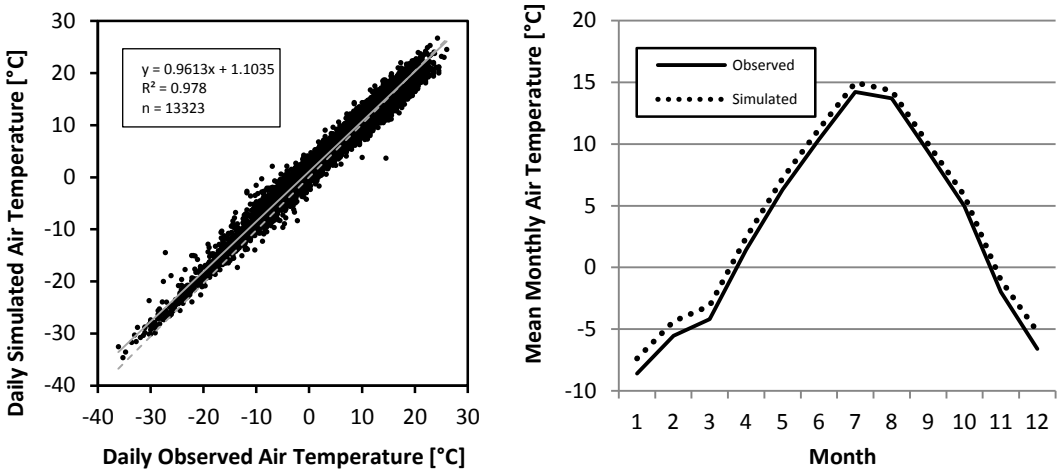

Figure 4.15 Results of model output for the 10 km Grid base stations. Linear regression scatterplot of daily simulated and observed air temperature (left). Mean monthly simulated and observed air temperature for four climate stations (right).

Table 4.6 Model performance for daily and monthly temperature [°C], SWE [mm] and streamflow [$m^3 s^{-1}$] data in the CRW using the 10 km Grid driver stations. Daily and monthly streamflow [$m^3 s^{-1}$] are separated into three decadal periods: 1971-1980 calibration period, 1981-1990 validation period and 1951-2010.

	Temperature		SWE		Daily Streamflow			Monthly Streamflow		
	Daily	Monthly	Snow Course	Snow Pillow	1971-1980	1981-1990	1961-2010	1971-1980	1981-1990	1961-2010
Sample Size (n)	13323	331	259	6564	3653	3652	18262	120	120	600
[%] Difference of the Mean	n/a	n/a	-11.61	0.05	-3.82	-5.87	-6.52	-3.70	-5.88	-6.45
P(T<=t) two tail	0.00	0.00	0.00	0.95	0.01	0.00	0.00	0.46	0.12	0.02
[%] Difference of Variance	5.87	-5.14	-12.47	-3.97	-24.84	-3.12	-31.97	-11.57	-3.88	-14.40
Coefficient of Determination (r^2)	0.978	0.990	0.463	0.609	0.788	0.849	0.720	0.877	0.898	0.797
Regression Coefficient (Slope)	0.96	0.97	0.64	0.77	0.79	0.91	0.74	0.89	0.93	0.84
Regression Intercept	1.10	1.03	106.10	70.16	0.27	0.05	0.31	0.12	0.02	0.16
Nash Sutcliffe Coefficient of Efficiency	n/a	n/a	n/a	n/a	0.79	0.84	0.72	0.88	0.90	0.79
Standard Deviation	n/a	n/a	n/a	n/a	2.51	1.94	2.25	2.01	1.54	2.04

4.3.2 SWE

Modelled output was verified against one snow pillow and two snow courses from the Gardiner Creek HW and West Castle monitoring stations. Comparisons of simulated and observed SWE output illustrating the magnitude and timing of snowpack development in the CRW is shown using a snow pillow and snow course (Figure 4.16). The snow pillow data at Gardiner Creek HW was simulated very well in terms of magnitude and seasonality for the years 1987-1988 and 1991-1994. SWE simulations from 1988 to 1990 were more representative of snow course measurements and are also considered to be in good agreement. Similar to the results in the Beaver Mines verification, simulation for the 1990-1991 period was also significantly under-estimated, this time, by approximately 30%.

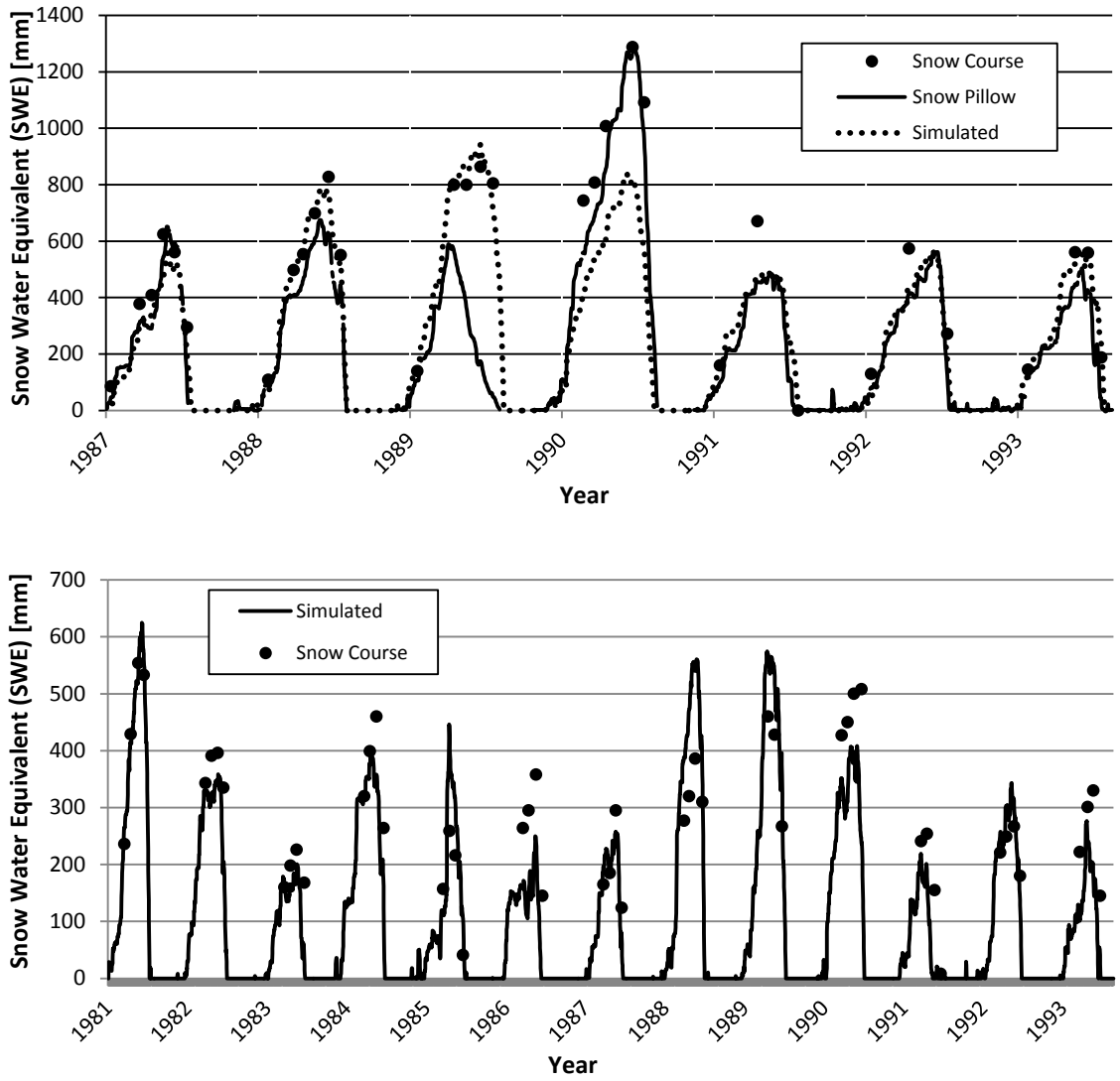

Figure 4.16 Simulated and observed SWE [mm] from snow course and snow pillow measurements at Gardiner Creek Monitoring Station (1987-1994) (top), and thirteen years (1981-1994) of simulated and observed SWE [mm] at West Castle snow course in the CRW (bottom). The 10 km Grid was used as a group of multiple (9) driver stations for the production of these simulated time series.

At West Castle, the 10 km Grid simulation improves in that the under-estimation has a lower magnitude when compared to the Beaver Mines simulation for this location (Figure 4.16). During this model run, the 10 km Grid performed well in simulating mean monthly SWE to within 1% of that observed with the snow pillow at Gardiner Creek HW, and under-simulated 11.61% using the combined snow course data from both stations. The percent difference in variances for simulated and observed snow

pillow (daily) was low (-3.97) and high (-12.47) for snow course data. The coefficients of determination for snow pillow are $r^2 = 0.609$ (n = 6564), and snow course $r^2 = 0.463$ (n = 259) respectively. A scatter-plot showing the comparison between simulated and observed SWE and a seasonal plot of simulated and observed mean monthly SWE is shown in Figure 4.17.

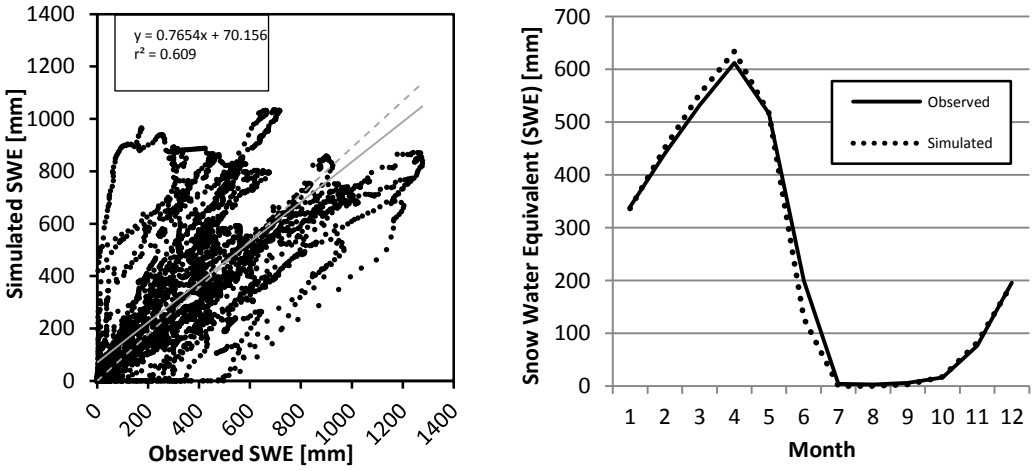

Figure 4.17 Scatter plot of daily simulated and observed SWE [mm] (left) and seasonal plot of mean monthly SWE [mm] at the Gardiner Creek HW (right).

4.3.3 Streamflow

Calibration results (Table 4.6) during the period 1971-1980 show an under estimation of total daily (3.82%) and monthly (3.7%) water yield. Under-estimation slightly increased during model validation (1981-1990) to 5.87% (daily) and 5.88% (monthly). Over the simulation period of 1961-2010 however, model under-estimation is further enhanced to 6.52% (daily) and 6.45% (monthly). P-values from the two tailed t-tests (1981-1990) indicate a significant difference between simulated and observed daily discharge and no significant difference between monthly means. During the total simulation period (1961-2010) however, mean monthly comparisons become insignificant for daily and significant for monthly output potentially due to negative influences of extreme wet or dry years. Percent differences in variance during the 1981-1990 validation period are slightly under-estimated for daily (3.12) and monthly (3.88) comparisons indicating preservation of peak and low flow periods during that decade. Over the simulation

period (1961-2010) however, differences in variance increase to approximately 32% (daily) and 14% (monthly). The coefficient of determination for daily (0.849) and monthly (0.898) validation (1981-1990) are strong, and slightly weaken over the total period of simulation where the r^2 value decreases to 0.720 (daily) and 0.797 (monthly). The NSE during the 1981-1990 validation period of record is reported as 0.84 (daily) and 0.90 (monthly). These also slightly decrease over the total simulation period (1961-2010) to 0.72 (daily) and 0.79 (monthly) but remain as strong indicators of overall fit to the 1:1 line. Figure 4.18 shows a comparison of simulated and observed mean annual streamflow, which provides insight to the magnitude of over- and under-simulated years. Years representing the five best and five worst simulations (1961-2010) including plots of standard deviation are represented in Figure 4.19. Finally, a linear regression showing the 1:1 trendline shows the strength of daily simulated and observed streamflow comparisons as well as a monthly seasonal plot are shown in Figure 4.20.

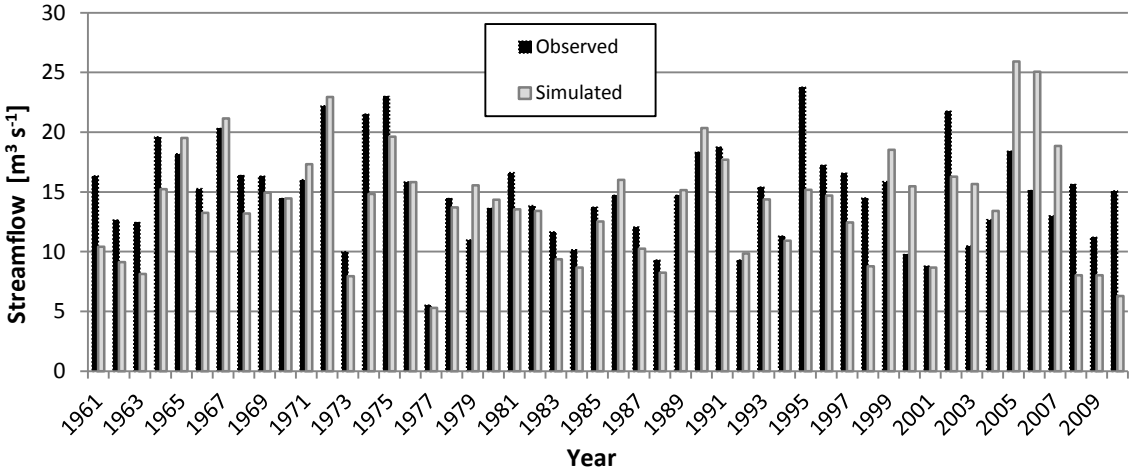

Figure 4.18 Mean annual comparison of simulated and observed streamflow [$m^3 s^{-1}$] (1961-2010) from model runs using the 10 km Grid.

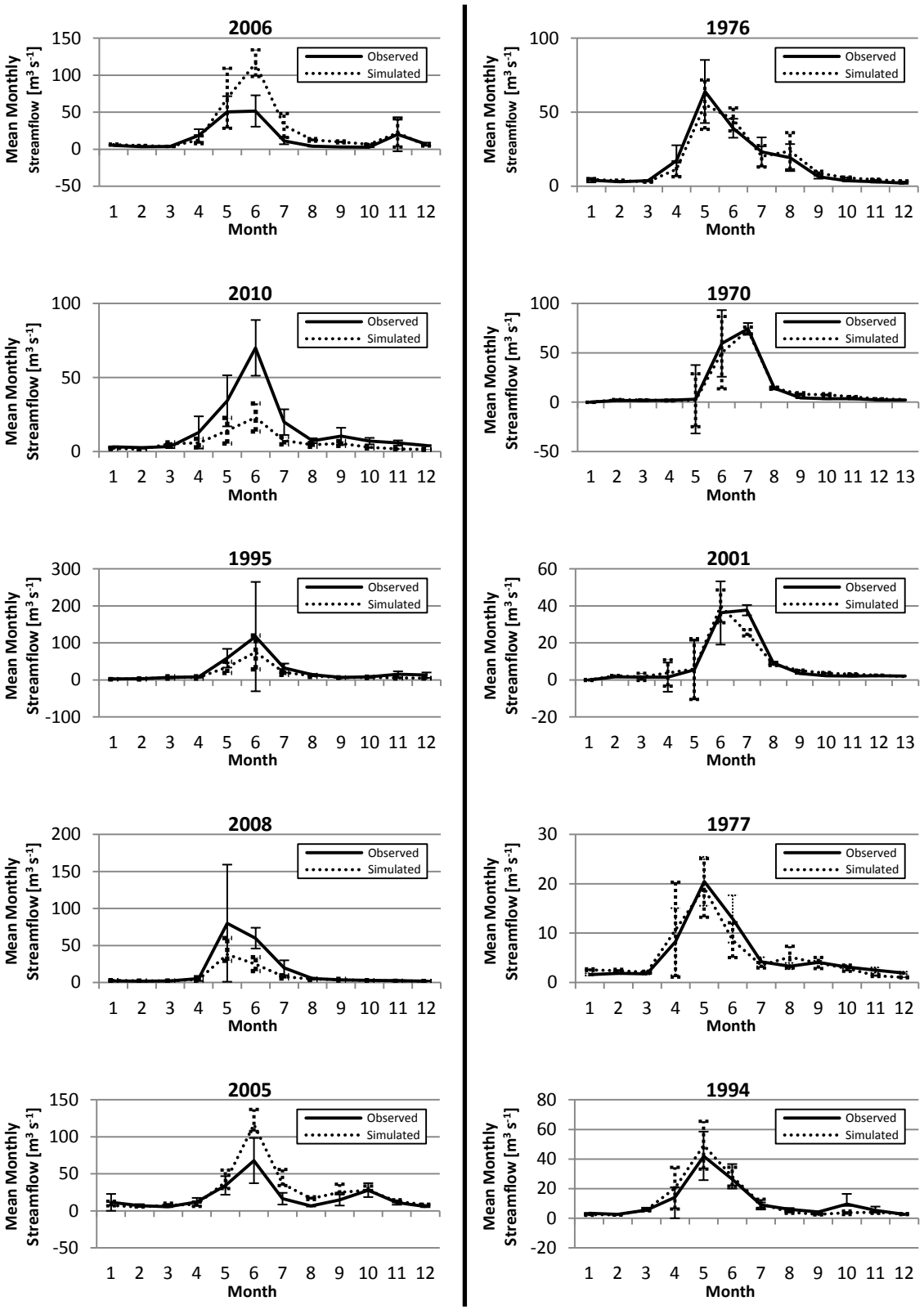

Figure 4.19 Standard deviation plots of observed and simulated streamflow [$m^3 s^{-1}$] using the 10 km Grid model runs. Plotted are the five worst (left column) and best (right column) years in descending order.

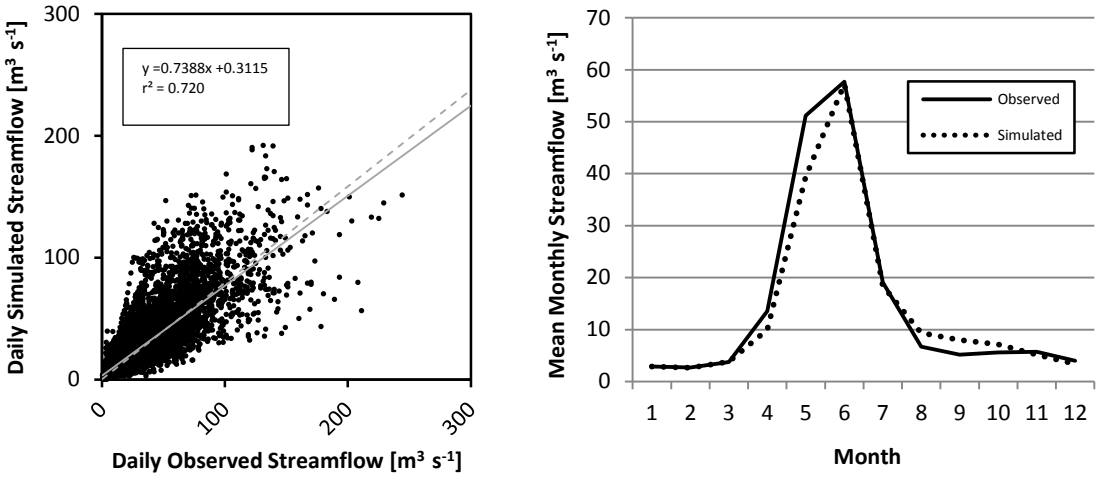

Figure 4.20 Results from 10 km Grid model output (1961-2010). Linear regression scatterplot of daily simulated and observed streamflow [$m^3 s^{-1}$] (left). Mean monthly simulated and observed streamflow [$m^3 s^{-1}$] (right).

4.4 Sensitivity Analysis

Snow accumulation and melt are considered dominant hydrological processes in most inland forested watersheds. As forest cover increases, snow accumulation on the ground is generally reduced due to the ability of the forest canopy to intercept snow and subsequently return a portion of the snowfall to the atmosphere through the process of sublimation. According to Schmidt and Gluns (1991), sublimation rates may vary significantly with changes in slope, aspect and in particular elevation, because of associated changes in the energy balance. Accordingly, previous research has demonstrated that sublimation has the ability to significantly reduce the amount of SWE available for spring runoff and water supply (Schmidt and Gluns, 1991), but that it is also the least known term of the winter water-balance equation in forested canopies (Lundberg and Halldin, 2001).

A sensitivity analysis of the impact that forested canopy interception has on peak SWE for the CRW was carried out using the ACRU model. Modelling the amount of snow intercepted by forest canopies requires information on specific tree species and their distribution throughout the watershed. However, current land cover classification for the CRW only separates forested areas into coniferous and broadleaf types. According to Kershaw's (2008) extensive notes on the Castle Wilderness area, groves of

trembling aspen are typically found on the upland slopes of the foothills parkland ecoregion (1250-1500 m), montane forests are distinguished by the presence of Englemann spruce, subalpine fir, Douglas fir and lodgepole pine. These coniferous forests primarily grow in the lower subalpine ecoregion (1650-1950 m) throughout the Rocky Mountain Cordillera (Kershaw, 2008). Interception efficiencies, which describe the collection efficiency of individual branches that comprise a canopy (Hedstrom and Pomeroy, 1998) for coniferous and broadleaf species have been reported in the literature, but for locations outside Alberta. For example, Bunnell et al. (1985) provides values of maximum SWE interception on Douglas fir stands (50%) in southwestern British Columbia, while Schmidt and Gluns (1991) provide canopy efficiencies for Englemann's spruce (50%), lodgepole pine (45%) and subalpine fir (45%) in locations in British Columbia, Canada and Colorado, USA. Other Canadian-based studies relevant to the CRW, focusing on mixed white spruce/trembling aspen (23%), were performed in central Saskatchewan, Canada (Hedstrom and Pomeroy; Pomeroy et al., 1998).

Two objective functions were used to evaluate the sensitivity of snow canopy interception on forested HRUs in the determination of SWE. The first objective function describes the percentage of canopy cover (ICC) for forested HRUs for each month throughout the year. This monthly canopy cover estimation determines the intercepted area where sublimation can take place. According to Pomeroy et al. (1998), subalpine and boreal forests located at high altitude and latitudes are primarily composed of evergreen conifer species, which retain their needles and therefore intercept snow through the winter. Deciduous forests however, lose a large percentage of their canopy structure during fall and winter months which reduces the volume of water intercepted as snow and increases the amount stored on the ground. According to several authors (Hedstrom and Pomeroy, 1998; Montesi et al., 2004; Pomeroy and Schmidt, 1993; Storck et al., 2002), conifer canopies may intercept up to 60% of the annual snow fall in the boreal forest and sublimation of this snow can return over 30-40% to the atmosphere as water vapour. Other studies (Pomeroy and Gray, 1995; Troendle and Meiman, 1986) report varying sublimation rates depending on climate and forest type.

The second objective function is the calculation of the canopy interception capacity of SWE in percent on the branches of trees in HRUs exhibiting forest cover. The variable in ACRU responsible for defining snow interception capacity is SNCAPI (the proportion of a tree that can hold snow), which is parameterized for each HRU according to the areal coverage of forest land cover, Values of SNCAPI range from 5 to 25% in studies by Kitahara and Saito (1994) and Pomeroy et al. (1998a). In ACRU, the default value for SNCAPI is 15%.

For the assessment of the sensitivity that canopy coverage has on forested HRUs, the percentage of canopy coverage was incremented by 10% ranging between 40% and 90% for dense coniferous forest, while percentage of canopy coverage for all other land cover types present in the CRW remained static for each respective month.

The sensitivity of the snow interception capacity variable in ACRU was also tested on dense coniferous forests. This parameter was incremented at 15% intervals ranging between 15% and 90%, while the broadleaf forest type remained static at 15%.

Results of the sensitivity analysis are displayed in Figures 4.21 and 4.22. Results in Figure 4.21 show the effect of change that canopy coverage has on dense coniferous forest canopies located at the West Castle and Gardiner Creek Climate Stations was minimal. At West Castle, each increase (10%) in the forest canopy resulted on average a 5 mm decrease of mean monthly SWE that would have been stored on the ground and later released into the CRW as runoff. These increases were less sensitive however at the Gardiner Creek Climate Station as the 10% increments resulted on average a 0.8 mm decrease in mean monthly SWE.

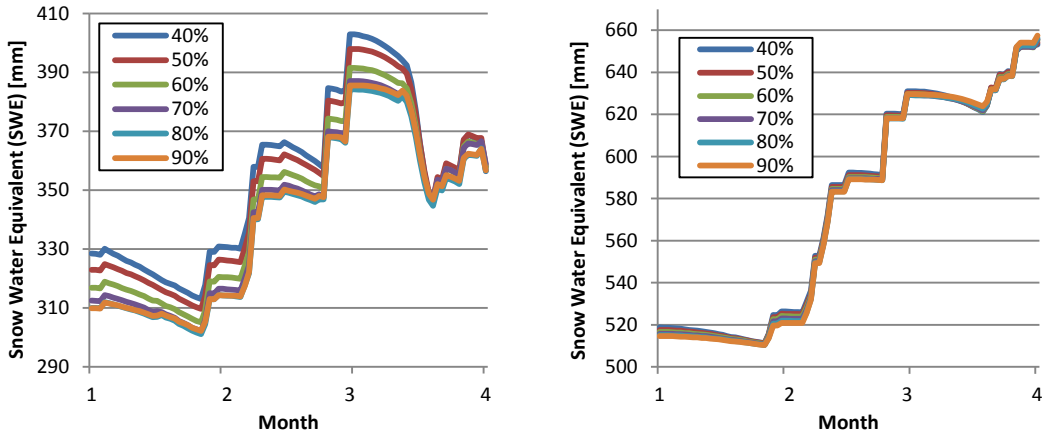

Figure 4.21 First objective function for the sensitivity analysis is canopy coverage (ICC) expressed as a percent. The effect of the change of canopy coverage on SWE for dense coniferous forest located at West Castle Monitoring Station in 1985 (left), and the effect of the change of canopy coverage on SWE for dense coniferous forest located at Gardiner Creek Monitoring Station in 1985 (right).

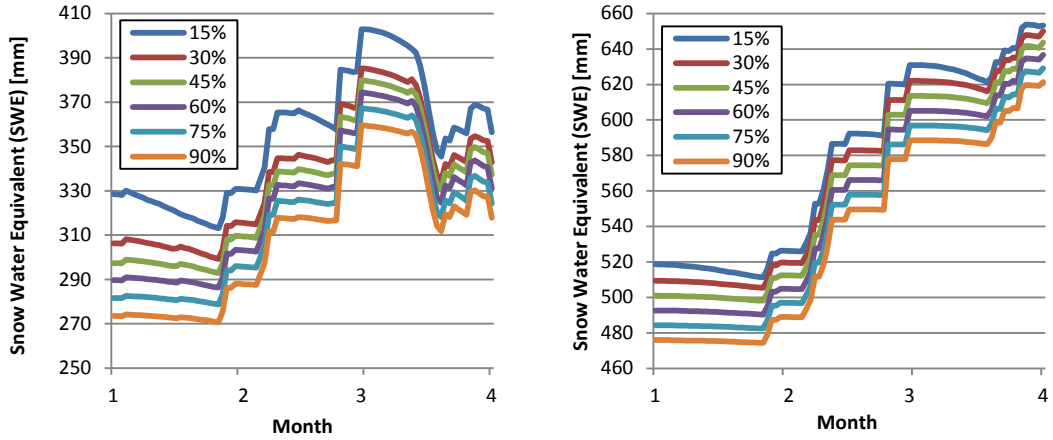

Figure 4.22 Second objective function for the sensitivity analysis of snow canopy interception capacity (SNCAPI) in mm. The effect of change of SNCAPI on SWE for dense coniferous forest located at West Castle Climate Station in 1985 (left), and the effect of change of SNCAPI on SWE for dense coniferous forest located at Gardiner Creek Climate Station (1985)(right).

Results in Figure 4.22 show the effect of change in SNCAPI for dense conifer forests at the West Castle and Gardiner Creek Monitoring Stations. At West Castle, increasing the capacity of the canopy to intercept snow by 15% increments from 15% to 90% resulted in an average decrease of approximately 9 mm from SWE storage on the ground. At Gardiner Creek, this decrease of SWE stored on the ground as a result of increased canopy interception was slightly less in quantity at approximately 8.75 mm SWE.

4.5 Discussion

4.5.1 Temperature

Verification analysis using four climate stations with varying lengths and frequencies of daily observations revealed that although the 10 km Grid out-performs the BMCS in temperature simulation, both are able to simulate daily air temperature across the CRW with a high degree of accuracy. Hydrological models commonly employ the use of linear lapse rates to extrapolate near-surface air temperatures from meteorological stations to locations where observations do not exist (Bolstad et al., 1998; Dodson and Marks, 1997; Running et al., 1987; Thornton et al., 1997). ACRU uses lapse rates to make temperature corrections to each HRU based on elevation for the partitioning of precipitation into rain or snow. Additionally, lapse rates are also applied with inputs of mean monthly incoming solar radiation and mean monthly LAI to compute rates of ET, sublimation and snowmelt (Kienzle, 2013). These adjustments are the same for each driver station approach, BMCS and the 10 km Grid.

The calibration of temperature consisted of making adjustments to the regional mean monthly lapse rates reported in Table 3.2 and shown in Figure 4.3. The challenges associated in lapse rate calibration can be attributed to a variety of explanations, including for example, those listed in Section 3.5.1.1. As a consequence of the relatively small difference in elevation between the BMCS and the two valley stations (Castle and West Castle, Table 4.1), any meaningful lapse rate adjustment causes only minor change in the temperature at the corresponding HRU locations making temperature calibration across the watershed difficult to achieve, especially when observed temperature differences between these stations is large. For instance, the average difference in Tmax observations between Beaver Mines and the West Castle Climate Station ranges from 1.7°C to 4.3°C, while the differences in Tmin range from 0.5°C to 2.5°C. The largest seasonal differences for both Tmax and Tmin occur during December and the smallest differences occur during July. The Gardiner Creek and Carbondale Lo Stations are situated at higher elevations but the Carbondale is seasonal (April to October) so that verification could not be made for winter months. The Gardiner Creek station records all year round but is located near the continental divide in a bowl-shaped valley where the influence of snow cover on near surface air temperatures

stretches into the late spring and early summer. In contrast, snow cover melts out earlier at Beaver Mines as a result of its location in the transition zone between the prairie and foothills landscape causing difficulty in approximating meaningful lapse rates between stations.

A study by Pigeon and Jiskoot (2008) focused on the derivation of temperature lapse rates in the West Castle Valley where temperature observations were obtained from climate stations on the nearby ski resort at West Castle. Due to the influence of inversions created by cold air drainage during winter, inversion days were separated, wet and dry precipitation days were categorized and a more accurate lapse rate approximation was made based on the multi-year lapse rate mode as opposed to lapse rate averages (Pigeon and Jiskoot, 2008). Due to time constraints, this method was not investigated but should be considered for future studies.

The problematic nature of quantifying the relationship of temperature and altitude through the use of near-surface lapse rates in mountain environments has been documented (Blandford et al., 2008; Bolstad et al., 1998; Gardner et al., 2009; Minder et al., 2010; Pigeon and Jiskoot, 2008; Rolland, 2003; Tang and Fang, 2006). According to Dodson and Marks (1997) the Tmin measurement is more susceptible to local conditions such as cold air drainage (which leads to temperature inversions) than Tmax. Bolstad et al. (1998) and Blandford et al. (2008) both add that other influential variables such as katabatic winds, insolation and the diurnal and seasonal variation of lapse rates also contribute to the complexity of lapse rate prediction. Given that the CRW lies directly south of a major mountain pass (Crowsnest Pass), the addition of channeled cross-mountain flow as explained by Steenburgh et al. (1997) likely accounts for discrepancies especially in the northern portion of basin. It should be noted that ACRU does not currently consider any of these variables in its model routines. Thus, given the fact that these factors considerably confound the relationship between temperature and altitude, especially for Tmin measurements, the difficulty in calibrating mean monthly lapse rates for Tmin and Tmax is justified. Comparisons between the verifcation at Beaver Mines and that on the 10 km Grid, reveal that with exception to the summer months using Beaver Mines as a base station, ACRU consistently over-simulated temperature throughout the year, with the largest variation occuring during the winter months. The timing of these discrepancies is

consisent with seasonal factors influencing temperature, such as cold air drainage and inversions that typically occur during winter (Pigeon and Jiskoot, 2008). Bolstad (1998) also contested that the quality of lapse rate prediction is susceptibile to temperature anomalies at a single station that are extrapolated across large areas, and that these susceptibilites can be reduced by using a larger network of climate stations for lapse rate delineation. Thus, the calculation of regional laspe rates in some remote mountainous or unpopulated areas like the CRW has proven to be difficult due to the sparseness of climate stations. Since ACRU uses temperature to partition precipitation into rain and snow, and given the fact that snowpack development and snowmelt are largley dependent on near surface temperatures, SWE becomes the next element of the hydrological cycle to be verified in the modelling process.

4.5.2 SWE

SWE verification in the CRW was carried out twice; first, with the BMCS and second, the 10 km Grid. Results showed the 10 km Grid performed well in simulating SWE especially at the Gardiner Creek HW Station. At Gardiner Creek, Alberta Environment uses a snow pillow as well as a snow survey to collect information on the development of the snowpack. At West Castle, measurements are made only from a surveyed snow course in an area of open and partial forest cover. A snow pillow is particularly useful in that it provides a daily measurement of SWE which can be compared with snow course measurements and aid in verification purposes. Snow course measurements are also valuable but have the limitation that measurements are usually taken on a monthly basis which offers a somewhat generalized or coarse view of the snowpack development for the area.

Since the site locations for the snow surveys were in areas of open and partial forest cover, and since ACRU classifies an area of forest as either fully forested or fully non-forested, a ratio of 50% forested and 50% non-forested SWE values were found to result in the closest simulation to observed data. However, during the verification and simulation of streamflow as well as during the evaluation of the impact of climate change on streamflow, forested HRUs remained fully forested. Shading in forested areas can slow snow melt processes that would otherwise take place at an increased rate. According to

Campbell (2014), the snow survey was said to follow the perimeter of a forested opening. The reduction of solar radiation input resulting from shading that occurs close to the forested canopy likely explains why the snow course data were consistently higher than that recorded by the snow pillow. Evidence of this can be seen by making comparisons between the Gardiner Creek snow pillow and snow course data. In Figures 4.10 or 4.16, comparisons of the snow pillow and snow course observations (excluding the simulations) reveal that during the spring melting period, the rate of melt is faster on the snow pillow than that observed by the snow course. For example, in the spring of 1988 at Gardiner Creek, snowpack measurements reveal that on the date 26 April, snow pillow SWE was 593 mm and snow course was 561 mm. Exactly one month later (26 May), significant melt had occurred causing a decrease in snow pillow SWE to 103 mm representing a percentage change of 82%, while snow course measurements showed a decrease to 266 mm representing a negative rate of change of 47%. Similar melt rates are revealed for other years where the snow pillow and snow course data are relatively consistent with each other (1990-1991 and 1993-1994), supporting slower melt in shaded areas. These findings provide insight to the variability of snowpack melt rates occurring in the mountains at macro- and micro-scales revealing the degree of complexity that exists in snowpack modelling in alpine environments.

Simulated and observed snow development at Gardiner Creek HW and West Castle Bush Stations as shown in Figures 4.10 and 4.16 illustrate that modelling the timing and magnitude of SWE can be a challenge in mountainous areas. Some years are represented well in modelled output, whereas other years are characterized by over and under-estimations of SWE. The location of the Gardiner Creek HW snow pillow and snow course sites are in an area directly east of the continental divide in a bowl-shaped valley where large amounts of snow redistribution most likely takes place. The redistribution of snow in alpine terrain has been explained by Winstral et al. (2002), where vertical flow constrictions over topographic obstacles (e.g. mountains) cause wind speeds to increase, thus increasing scour rates and snow entrainment. Upon cresting the topographic feature, expansion of flow occurs, leading to reduced wind speeds, decreased snow transport fluxes and a potential for snow deposition. Winstral et al. (2002) also state that where wind speeds at the topographic obstacle are strong enough and a sufficient slope

break exists downwind of the obstacle (e.g. location of Gardiner Creek HW), flow separation can occur, whereby the air stream is no longer in contact with the ground, forming a lee eddy, which is the basis for snow drift development. It is also possible for flow-separation eddies to develop at the base of windward-facing topographic obstacles (e.g. location of West Castle Bush snow course) (Winstral et al., 2002). Although much of the spatial heterogeneity of SWE in alpine regions is the result of redistribution by wind and many other factors (Balk and Elder, 2000; Elder et al., 1991), the current setup of ACRU is not able to model these complexities, limiting ACRU's ability to accurately simulate physically-based snow processes. Considering these limitations, the seasonality of mean monthly SWE shown in Figure 4.11 using the BMCS and Figure 4.14 using the 10 km Grid, suggest, that despite the over and under estimation of SWE over multi-year periods, mean monthly SWE is being modelled resonably well in terms of timing of snowpack development, magnitude and melt throughout the season.

Results of the sensitivity analysis provide insight to the fact that the snow canopy interception routines in the ACRU model are not sensitive enough to make significant changes to the overall accumulation and storage of SWE in mountain regions exhibiting canopies of dense coniferous forest. Snow interception processes are usually best simulated by models specifically developed for those purposes. For example, in their review of snow interception measurement techniques, processes and models, Lundberg and Halldin (2001), stated that except for models that have been developed to simulate snow interception storage and evaporation/sublimation processes, snow interception processes are treated as very basic if at all in hydrological models. Pomeroy et al. (1998b) also suggested that little progress has been made in modelling snow interception in hydrological models. The routines in the ACRU model that deal with snow interception were added as a suite of physically based processes associated with cold environments and terrain dependent hydrological variables. However, the overall results of the snow verification prove that these cold environment routines are sufficient for the relatively large hydrological modelling units (the average size of an HRU is about 3.5 km^2). With the distribution of SWE being one of the controlling factors in the timing of runoff (Balk and Elder, 2000), it is important to consider the influence SWE and temperature has on the modelling of streamflow in the CRW.

4.5.3 Streamflow

Modelling streamflow in the CRW required calibration and verification of streamflow data recorded at the hydrometric gauges at Ranger station and near Beaver Mines. Measured streamflows during the 1971-1980 period of record were used to calibrate ACRU. Streamflow calibration refers to the process where streamflow parameters are estimated by comparing model predictions (output) for a given set of assumed conditions and minimizing the difference between measured and simulated streamflow at the watershed outlet (Moriasi et al., 2007). The verification period was chosen based on data availability and streamflow conditions consisting of low flow, high flow and normal years. The years 1961-2010 were also chosen as a period of record to make comparisons against streamflow generation as it represents the whole historical period including the inter-decadal variability of normal, wet and dry conditions.

Meteorological observations can only be obtained from point locations. In hydrological modelling however, the number of point locations available will either limit or support predicted output of the measured variable of interest (e.g. streamflow). Balk and Elder (2002) suggested, point measurements are only satisfactory for normal precipitation years and errors in streamflow prediction dramatically increase for abnormally wet or dry years.

Comparisons of output from model runs using Beaver Mines data with the 10 km Grid support the assumption that since Beaver Mines is a point location from which meteorological conditions are extrapolated across the watershed, uncertainties in resulting streamflow volumes are to be expected. Since the 10 km Grid offers an increasing number of virtual base stations spatially distributed evenly across the watershed, better predicted results were expected. These assumptions were solidified by the resulting comparisons of modelled output which included larger percent differences of variance for the point based over gridded datasets. For example, results of mean monthly model runs using the BMCS showed differences in variance of 24.66%, 75.48% and 25.23% for the calibration (1971-1980), verification (1981-1990) and historical (1961-2010) periods. The 10 km Grid yielded better results, such as, 11.57%, 3.88% and 14.40% for the same periods of record. Percentage differences between simulated means were not as large (Table 4.6).

Annual comparisons of simulated and observed streamflow were made to identify whether or not systematic errors exist within the streamflow modelling routines. This was accomplished by calculating the difference between simulated and observed annual streamflow to determine the five worst and best years during the simulation record. Standard deviation was then plotted for simulated and observed time series for mean monthly streamflow. Model runs based on the BMCS showed consistent over-simulation beginning in April, peaking in May to June and returning to a better model fit in the early autumn. Similarities between standard deviations (Figure 4.13) revealed a preservation of the dispersion around the mean for both simulated and observed streamflow. This means that over-simulation during late spring and early summer could be a result of some hydrological component of the physical environment that is unaccounted for or simply a result of error associated with extrapolating measurements in time and space. Beven (2001) has stated that despite many advances in knowledge and measurement of hydrological variables, process hydrology is very complex and changes strongly in non-linear ways. Results from the 10 km Grid were more inconsistent in that the worst years were characterized by over- and under-simulations more during the months May to July, but overall dispersion around the mean (standard deviation) was generally consistent (Figure 4.19). A large difference in standard deviation was noted during the 1995 flood year as well as 2008. Modelling from a single point location as opposed to gridded datasets, can, under certain conditions, provide a better estimation of extreme events. This results from the fact that the gridded dataset is comprised of spatial averaging of observations over a larger geographical area, whereas the point location (Beaver Mines) has the ability to capture a more representative measurement of the variable of interest.

Particular attention was given to the worst simulation years for both (Beaver Mines and 10 km Grid) model runs and showed that 7 out of 10 years occurred since the year 2001 whereas the other 3 occurred during 1995, 1996 and 1997. It has been alluded to that the climate change signal had yet to be measured prior to the 1990s Diaz-Nieto and Wilby, 2005), which may explain why the worst years of model simulation have all taken place since 1995. A commonly held opinion in the climate change community is that an increased frequency of extreme events is a result of climatic change. Large

thunderstorms are often accompanied by large amounts of precipitation, which can drop considerable amounts of rain in small areas in a short amount of time. Due to the scarcity of climate stations located in mountain environments and the fact that large thunder storms often occur over very small areas, observations of precipitation for an area may not be representative of actual inputs received and yet a signal of the storm event may show up in downstream streamflow records. For example, in some instances, climate stations may pick up the edge of a large storm and thus record only a small portion of what was received by the surrounding region, or it may be that a storm skips over a climate station altogether while dropping large amounts of rain nearby. In other cases, a large storm may occur directly over a climate station with the surrounding area not experiencing any rainfall.

It is a generally accepted notion that hydrological modelling is often comprised of general over- and under-simulations. For example, Beven (2001) has stated that of all the hydrological inputs used in streamflow modelling, precipitation is the most important, where models have shown more sensitivity to precipitation inputs as opposed to topography and vegetation and that significant over- and under-simulation takes place in individual years. Hence, it can be difficult to determine the exact cause of over- and under-simulation, especially when modelling the hydrology of mountain environments.

4.5.4 The Choice of the Beaver Mines Climate Station or the 10 km Grid

In hydrological modelling, the application of correction factors is commonly used to extrapolate measures of temperature, precipitation and other variables from point locations to unmonitored sites within a study region. Hungerford et al. (1989) has stated that as a result of changes in air masses, cloud cover and precipitation, the accuracy of extrapolation decreases as horizontal distance between a base station and study site increases. This decreased accuracy was more prevalent in the application of the BMCS over the 10 km Grid. Verification analysis provided the opportunity to make an assessment between datasets. Since the overall statistical results show that the 10 km Grid is a superior dataset for driving hydroclimatological variables in the CRW, the 10 km Grid is chosen to simulate the future hydrology of the CRW.

Chapter 5: Simulating impacts of climate change on the Castle River hydrology using a future GCM projection

5.1 Introduction

In Canada, most studies focusing on the effects of climate change on watershed hydrology have concentrated on watersheds where snowmelt is the major proportion of streamflow. This is due to the strong influence that climate change has on snow-dominated regions throughout the world (Barnett et al., 2005; Christensen et al., 2004; Middelkoop et al., 2001).

As described in Chapter 1, the overall goal of VACEA is to better understand the vulnerability facing rural agriculture and indigenous communities in the Americas and provide new knowledge that can be used to strengthen their capacity to adapt to shifts in climate variability and the frequency of extreme events. In Canada, impact assessments of climate change on hydrology are focused on three watersheds: The Oldman River Basin (ORB), the Castle River Watershed (CRW) and the Swift Current Creek Watershed (SSCW). The hydrological changes expected in the CRW are assessed by applying a future climate projection from GCM output downscaled to a regional scale. Climate scenarios in the form of Regional Climate Models (RCMs) are provided by Dr. Elaine Barrow of the Prairie Adaptation Research Collaborative (PARC) at the University of Regina, Saskatchewan. Dr. Barrow works under the direction of research team leader and climate specialist Dr. David Sauchyn of the University of Regina.

GCMs are designed to replicate the physical processes and known feedbacks between the ocean, atmosphere, cryosphere and land surface (Barrow and Yu, 2005). Although they have the capacity to simulate climates of the past and present, GCMs are often used to make projections of future climates over large regions. The typical resolution for current GCMs is roughly in the hundreds of kilometers (250-600 km) horizontally (grid spacing) with the ability to assess numerous vertical layers of the atmosphere (10-20 layers) and the ocean (as many as 30 layers) (Barrow and Yu, 2005; Flato et al., 2013). Output from GCM experiments provides the basis for the construction of climate change scenarios. According to Barrow and Yu (2005), a scenario is constructed by calculating mean differences between simulated

current climate and the climate of some future time period (typically a 30-year period) at a monthly or seasonal scale.

According to Flato et al. (2013), regional-scale climate information can be obtained directly from global models. However, their resolution is often too coarse for small-scale analysis. Issues with scale can be resolved through the application of downscaling techniques. According to Poyck et al. (2011), several ways of downscaling GCM output exist. For example, from simple statistical methods which extract change parameters between current and future GCM simulations and apply those to measured data (e.g. delta-change method), to more complicated methods, such as embedding an RCM into a GCM (nesting technique). Details of embedding an RCM into a GCM are given by Hudson and Jones (2002). Methods based on RCMs are more able to represent physical processes on a relevant scale which allows them in some cases to be simulated directly in climate impact studies (Poyck et al., 2011). However, one drawback of the nesting technique is the requirement of significant bias correction to be applied to original model results (Poyck et al., 2011). In the 2013 *Contribution of Working Group I* to the Fifth Assessment Report (AR5) of the IPCC, Flato et al. (2013) reported not only had the use of RCMs for dynamical downscaling increased since the Fourth Assessment Report (AR4) in 2007, their resolution had increased from around 50 km to around 25 km, and process descriptions have been further developed with added components while overall use has become more widespread. Principles based on the embedding of an RCM into a GCM describe the methodology adapted by this study.

5.2 Selection of a climate change scenario

Simulating climate change impacts on hydrological processes for an area requires the choice and application of scenarios depicting future climate. A main problem identified by Barrow and Yu (2005) is the selection of the number of scenarios to use for impacts analysis. The IPCC Task Group on Data and Scenario Support for Impact and Climate Analysis (TGICA) currently recommends the selection of a range of scenarios that will help build a complete picture of the range of future climate variability of a region (IPCC-TGICA, 2007). In partnership with the VACEA project, prior agreement was made with climate

specialist Dr. David Sauchyn (University of Regina) that his team would provide multiple climate scenarios for the CRW at a spatial resolution of 10 km. Five scenarios were selected following the same methodology set forth by Barrow and Yu (2005); four representing more extreme changes in temperature and precipitation and one representing median conditions. The scenarios are listed first by scenario type, followed by the RCM/GCM acronym which was applied for climate modelling.

1. Cooler/drier – RCM3-gfdl
2. Cooler/wetter – RCM3-cgcm3
3. Median – CRCM-cgcm3
4. Warmer/wetter – CanRCM4-canesm2
5. Warmer/drier – HRM3-gfdl

Unfortunately, only one scenario (#4) was made available in the spring of 2014 at an undesired resolution (25 km), requiring significant additional time for additional downscaling to the resolution of the 10 km Grid used in this study. However, the application of this one scenario provides a methodology which is recommended to be followed applying the remaining four scenarios and provides a framework upon which to build a conceptual representation of future climate in the CRW.

5.3 Downscaling of the RCM to match the 10 km Grid

CanRCM4, a fourth generation regional climate model for Canada, was coupled with and driven using the second generation Canadian Earth System Model (CanESM2) GCM creating regional climate projections for Southern Alberta at a spatial resolution of 25 X 25 km. Prior to it being made available, a bias correction was applied by Dr. Barrow for the purpose of eliminating systematic errors associated with general downscaling of climate model output. An established view in the hydrological modelling literature is that an adjustment for model bias is essential for interpreting regional climate change predictions (Hamlet and Lettenmaier, 1999; Nijssen et al., 2001). Model bias can be introduced as systematic model errors caused by imperfect conceptualization, partitioning of units and spatial averaging within grid cells (Teutschbein and Seibert, 2012). Bias can be pronounced as, for example, the occurrence of too many wet

days with low intensity rain or incorrect estimation of extreme temperatures, but also general under – or over-estimations and incorrect seasonal variations of precipitation (Teutschbein and Seibert, 2012). Bias correction performed by Dr. Barrow follows the methodology set forth in Boe et al. (2007). The method used was also reported in Teutschbein and Seibert (2012) in their comparative review of different bias correction methods. Following bias correction, CanRCM4 output for a historical (1971-2000) and future (2041-2070) time series were made available by Dr. Barrow. Although this dataset represents a downscaled version of GCM output, the spatial scale between the CanRCM4 (25 km) and 10 km Grid did not match (see Figure 5.1).

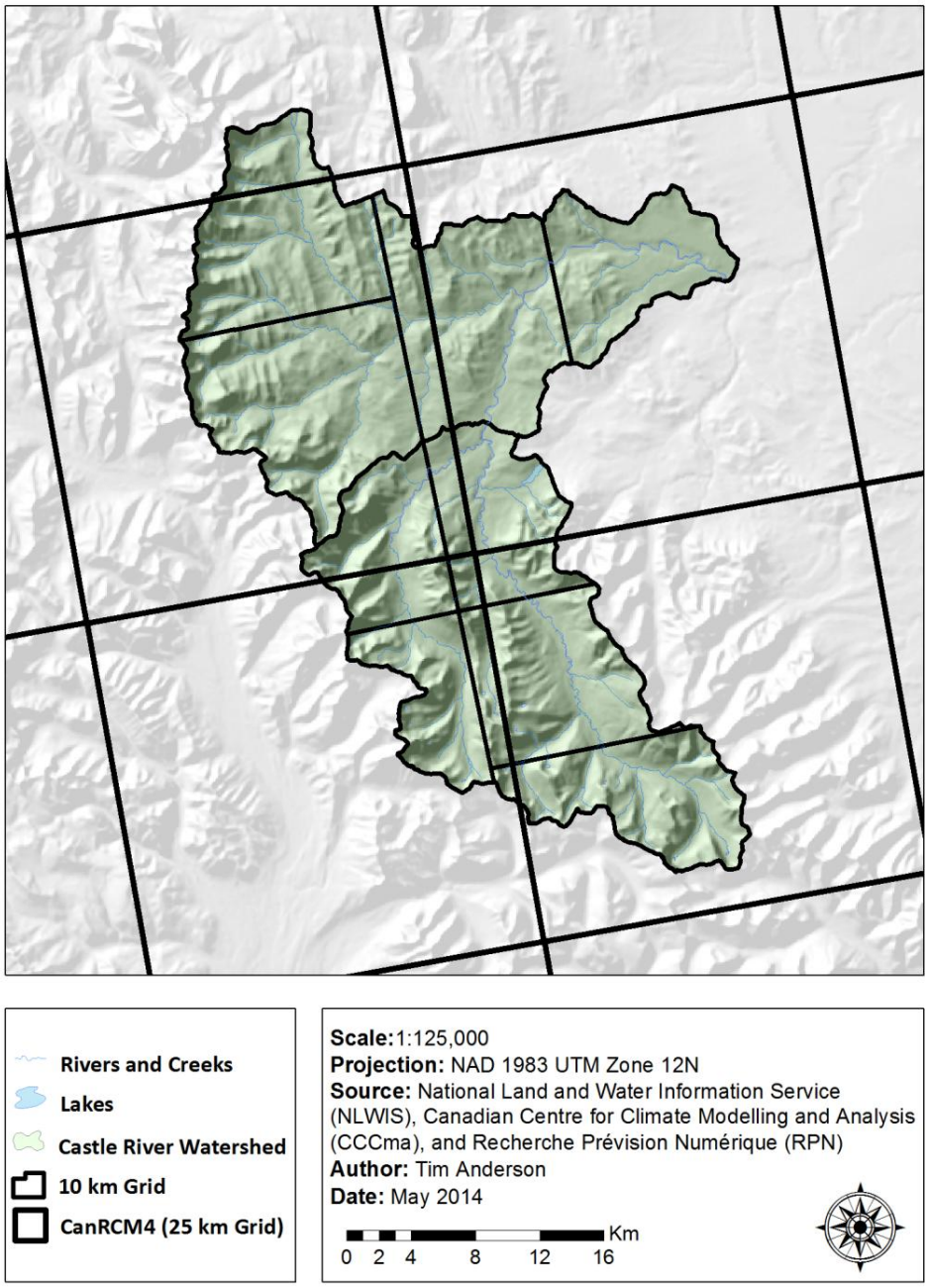

Figure 5.1 A comparison of spatial scales between the 10 km Grid and the CanRCM4 which has a spatial resolution of 25 km.

In order to provide consistency of climate input for the ACRU model, the RCM grid needed to be downscaled to the spatial scale of the 10 km Grid. This was accomplished through extensive GIS spatial analysis using area weighting based on spatial proportions of each CanRCM4 grid that spatially overlaid a

10 km Grid polygon. The hydroclimatic variables upon which these ratios were made were based on available PRISM surfaces (100 m) for temperature and precipitation. To run ACRU using downscaled RCM data, new climate input files were created to simulate the future hydrological impacts in the CRW. Changes to the new climate input files included the insertion of RCM-based temperature and precipitation, while keeping static all other hydroclimatic variables such as wind, relative humidity, hours of sunshine duration and solar radiation. The downscaling of hydroclimatic information to each of the 230 HRUs across the watershed takes place internally within the ACRU model.

5.4 Applying future climatic simulations to the CRW

ACRU was rerun with the climate input files created from the downscaled RCM-based simulations. The only difference from those used in the verification process is the replacement of the RCM-based simulated variables of temperature and precipitation, where precipitation is adjusted using RCM-based CORPPT (refer to section 3.5.1.2 for the calculation of CORPPT). ACRU was run for two climate periods, one for the 1971-2000 period, which established a baseline hydrological response from the RCM-based output, and once for the future (2041-2070) period, to represent the future hydrological behavior of the CRW. Results from the 1971-2000 historical and RCM 1971-2000 baseline were compared to assess the degree of confidence that can be put into the future RCM projections.

5.5 Results and Discussion

5.5.1 Comparison of historical 30-year time series

Following model simulation for 1951-2010, all 230 HRUs were area weighted for the entire CRW to obtain values representative of the watershed as a whole. Area weighting was applied to simulated output of mean temperature, rainfall, snowfall, total precipitation and SWE. The partitioning of precipitation into rain and snow as mentioned in section 4.1 and 4.5.1 provides the opportunity to compare historical amounts of rainfall, snowfall and total precipitation for the study area. Streamflow output is obtained as ACRU internally accumulates streamflow volumes from each HRU within the

watershed. Streamflow accumulation begins in the far reaches of the upper watershed, down to the HRU situated at the mouth and location of the hydrometric gauge at Beaver Mines. Therefore, mean monthly and annual streamflow was calculated directly from simulated output of the HRU representing the Beaver Mines gauge location.

It is important to note that Area weighted values for 1951-2010 were divided into four 30-year time series (e.g. 1951-1980, 1961-1990, 1971-2000 and 1981-2010) to evaluate how each 30yr normal period has progressively changed (Figure 5.2). Results are reported in Tables 5.1 to 5.6. Comparisons between time series refers to, for example, the comparison of how a variable has changed between an earlier 30-year period (e.g. 1951-1981) and subsequent 30-year periods (e.g. 1961-1990). The 30-year periods will be referred to as first, second and third periods of comparison, where the 1951-1980 vs. 1961-1990 periods refer to the 'first' comparison period, 1961-1990 vs. 1971-2000 refers to the 'second' comparison period and 1971-2000 vs. 1981-2010 refers to the 'third' comparison period. In comparative analysis, change is usually expressed as a percent. Percent change can often be misleading however, as a result of change between two seemingly small numbers. Examples of this in Tables 5.1 to 5.13 (with exception to Table 5.7) occur frequently and are expressed as a large percentage change, sometimes more than 100%. For example, in Table 5.5, the percentage change of August SWE for the third period of comparison is 2615%. This large percent change is a result of a mere increase from 0.004 mm to 0.110 mm of SWE in that month, which is likely the result of a rare, single snowfall event within the 30-year period. As a result, the mean monthly values for each variable, along with the difference and percent change, are reported.

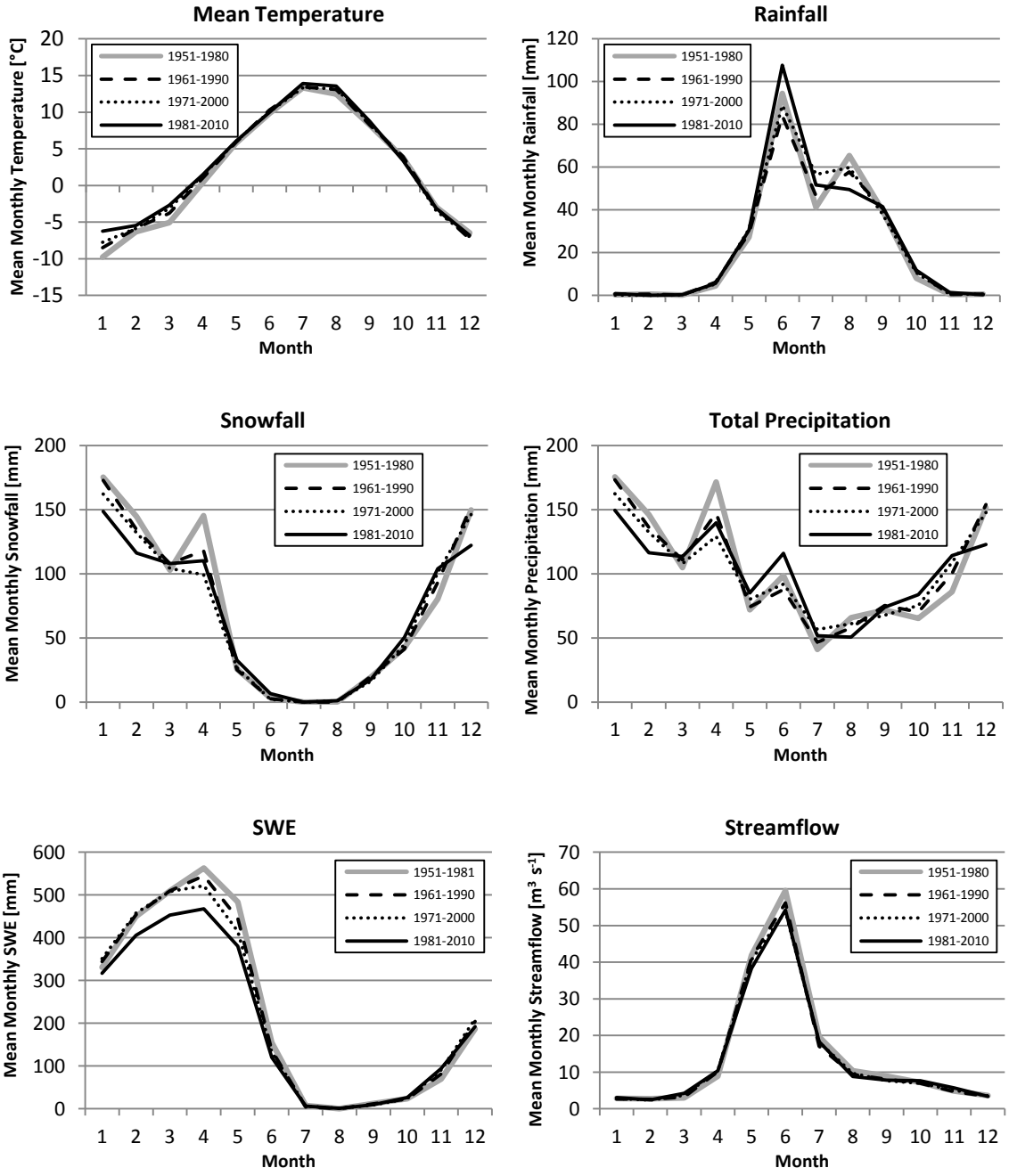

Figure 5.2 Historical 30yr (1951-2010) time series for mean temperature [°C], rainfall [mm], snowfall [mm], total precipitation [mm], SWE [mm] and streamflow [$m^3 s^{-1}$].

5.5.1.1 Mean Temperature

Mean annual temperatures have increased by approximately 0.8°C over the past 60yrs (1951-2010) in the CRW (Figure 5.2 and Table 5.1). These findings are in agreement to those found in other

historical comparisons where increases ranged between 1°C and 2°C since the 1940s in the North Western part of North America (Cayan et al., 2001) and a 0.9°C increase relative to the 1961-1990 mean for southern Canada, south of 60°N (Zhang et al., 2000). Seasonal increases occur 10 out of 12 months during the year, with the largest increases taking place between January and April (Figure 5.2 and Table 5.1). For example, January mean temperatures gradually increase from -9.8 °C during the 1951-1980 period to -6.3°C by the 1981-2010 period. March temperatures increased from -5.1°C to -2.7°C for the same period. Cayan et al. (2001) and others have also found this seasonal increase in temperature to be more pronounced during the winter and spring months with the largest increases taking place in March. The month of August experienced slight gradual warming with 4.7%, 0.9% and 2.7% increases over the first, second and third periods of comparison. In contrast, the months of June and October have shown slight decreases throughout the three comparative periods.

Table 5.1 Comparisons of simulated mean monthly and annual temperature based on four 30-year historical periods. Change between periods is expressed as a difference [°C] (A = Annual).

Time Series Comparisons		Month												
		1	2	3	4	5	6	7	8	9	10	11	12	A
1951-1980		-9.8	-6.3	-5.1	0.4	5.8	9.8	13.3	12.5	8.3	3.8	-3.0	-6.5	2.0
1961-1990		-8.5	-5.8	-3.8	1.0	5.9	10.3	13.4	13.1	8.3	3.9	-3.1	-7.3	2.3
1971-2000		-7.7	-5.8	-3.1	1.4	6.0	10.1	13.3	13.2	8.5	3.6	-3.5	-7.0	2.5
1981-2010		-6.3	-5.5	-2.7	1.5	6.0	10.0	13.9	13.6	8.8	3.4	-3.1	-6.8	2.8
1st Period	Diff	1.3	0.5	1.3	0.6	0.1	0.5	0.1	0.6	0.0	0.1	-0.2	-0.8	0.3
2nd Period	Diff	0.7	0.0	0.7	0.4	0.1	-0.3	-0.1	0.1	0.2	-0.3	-0.3	0.3	0.1
3rd Period	Diff	1.5	0.4	0.4	0.1	0.0	-0.1	0.6	0.4	0.3	-0.2	0.4	0.2	0.3

5.5.1.2 Rainfall

Mean annual rainfall decreased during the first comparison period (negative change of 1.6%) and has increased by 23.4 mm since 1961. A study by Zhang et al. (2000) revealed that annual precipitation has increased by 5% to 35% for all of Canada relative to 1950-1998 with significant increases taking place in all seasons. Akinremi et al. (1999) has stated that across the Canadian Prairies there has been an increase in rainfall amount within the last 75 years. Seasonal changes of rainfall in the CRW between the

30 yr periods have occurred most significantly during the months of June, July and August (Figure 5.2 and Table 5.2). In June, rainfall decreased during the first comparison period and increased throughout the second and third periods by 5.6% and 21.2% for an equivalent of 23.5 mm. The month of July steadily increased for the first two periods and decreased again during the last. In August, however, changes were variable in that a decrease occurred during the first period, an increase in the second, followed by another decrease in the third signifying an overall decreasing pattern (negative change 24.3%). Although the reported values are based on the period Jun-Aug, these seasonal observations are similar to reported precipitation amounts between May and August over the 20th century for southern Alberta (Shen et al., 2005) and, if continued, will agree with future projections made by Barrow and Yu (2005) that state the largest decreases in precipitation will occur during the summer season.

Table 5.2 Comparisons of simulated mean monthly and annual rainfall based on four 30-year historical periods. Change between periods is expressed as a difference [mm] and percent change [%] (A = Annual).

Time Series Comparisons		Month												
		1	2	3	4	5	6	7	8	9	10	11	12	A
1951-1980		0.3	0.6	0.1	4.4	27.2	94.4	41.2	65.4	39.5	8.1	0.4	0.6	282.3
1961-1990		0.5	0.6	0.1	6.2	29.0	84.1	46.6	57.8	40.5	11.2	0.4	0.6	277.7
1971-2000		0.2	0.0	0.2	5.3	31.0	88.8	56.6	59.8	38.0	10.6	0.5	0.6	291.7
1981-2010		0.9	0.0	0.3	5.6	30.4	107.6	51.7	49.5	41.6	11.7	1.4	0.3	301.1
1st Period		0.2	0.0	0.0	1.8	1.8	-10.3	5.3	-7.6	1.0	3.2	0.0	0.0	-4.5
	[%] Change	68.2	0.1	0.9	41.5	6.7	-10.9	12.9	-11.6	2.7	39.2	-1.4	-0.7	-1.6
2nd Period	Diff	-0.3	-0.6	0.0	-0.9	2.0	4.7	10.0	2.0	-2.6	-0.6	0.1	0.1	13.9
	[%] Change	-58.6	-99.3	33.7	-14.3	6.9	5.6	21.6	3.5	-6.4	-5.3	19.8	11.6	5.0
3rd Period	Diff	0.7	0.0	0.2	0.3	-0.6	18.8	-4.9	-10.3	3.6	1.1	0.9	-0.3	9.4
	[%] Change	323.0	-100.0	96.6	4.9	-1.9	21.2	-8.6	-17.2	9.5	10.6	169.0	-51.6	3.2

5.5.1.3 Snowfall

The simulation of annual snowfall relative to 1951-2010 shows steady decreases at a rate of 2.3%, 3.7% and 2.3% between the three comparison periods (Figure 5.2 and Table 5.3). Seasonal decreases occurred mostly between December and February, with snowfall amounts in March fluctuating

between periods. Attention is drawn to significant decreases in April snowfall (decreases of 18.7% during the first period and 15.8% during the second period), which is most likely attributable to warming temperatures that decrease the ratio of snow to rain. During November, snowfall has continually increased since the 1951-1980 period by 29.3% (23.6 mm). Zhang et al. (2000) found increasing trends in Canadian snowfall linked to autumn months which may coincide with increases seen in November for the 2041-2070 projection period.

Decreases in snowfall amounts have occurred during months (October to April) where snowfall historically has been the greatest. For example, Clow (2010), found decreases in 8 out of 14 regions throughout the southern Rocky Mountains in Colorado, during 1978-2007, while Knowles et al. (2006), observed similar results for the western United States. The primary mechanism responsible for decreases in snowfall and the subsequent phase change to rain has been attributed by many to be a result of increasing temperatures. Influences of Pacific circulation events such as El Nino-Southern Oscillation (ENSO) and Pacific Decadal Oscillation (PDO) have, according to Stewart et al. (2004) and others, clearly contributed to changing temperatures in the West. For example, linkages have been made and describe to a certain extent decreases in winter precipitation in the American southwest (Clow, 2010) and Cascades (Mote el al., 2005). However, there is uncertainty as to how much of an influence Pacific climate patterns such as ENSO or PDO contribute to warming temperatures in the Canadian Rockies.

Table 5.3 Comparisons of simulated mean monthly and annual snowfall based on four 30-year historical periods. Change between periods is expressed as a difference [mm] and percent change [%] (A = Annual).

Time Series Comparisons		Month												
		1	2	3	4	5	6	7	8	9	10	11	12	A
1951-1980		175.4	144.8	102.9	145.4	26.0	3.4	0.1	0.3	19.4	42.5	80.5	149.8	890.3
1961-1990		173.0	134.5	108.0	118.2	25.5	2.7	0.1	0.2	20.2	41.3	93.4	152.8	869.6
1971-2000		162.4	132.1	104.4	99.4	26.9	2.4	0.2	1.2	16.4	44.9	101.0	146.3	837.6
1981-2010		148.7	116.3	108.1	110.3	32.8	6.7	0.1	1.2	17.6	50.4	104.1	122.2	818.6
1st Period	Diff	-2.4	-10.3	5.1	-27.2	-0.5	-0.7	0.0	-0.1	0.8	-1.1	12.9	3.0	-20.8
	[%] Change	-1.3	-7.1	5.0	-18.7	-2.0	-19.7	79.7	-45.3	4.0	-2.7	16.0	2.0	-2.3
2nd Period	Diff	-10.6	-2.4	-3.6	-18.7	1.5	-0.3	0.1	1.1	-3.8	3.6	7.6	-6.5	-32.0
	[%] Change	-6.2	-1.8	-3.3	-15.8	5.9	-12.2	69.7	705.3	-18.7	8.6	8.1	-4.2	-3.7
3rd Period	Diff	-13.7	-15.8	3.7	10.9	5.9	4.4	0.0	0.0	1.2	5.5	3.1	-24.1	-18.9
	[%] Change	-8.4	-11.9	3.5	11.0	21.8	183.4	-24.0	0.5	7.6	12.3	3.1	-16.5	-2.3

5.5.1.4 Total Precipitation

Combining rainfall and snowfall into total precipitation reveals a consistent decrease in annual precipitation amounts since the 1951-1980 period. Although annual decreases have been consistent over the three periods (decreasing amounts of 16.4 mm, 12.4 mm and 4.2 mm), seasonal decreases have shown higher rates, especially between the months of December to February and April (Figure 5.2 and Table 5.4).During the December to February period, decreases in total precipitation are influenced by decreases in snowfall because of the cold temperatures which restrict the amount of rain that can fall. However, total precipitation in April was also strongly influenced by snowfall amounts (Table 5.3). Reported mean temperatures in April (Table 5.1) ranging between 0.4°C and 1.5°C are above freezing, which suggests a generally higher proportion of rainfall than snowfall (Table 5.3). Due to the continental climate and regular occurrence of strong winds (Chinook) during the spring and autumn, snowfall in southern Alberta can occur over a very wide range of mean daily temperatures (Kienzle, 2008). For example, in Kienzle (2008), reports from similar based studies show seasonal variations of threshold temperature ranges (defining the partitioning of precipitation), where the lowest threshold temperature (1.4°C) occurred in January , and the highest (2.6°C) in April. With mean temperatures in April being above

zero for comparison periods (Table 5.1), but falling below a threshold where precipitation can occur as snow, April snowfall amounts predominating seasonal decreases in total precipitation are supported.

Many studies have focused on a shift in precipitation phase changes as a result of increasing temperatures. For example, according to Knowles et al. (2006) and others, the fraction of snowfall to total precipitation will continue to decline as warming trends continue to increase across the western United States. Although these changes have been observed throughout North America, a detailed analysis identifying the timing of the rain to snow ratio in the CRW has yet to be accomplished.

Table 5.4 Comparisons of simulated mean monthly and annual total precipitation on four 30-year historical periods. Change between periods is expressed as a difference [mm] and percent change [%].

Time Series Comparisons		Month												
		1	2	3	4	5	6	7	8	9	10	11	12	A
1951-1980		175.7	146.4	105.0	171.6	72.1	98.8	41.3	65.9	72.0	65.4	86.0	151.6	1251.6
1961-1990		173.5	136.3	111.0	147.5	74.2	87.8	46.6	58.0	75.5	70.4	100.4	154.1	1235.2
1971-2000		162.6	132.5	108.2	129.1	80.3	92.1	56.7	61.1	67.8	75.4	109.1	147.8	1222.8
1981-2010		149.6	116.6	113.6	139.9	85.2	116.0	51.8	50.8	74.2	83.8	114.2	122.9	1218.6
1st Period	Diff	-2.2	-10.1	6.0	-24.1	2.2	-11.0	5.4	-7.8	3.5	5.1	14.3	2.5	-16.4
	[%] Change	-1.2	-6.9	5.7	-14.0	3.0	-11.1	13.0	-11.9	4.9	7.7	16.7	1.6	-1.3
2nd Period	Diff	-11.0	-3.8	-2.8	-18.4	6.0	4.3	10.1	3.1	-7.6	5.0	8.7	-6.3	-12.4
	[%] Change	-6.3	-2.8	-2.6	-12.4	8.1	4.9	21.6	5.4	-10.1	7.1	8.7	-4.1	-1.0
3rd Period	Diff	-13.0	-15.9	5.4	10.8	4.9	23.9	-4.9	-10.3	6.4	8.4	5.1	-24.9	-4.2
	[%] Change	-8.0	-12.0	5.0	8.4	6.1	25.9	-8.7	-16.8	9.4	11.1	4.7	-16.8	-0.3

5.5.1.5 SWE

SWE has shown consistent annual decline since the 1951-1980 period, where negative changes of 3.1%, 4.2% and 9.5% have occurred (Figure 5.2 and Table 5.5). Substantial decreases occurred seasonally, from December to June (winter and spring seasons) during the third comparison period, where significant decreases occurred (Table 5.5). The large seasonal decreases can be linked to decreasing amounts of snowfall that has mostly occurred from December to February and April. March snowfall has fluctuated, but on a small scale that seems to be consistent with the stagnant depths of SWE over the

historical periods. The last period during March however shows a large decrease in SWE depths which is likely to be partially explained by linkages to increasing amounts of precipitation falling as rain than snow in recent years. This assumption is supported by the notion that the decadal period of the 1990s may already include a climate change signal (Diaz-Nieto and Wilby, 2005), linking these decreases in SWE as an impact of climate change. Decreases in SWE depths during April and May may also correspond to recent influences of climate change, where an influence of increasing mean temperatures (0.4°C to 1.5°C, Table 5.1), being more pronounced in April, has the ability to increase melt rates as explained by Clow (2010), Stewart (2009), Knowles et al. (2006) and others causing declining snowpacks in the Western United States.

Table 5.5 Comparisons of simulated mean monthly SWE on four 30-year historical periods. Change between periods is expressed as a difference [mm] and percent change [%] (A=Annual).

Time Series Comparisons		Month												
		1	2	3	4	5	6	7	8	9	10	11	12	A
1951-1980		331.1	449.4	509.8	563.2	483.8	155.1	7.8	0.3	12.3	23.4	69.4	187.0	574.4
1961-1990		344.4	453.5	509.8	544.8	445.0	136.7	4.2	0.1	11.4	22.7	81.7	204.6	556.7
1971-2000		351.3	457.8	508.4	521.6	414.9	132.0	6.4	1.0	9.1	23.6	90.9	210.1	533.6
1981-2010		316.8	405.5	453.1	467.9	380.5	120.4	6.3	1.0	9.7	26.5	94.2	192.2	482.6
1st Period	Diff	13.2	4.1	0.0	-18.4	-38.8	-18.4	-3.7	-0.1	-0.8	-0.7	12.3	17.5	-17.7
	[%] Change	4.0	0.9	0.0	-3.3	-8.0	-11.9	-46.7	-43.8	-6.9	-2.9	17.7	9.4	-3.1
2nd Period	Diff	6.9	4.3	-1.4	-23.1	-30.1	-4.7	2.3	0.8	-2.3	0.8	9.2	5.5	-23.1
	[%] Change	2.0	0.9	-0.3	-4.2	-6.8	-3.4	54.0	599.7	-20.1	3.6	11.3	2.7	-4.2
3rd Period	Diff	-34.4	-52.3	-55.3	-53.7	-34.3	-11.6	-0.1	0.0	0.6	2.9	3.3	-17.9	-51.0
	[%] Change	-9.8	-11.4	-10.9	-10.3	-8.3	-8.8	-2.3	-0.8	6.2	12.4	3.6	-8.5	-9.5

5.5.1.6 Streamflow

Simulated flows in the CRW are characterized by small fluctuations during winter months, decreases in the summer and a mean annual decrease of approximately 0.2% since the first period of comparison (Figure 5.2 and Table 5.6). This rate is verified by Rood et al. (2004) and Byrne et al. (2006), where an approximate declining rate of 0.2% was observed for headwater streams in the Rocky Mountain

region near the Canada-United States border. Seasonal increases are identified in mean monthly streamflow for March and April and deceases occur during summer. These general findings are similar to trends observed by Zhang et al. (2001). As a result of warming temperatures, snowmelt derived streamflow from mountain rivers is occurring up to four weeks earlier in recent decades (Kienzle et al., 2012; Stewart et al., 2005; Cayan et al., 2001). Supplementary to an earlier spring runoff peak are three additional findings that correspond to simulated historic streamflow in the CRW. In analyzing declining summer flows from rivers that drain the Rocky Mountains, Rood et al. (2008), found slightly increased winter flows, an advancement and more gradual rising limb of the hydrograph and considerable decreased summer flows, especially in late summer and early autumn. Evidence of each of these findings are provided here (Table 5.6). For example, slightly increasing winter flows can be seen during January and March, rising discharge rates in April and slightly decreasing in May and June might be indicative of an advancement of a rising limb, and decreased flows during the months of August and September correspond to decreases observed in late summer early autumn.

Table 5.6 Comparisons of simulated mean monthly and annual streamflow on four 30-year historical periods. Change between periods is expressed as a difference [$m^3 s^{-1}$] and percent change [%] (A=Annual).

Time Series Comparisons		Month												
		1	2	3	4	5	6	7	8	9	10	11	12	A
1951-1980		2.8	2.8	3.0	8.9	41.9	59.5	19.6	10.4	8.9	7.2	4.9	3.6	14.5
1961-1990		2.7	2.6	3.2	10.1	41.1	56.2	17.1	9.3	8.0	7.0	4.7	3.4	13.8
1971-2000		2.8	2.4	3.7	10.5	40.7	53.9	18.1	9.6	7.7	6.9	5.1	3.5	13.8
1981-2010		3.1	2.5	4.2	10.4	38.3	54.3	18.3	8.8	7.8	7.6	5.7	3.4	13.7
1st Period	Diff	-0.1	-0.1	0.2	1.3	-0.8	-3.3	-2.5	-1.1	-0.9	-0.2	-0.2	-0.2	-0.7
	[%] Change	-4.1	-5.3	7.4	14.4	-1.9	-5.6	-12.8	-10.2	-10.0	-3.4	-3.6	-5.8	-4.6
2nd Period	Diff	0.1	-0.3	0.5	0.3	-0.4	-2.3	1.0	0.3	-0.4	0.0	0.4	0.1	-0.1
	[%] Change	3.3	-9.7	14.5	3.3	-1.1	-4.1	6.1	3.3	-4.5	-0.4	8.2	3.0	-0.4
3rd Period	Diff	0.3	0.1	0.5	-0.1	-2.4	0.4	0.2	-0.8	0.2	0.7	0.6	-0.1	0.0
	[%] Change	9.4	5.1	14.0	-0.9	-5.8	0.7	1.1	-8.4	2.2	10.1	12.3	-3.5	-0.3

5.5.3 Comparison of Historical and RCM-based 1971-2000 Time Series

To establish confidence in RCM-based projections of future climate time series for the CRW, comparisons of the historical and RCM-based 1971-2000 time series were compared. Results are shown in Figure 5.3 and Table 5.7. Results show a high degree of correlation for all hydrological variables, where, for example, the slopes of the 1:1 line are very close to unity for mean temperature, rainfall, snowfall, SWE and streamflow. The slope of the line for total precipitation is at unity. The coefficient of determination (r^2) for all variables is greater than or equal to 0.987, with an exception to streamflow, where r^2 is equal to 0.928. As a result of a high degree of correlation between historical and RCM-based 1971-2000 times series, there is high confidence in the RCM-based time series to represent the historical record as it is compared with future 2041-2070 climate scenarios.

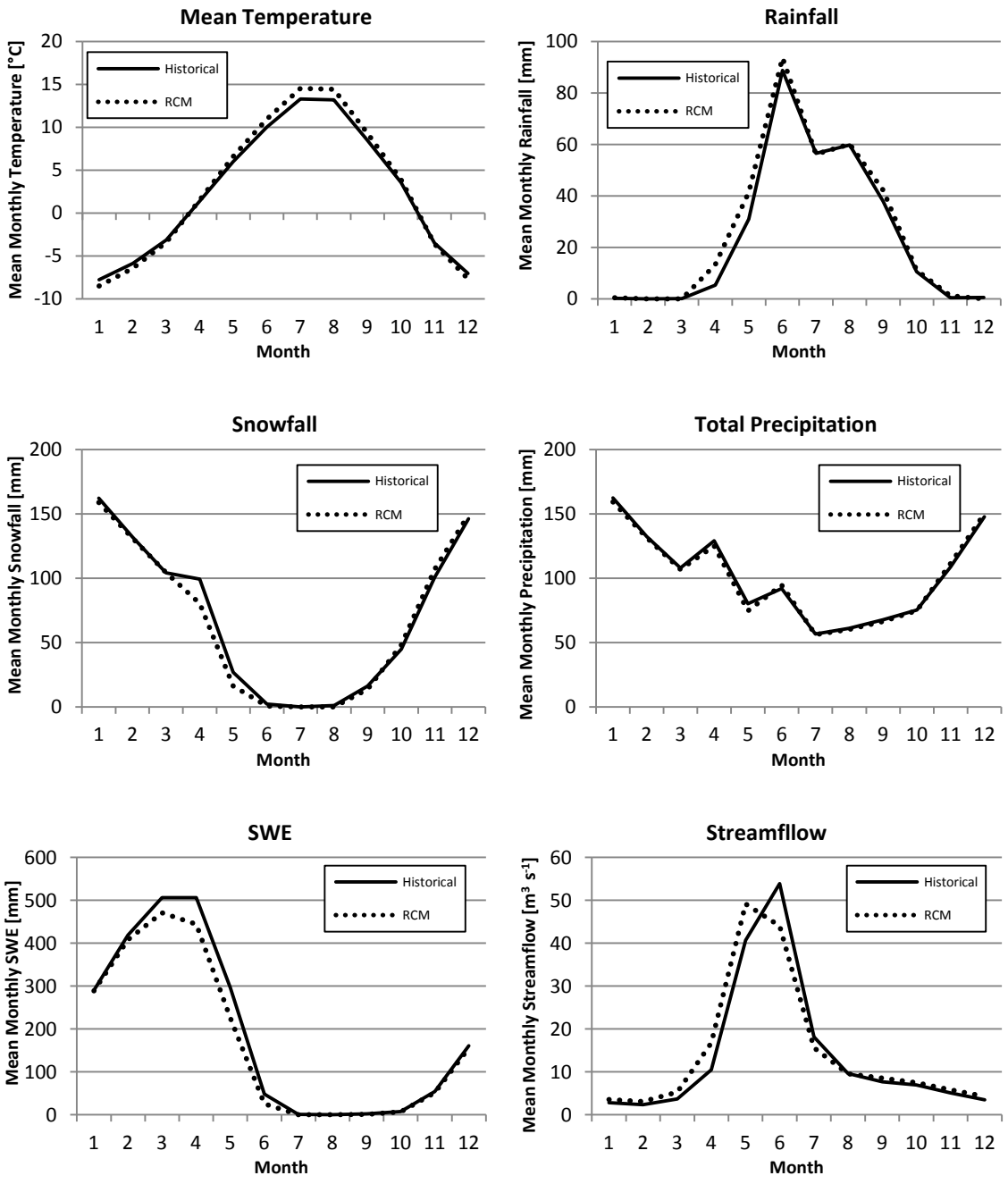

Figure 5.3 Comparisons of RCM-based vs. Historical 1971-2000 simulated mean temperature [°C], rainfall [mm], snowfall [mm], total precipitation [mm], SWE [mm] and streamflow [m^3 s^{-1}] for the CRW.

Table 5.7 Comparison of mean monthly historical and RCM 1971-2000 time series for mean temperature [°C], rainfall [mm], snowfall [mm], total precipitation [mm], SWE [mm] and streamflow [$m^3 s^{-1}$].

	Mean Temperature	Rainfall	Snowfall	Total Precipitation	SWE	Streamflow
Coefficient of Determination (r^2)	0.999	0.987	0.988	0.995	0.990	0.928
Slope	1.09	1.03	1.01	1.00	0.92	0.92
y-intercept	0.03	1.73	-2.57	-0.81	-2.50	1.87

5.5.4 Comparison of historical 1971-2000 and future 2041-2070 scenarios for hydrological variables in the CRW

With an established confidence in the RCM-based historical 1971-2000 time series, comparisons are made with future 2041-2070 RCM-based model output. The two 30-year periods are compared (Figure 5.4) for mean temperature, rainfall, snowfall, total precipitation, SWE and streamflow. Comparisons are made by calculating percent change between historical and future periods for each hydrological variable and are reported in Tables 5.8 to 5.13.

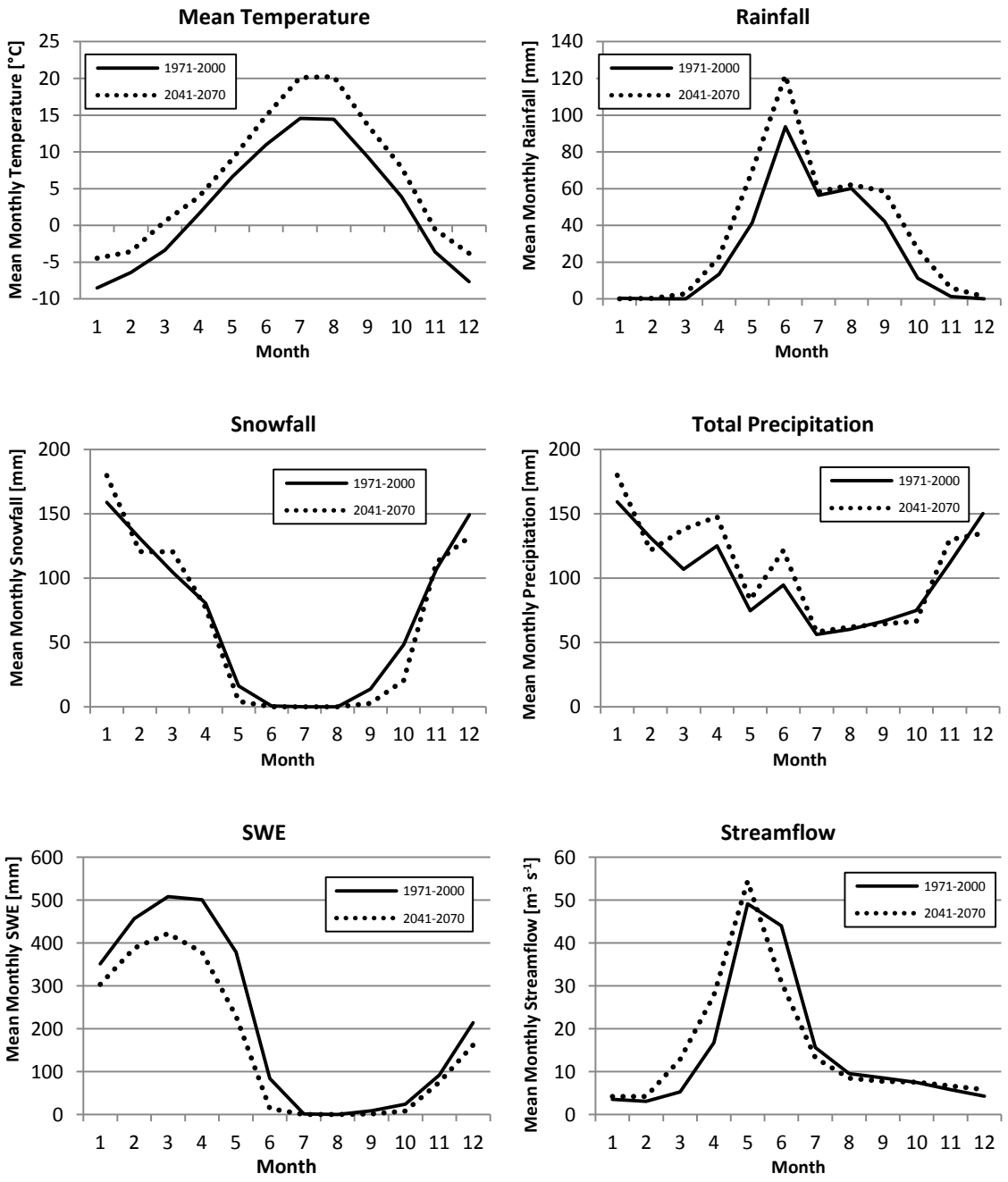

Figure 5.4 Downscaled historical (1971-2000) and future (2041-2070) climate simulations for mean temperature [°C], rainfall, snowfall [mm], total precipitation [mm], SWE [mm] and streamflow [$m^3 s^{-1}$] in the CRW.

5.5.4.1 Mean Temperature

According to simulated output (2041-2070) of mean temperature in the CRW, substantial increases are expected to occur for all months (Figure 5.4 and Table 5.8). The largest increases are expected in July and August, where increases of 5.6°C (38.2% change) and 5.8°C (40.2% change) are projected to take place. Significant increases during the winter months (December, January and February), are reported as 3.9°C, 4.0°C and 2.9°C.

Climate change studies generally agree that a warming is expected in future years under conditions of doubling of atmospheric CO_2 levels. According to reports by Barnett et al. (2005) and Gan (2000), GCMs project that temperature increases could be as much as 8°C during winter months by the mid-21st century. However, since GCMs project over large areas, for example, 250 -600 km, (Barrow and Yu, 2005; Flato et al., 2013), projected output is unable to accurately capture, inter alia, regional dynamics of topography and climate, thus rendering an 8°C increase in temperature as an unreliable projection for regional scale temperature change.

In a climate change study over North America using the third-generation Canadian RCM, Plummer et al. (2006) found seasonal mean air temperatures to increase by 3°C to 4°C for regions in the center of the continent by 2041-2060 and seasonal changes between +1.5 and +3°C during summer and autumn relative to a 1971-1990 gridded dataset. Comparisons with simulated 2041-2070 projections, CRW temperatures are about the same annually (+4.1°C) and higher seasonally (3.9°C, 5.6°C and 5.8°C during summer, and 4.3°C, 4°C and 3.1°C during autumn). Among other reasons, the choice of applying a single scenario that projects warmer and wetter conditions partially explains the higher seasonal temperature projections in the CRW.

According to Barrow and Yu, (2005), Canada's location in the high latitudes means that it is likely to experience some of the largest changes in climate, particularly in temperature. Rising temperatures will affect the regional hydrological cycle. For example, MacDonald et al. (2012) found that increasing temperatures in the central Rocky Mountains would result in substantial spatial changes in the date of minimum and maximum SWE, decreasing changes in the ratio of snow to rain and a shorter melt season.

Schindler and Donahue (2006) stated warming could create longer growing seasons and also exacerbate the effects of drought.

Table 5.8 Comparisons of mean monthly temperature for RCM based 1971-2000 and 2041-2070. Change between periods is expressed as a difference [°C] (A=Annual).

Time Series Comparisons (Mean Monthly)	Month												
	1	2	3	4	5	6	7	8	9	10	11	12	A
1971-2000	-8.5	-6.4	-3.4	1.5	6.6	11.0	14.6	14.4	9.3	3.9	-3.6	-7.6	2.5
2041-2070	-4.4	-3.6	0.5	3.9	9.1	14.9	20.1	20.2	13.6	7.9	-0.5	-3.8	6.6
Difference	4.0	2.9	3.9	2.3	2.4	3.9	5.6	5.8	4.3	4.0	3.1	3.9	4.1

5.5.4.2 Rainfall

Annual increases of 34.3% (110 mm) are expected under a 2041-2070 warmer and wetter scenario where with exception to the month of January, rainfall is expected to increase in all months in the CRW (Figure 5.4 and Table 5.9). Large projected increases of 28.2 mm (68% change) are expected in May and 28 mm (29.9% change) in June. Other increases in rainfall are projected to occur during the months of September and October, where September rainfall amounts are expected to increase by 16.3 mm (38.6% change) and 15.8 mm in October (140.6% change). Barrow and Yu (2005) have stated that the greatest decreases in precipitation amounts will occur during future summer months. The 2041-2070 CRW projections show (Table 5.9) that during the months July and August, rainfall will increase, but at an insignificant amount (1.9 mm for both months). Under scenarios representing a range of future conditions, summer rainfall in the CRW would likely agree with Barrow and Yu`s (2005) results.

Plummer et al. (2006), found changes in seasonal precipitation over regions in North America between 1971-1990 and 2041-2060 to be generally small, less than ±10%. In a climate impact study on the SMRW, MacDonald et al. (2011) found predicted change from a range of future scenarios for three future periods relative to 1961-1990. Changes in precipitation for the period centered around 2025 ranged from a 4% decrease to a 5% increase. Change centered around 2055 ranged from a 1% decrease to a 7% increase, and change around 2085 ranged from a 2% decrease to a 14% increase.

Despite projected decreases in summer precipitation (Barrow and Yu, 2005) warmer temperatures in future summer periods have the ability to cause more rainfall events. This is based on the premise that an increase in atmospheric water vapour is driven by enhanced ET, with the effect to encourage convective activity promoting cloud growth and precipitation (Nkemdirim and Purves, 1994). According to Trenberth et al. (2003), rainfall intensity, duration and frequency are as much a concern as total amounts, as these factors determine the amount that runs off and generates streamflow. Although these latter variables of rainfall are not discussed here, they are important as they create conditions for floods and drought, which can have enormous impacts on the environment and society (Trenberth et al., 2003).

Table 5.9 Comparisons of mean monthly rainfall for RCM based 1971-2000 and 2041-2070. Change between periods is expressed as a difference [mm] and percent change [%] (A=Annual).

Time Series Comparisons (Mean Monthly)	Month												
	1	2	3	4	5	6	7	8	9	10	11	12	A
1971-2000	0.4	0.0	0.1	13.4	41.5	93.7	56.3	60.1	42.3	11.2	1.29	0.1	320.4
2041-2070	0.1	0.4	2.8	22.8	69.7	121.7	58.2	62.1	58.6	27.0	5.9	1.27	430.4
Difference	-0.4	0.4	2.7	9.4	28.2	28.0	1.9	1.9	16.3	15.8	4.6	1.2	110.0
Percent Change [%]	-86.4	2048.4	3663.7	70.3	68.0	29.9	3.3	3.2	38.6	140.6	359.0	1255.0	34.3

5.5.4.3 Snowfall

It has been documented that the largest snow producing months for mountain ranges including the Sierra Nevada, Pacific Northwest ranges and Rocky Mountains are the months of January and March (Knowles et al., 2006). Future CRW projections support this statement, as all other months with exception of November show monthly decreases in snowfall amounts. The ratio of snowfall to total precipitation relative to 1961-1990 amounts at higher elevations in the SMRW is more than 70% (MacDonald et al., 2011). Over a range of future scenarios, this ratio is expected to decline to percentages as 65% in 2025, 54% in 2055 and 40% by 2085 (MacDonald et al., 2012). Projections of reduced snowfall for future periods

in Scotland revealed an almost total disappearance of snow in the southern lowlands, but a decreasing percentage in higher altitudes (Harrison et al., 2001).

Annual snowfall amounts for the 2041-2070 period are expected to decrease by approximately 5% (Table 5.4), most likely as a result of future warming causing snow-based precipitation to increasingly fall as rain instead of snow. Projected winter decreases occur during December and February and autumn decreases occur in September and October, where October decreases account for the largest mean monthly loss throughout the year (27.8 mm)

Decreasing snowpacks in mountain watersheds around the world are creating significant threats to water resources in downstream communities under a warming climate. The effective storage capacity that mountains exhibit is vital to the timing of streamflow that are needed throughout the year. Summer months are especially important as evaporative demand is at its peak and instream flow needs are often high due to a variety of water users. An example of this is shown in Barnett et al. (2005) where less winter snowfall in the Columbia River system will force residents, by 2050 or earlier, a choice of water releases for summer and autumn hydropower or spring and summer releases for salmon runs. Additionally, as a result of climate change the river system could not accommodate both without accepting considerable losses to either cause.

Table 5.10 Comparisons of mean monthly snowfall for RCM based 1971-2000 and 2041-2070. Change between periods is expressed as a difference [mm] and percent change [%] (A=Annual).

Time Series Comparisons (Mean Monthly)	Month												
	1	2	3	4	5	6	7	8	9	10	11	12	A
1971-2000	158.9	131.3	104.6	80.6	16.2	0.69	0.01	0.1	13.9	48.3	107.2	149.5	811.5
2041-2070	180.0	120.8	120.5	76.9	4.2	0.01	0.0	0.0	2.8	20.6	112.6	132.0	770.2
Difference	21.0	-10.5	15.8	-3.8	-12.0	-0.7	-0.01	-0.1	-11.1	-27.8	5.5	-17.5	-41.3
Percent Change [%]	13.2	-8.0	15.1	-4.7	-74.1	-99.1	-100.0	-100.0	-80.0	-57.4	5.1	-11.7	-5.1

5.5.4.4 Total Precipitation

Most climate studies suggest that under future conditions of climatic warming, the ratio of snow and rain to total precipitation is changing. For example, MacDonald et al. (2011) concluded that by 2085 decreases from 70% to 40% in the proportion of snow to rain in the SMRW will occur. Other studies (Groisman et al., 1999; Lapp et al., 2005; Lueng and Ghan, 1999; MacDonald et al., 2012) supporting these findings in alpine regions are also found in the literature. Increases in ET, groundwater recharge, soil moisture and streamflow in the Cline River watershed, in the Alberta Rocky Mountains, is expected to occur due to predicted increases in precipitation (Kienzle et al., 2012). These implications suggest that under similar conditions of increased precipitation and projected climate scenarios, the CRW could experience similar results.

Annual projections in the CRW show an approximate 8% increase in precipitation between 2041-2070 relative to the 1971-2000 period (Figure 5.4 and Table 5.11). The largest seasonal increases are expected to take place during March (29.1% change), April (18.1% change) and June (28.6% change). Increases in January are also projected to be high as a result of January being one of the highest snow producing months in the American northwest (Knowles., et al, 2006).

Table 5.11 Comparisons of mean monthly total precipitation for RCM based 1971-2000 and 2041-2070. Change between periods is expressed as a difference [mm] and percent change [%] (A=Annual).

Time Series Comparisons (Mean Monthly)	Month												
	1	2	3	4	5	6	7	8	9	10	11	12	A
1971-2000	159.4	131.6	107.1	125.3	74.8	94.7	56.3	60.2	66.6	75.0	111.7	150.3	1213.1
2041-2070	180.0	121.7	138.2	147.9	83.2	121.7	58.2	62.1	64.6	66.6	130.0	135.1	1309.2
Difference	20.6	-9.9	31.1	22.6	8.4	27.1	1.9	1.9	-2.0	-8.5	18.3	-15.2	96.1
Percent Change [%]	12.9	-7.5	29.1	18.1	11.2	28.6	3.3	3.1	-3.1	-11.3	16.4	-10.1	7.9

5.5.4.5 SWE

Snow processes have been considered a major controlling factor for a range of environmental systems in mountain regions (Beniston et al., 2003). Although factors such as temperature and

precipitation influence snow duration and timing of melt, it has been found that increases in air temperature, independent of precipitation, can have a substantial effect on declining SWE depths in the Rocky Mountains (MacDonald et al., 2012) and Pacific Northwest (Mote, 2003; Leung and Wigmosta, 1999). Future (2041-2070) CRW projections relative to 1971-2000, reveals that despite increases in snowfall during January and March (Figure 5.4 and Table 5.12), SWE depths are expected to experience substantial decreases between January and May. For example, SWE depths in January declined from 288.8 mm to 224.7 mm (negative change of 22.2%). February SWE declined from 408.3 mm to 339.5 mm (negative change of 16.9%), March SWE declined from 471 mm to 376.5 mm (negative change of 20.1%), April SWE declined from 444.6 mm to 311.1 mm (negative change of 30%) and May SWE declined from 225.6 mm to 101.3 mm (negative change of 55.1%).

It has been found that as a result of an average increase of 1°C in mountain temperature, a general rise in the altitude of the snowline by about 150 m can occur (Beniston et al., 2011). MacDonald et al. (2011, 2012) have concluded that due to warming temperatures in two separate high elevation watersheds in the Rocky Mountains, significant loss in snow extent and depth will occur. For example, snowpack in the North Saskatchewan headwater region could see significant decreases where, under scenarios of future warming relative to 1961-1990, the historical 30-year average snowline could increase from 2700 m to 3100 m by the 2020s, and an exhaustion of the peri-annual snow cover by the 2050s and 2080s. Additional to losses in snow duration and extent is the expected shift in snowmelt runoff affecting the timing of streamflow seasonality and the resulting negative impacts on the environment and society.

Table 5.12 Comparisons of mean monthly SWE for RCM based 1971-2000 and 2041-2070. Change between periods is expressed as a difference [mm] and percent change [%] (A=Annual).

Time Series Comparisons (Mean Monthly)	Month												
	1	2	3	4	5	6	7	8	9	10	11	12	A
1971-2000	288.8	408.3	471.0	444.6	225.6	25.5	0.3	0.002	0.9	6.6	51.7	155.3	521.4
2041-2070	224.7	339.5	376.5	311.1	101.3	2.6	0.0003	0.0	0.1	1.4	34.3	115.7	435.3
Difference	-64.1	-68.9	-94.5	-133.5	-124.3	-22.9	-0.3	-0.002	-0.8	-5.2	-17.4	-39.5	-86.1
Percent Change [%]	-22.2	-16.9	-20.1	-30.0	-55.1	-89.8	-99.9	-100.0	-86.8	-78.5	-33.7	-25.5	-16.5

5.5.4.6 Streamflow

The most serious risk from recent and projected climate warming in western Canada is a shift in the amount and timing of streamflow (Axelson et al. 2009; Regonda et al., 2005). The projected 2041-2070 streamflow runoff peak in the CRW relative to 1971-2000 is expected to take place during May (Figure 5.4 and Table 5.13). To identify the date of and possible shift in the spring runoff peak, an analysis of the weekly and or daily streamflow records is needed. Although differing methods exist (Regonda et al., 2005), this analysis will not be carried out at the time and scope of this research. The annual hydrograph for the CRW shows increases in the projected streamflow runoff record (Figure 5.4) during March (7.6 m^3 s^{-1} and 144.2% change), April (11.1 m^3 s^{-1} and 66.3% change) and May (5.2 m^3 s^{-1} and 10.7% change), while the month of June is represented by a steepening of the slope of the recession curve which gradually levels out between July and September.

According to Kienzle and Mueller (2013), the CRW contributes on average during the 1971-2000 period, approximately 15% of the total water yield to the larger ORB. As a result of the intensified demand on irrigated agriculture, the ORB is heavily dependent on contributions from its upstream headwater sub-regions. Therefore, as a seasonal shift resulting in decreased summer streamflow volumes is expected, it is inevitable that there will be added stress to the ORB system during peak demand periods when ET is high. Climate change simulations of projected warming in many watersheds around the world are expecting an earlier shift in streamflow runoff. For example, in the Rhine River basin in Europe, projected warming of 1°C to 2.4°C is expected to cause a shift in the precipitation regime into one dominated by rainfall, causing increased winter discharge, an increased frequency and magnitude of peak flows and longer and more frequent periods of low flow throughout the summer (Barnett et al., 2005). MacDonald et al. (2011), have found that according to future projections centered around 2025, 2055 and 2085, an earlier onset of snowmelt and probable declines in max SWE infers an overall earlier onset of spring in the SMRW. Similarly, Kienzle et al. (2012) have found that in the UNSRB, projected warming will cause an earlier shift of approximately 18 days in the 2020s, 21 days in the 2050s and 26 days in the 2080s, which

suggests that these shifts will have important economic and environmental implications on water resources in the future.

Table 5.13 Comparisons of mean monthly streamflow for RCM based 1971-2000 and 2041-2070. Change between periods is expressed as a difference [$m^3 s^{-1}$] and percent change [%] (A=Annual).

Time Series Comparisons (Mean Monthly)	Month												
	1	2	3	4	5	6	7	8	9	10	11	12	A
1971-2000	3.6	3.1	5.3	16.7	49.2	44.0	15.6	9.5	8.5	7.5	5.8	4.3	14.5
2041-2070	4.2	4.3	12.9	27.8	54.4	30.9	13.2	8.5	7.8	7.5	6.7	5.8	15.4
Difference	0.6	1.1	7.6	11.1	5.2	-13.1	-2.4	-1.1	-0.7	0.0	0.9	1.5	0.9
Percent Change [%]	17.8	36.5	144.2	66.3	10.7	-29.8	-15.3	-11.2	-8.7	0.3	15.4	35.1	6.4

Chapter 6: Summary, Conclusions and Recommendations

6.1 Summary and Conclusions

The ACRU agro-hydrological modelling system has been used in this research to estimate critical historical and future hydro-climatological variables, including streamflow that have occurred during 1951-2010, and will occur in the future period 2041-2070 in the Castle River watershed (CRW). To accomplish this objective, hydrological processes in the CRW are driven by ACRU using hydro-meteorological data. In the recent past, ACRU has simulated historical and future hydro-climatological variables using a driver station method as described by Hungerford et al. (1989) for watersheds in the Alberta Rocky Mountains (Kienzle et al., 2012; Nemeth et al., 2012) and foothills (Forbes et al., 2010) regions. In each study, a base or driver station was chosen to drive the hydrological model by extrapolating meteorological variables across the watershed, making corrections for differences between elevation, slope and aspect between the station and the watershed. In this case, the Beaver Mines Climate Station (BMCS, 05AA022) was chosen to drive the hydrological processes in the CRW. During model setup, a newly created spatially gridded dataset of 10 x 10 km resolution (Hutchinson et al., 2009) was made available (here after referred to 10 km Grid). The 10 km Grid offers an increasing number of virtual base stations spatially distributed evenly across the watershed. Therefore, in consequence of obtaining a dataset which offered expectations of a better simulation, a sub-objective was formalized in comparing the two datasets to identify which one had the ability to drive a superior simulation. The dataset which performed the best would then be applied to simulate the future 2041-2070 hydrological behavior of the CRW. This represents the first time the 10 km Grid has been applied by the ACRU model and also represents the first study where the 10 km Grid was compared directly to the performance of a single driver station (BMCS).

ACRU was parameterized twice, first by using the BMCS and its associated meteorological variables, and second by using nine virtual driver stations from the 10 km Grid and their associated meteorological variables. The parameterization of ACRU is based on the partitioning of the watershed into hydrological response units (HRUs), which can be described as sub-units that represent specific dynamics unique to the hydrological response in the watershed. HRUs were delineated based on watershed

boundary, land cover, elevation, and solar radiation. Each HRU is then parameterized according to variables unique to the CRW that influence the overall response of the hydrological system. For example, inter alia, temperature, precipitation, evapotranspiration (ET), land cover, soils, albedo, rooting depth and forest canopy coverage. In order to overcome instances where insufficient or no data were available (PTCs and LAI) for the CRW, data were taken from an earlier application of the ACRU model in the UNSRB (Nemeth, 2010, Nemeth et al. 2011) and applied with minor corrections (see Section 3.5.1.7) to the CRW. In addition to the contribution of data from Nemeth (2010,) other input parameters were checked against those used in other studies and changes were made where necessary. For example, as a result of finding a range of values that have been applied to simulate canopy interception capacity of snow, an analysis was performed on the sensitivity of ACRU to simulate snowpack by making changes to forest canopy coverage percentages and resulting interception capacities. The findings revealed general model insensitivity to these snow routines which will constitute the basis of future model improvements.

Model verification of ACRU on hydro-climatological variables in the CRW was carried outfor each dataset, the BMCS and the 10 km Grid. Model verification was based on the 10-year 1981-1990 period of record where verification of mean temperature, snow water equivalent (SWE) and streamflow was carried out. Data used for model verification were collected from surrounding climate stations containing observations independent of driver station input data. For example, measures of mean temperature were obtained from seasonal climate stations located in the watershed; measures of SWE were obtained from snow pillow and snow survey data and streamflow measurements from hydrometric gauges maintained by Environment of Canada.

Results of the verification for the 10 km Grid relative to the Beaver Mines data showed that for mean temperature, the 10 km Grid had a superior simulation (r^2 = 0.978) daily and (r^2 = 0.990) monthly compared to that of the Beaver Mines daily (r^2 = 0.921) and monthly (r^2 = 0.978). Verification of SWE using Beaver Mines resulted in a stronger coefficient of determination daily (r^2 = 0.622) and monthly (r^2 = 0.755) monthly than the 10 km Grid daily (r^2 = 0.463) monthly (r^2 = 0.609), but by comparison of the simulated and observed means of accumulated SWE depths, the percentage difference pertaining to the 10 km Grid

resulted in a daily under-simulation by 11.01% compared to a 19.36% under-simulation by the Beaver Mines and monthly 0.05% over-simulation by the 10 km Grid versus a 3.26% over-simulation by the Beaver Mines.

According to Legates and McCabe (1999), the goodness of fit tool of r^2 suffers from limitations that can make it a poor evaluation of model performance. This is due to correlation based measures such as r^2 being more sensitive to outliers than observations around the mean. Thus, to increase the evaluation of streamflow modelling, the use of the Nash-Sutcliffe Coefficient of Efficiency (NSE), which is widely used to evaluate the performance of hydrological models, was used. Additional to using these statistical evaluation methods, the percent difference of variances were also compared.

In all cases of streamflow comparison during the 1981-1990 period, the BMCS dataset was out-performed by the 10 km Grid, where for example, superior results from the 10 km Grid were daily (r^2 = 0.849) and monthly (r^2 = 0.898), daily (NSE = 0.84) and monthly (NSE = 0.90) and daily (difference of variance = -3.12%) monthly (difference of variance = -3.88%) compared to Beaver Mines statistical results of daily(r^2 = 0.766) and monthly (r^2 = 0.809), daily (NSE = 0.75) and monthly (NSE = 0.78) and daily (difference of variance = -75.61%) monthly (difference of variance = -75.49%). As a result of the 10 km Grid out-performing the BMCS in simulating historical 1981-1990 hydro-climatological variables, the 10 km Grid was chosen to simulate future hydrological behavior of the CRW for the 2041-2070 period.

Simulating climate change impacts on hydrological processes for an area requires the choice and application of a range of scenarios depicting future climates. Prior to the inception of this research, an agreement was made that climate specialist Dr. David Sauchyn (University of Regina) and Elaine Barrow (Prairie Adaptation Research Collaborative, PARC) would provide five climate change scenarios in the form of downscaled GCM (CanESM2) to RCM (CanRCM4) climate output representing a range of future climate scenarios for the CRW, but within the time frame of this research only a single scenario was made available. This represents a main problem in climate scenario work (Barrow and Yu, 2005), where typically more than one scenario should be applied.

Two RCM-based datasets were provided, one representing a baseline period (1971-2000), and one representing future (2041-2070) projections. The RCM-based output for the future period of record represents a scenario of warmer and wetter conditions under global climate change for the CRW region. Further downscaling of the RCM data (resolution of 25 x 25 km) to match the resolution of the 10 km Grid was accomplished through extensive GIS spatial analysis using area weighting based on spatial proportions of each RCM grid that spatially overlaid a 10 km polygon. To establish confidence in the RCM-based 1971-2000 baseline, ACRU was run using the 10 km Grid for the 1971-2000 period of record and compared against the RCM-based 1971-2000 period. Comparisons of mean temperature, rainfall, snowfall, total precipitation, SWE, and streamflow, were made and confidence was established in the RCM-based 1971-2000 period as all variables showed an $r^2 > 0.987$, with exception to streamflow whose $r^2 = 0.928$. Before comparing the baseline RCM with future projections, model output from a 10 km Grid-based run (1951-2010) was separated in to four 30-year time series and (1951-1980, 1961-1990, 1971-2000, 1981-2010) and compared to identify how historical 30-year climate has changed since 1951-1981.

Results from the comparison of future 2041-2070 time series relative to 1971-2000 show substantial rises in mean temperatures and rainfall. Projected increases for the CRW are in line with expected changes reported by Plummer et al., (2006) and MacDonald et al., (2012). Rises in mean temperature will cause declines in snowfall amounts limiting the development of snowpack to take place (Barnett et al, 2005; Harrison et al., 2001; MacDonald et al., 2011). Considerable decreases of SWE depths are projected during all months including a shift in the snowmelt period to take place earlier in the year. Projections of declining SWE depths are in line with other climate change studies (Leung and Wigmosta, 1999; MacDonald et al., 2012; Mote, 2003). A substantial impact on water resources is expected in the CRW as an earlier melt period has the potential to create a shift in the peak streamflow hydrograph (Rood et al., 2008; Stewart et al., 2004; Stewart, 2009). Although a shift in the peak runoff period was not visually determined for the future, an earlier runoff peak has been associated in climate change impact studies as a precursor of added stress to water resources during peak demand summer months (Barnett et al., 2005; Kienzle et al., 2012; Regonda et al., 2005; Rood et al., 2008; Schindler and Donahue, 2006).

6.2 Recommendations

6.2.1 Improvement to Present Research

This study has demonstrated the ability of the ACRU model to accurately simulate historical hydro-climatological variables in a headwater Canadian Rocky Mountain region. Projections of future climate in the CRW were also simulated, but there is always uncertainty associated with making predictions about the state of climate and subsequent hydrological processes in a future period. According to Beven (2001), the main reason why we need to model rainfall-runoff processes results from the limitations of hydrological measurement techniques and measurements in space and time. Additionally, Beven (2001) suggested the ultimate aim of prediction using models must be to improve decision-making about hydrological problems, such as water resources planning, flood protection and the licensing of abstractions.

One of the major limitations of this research deals with the amount and quality of available data, which is a typical characteristic of mountainous watersheds. Currently, most climate stations in the mountains measuring temperature and precipitation are located in low elevation areas and in proximity to populated areas. In contrast, the scientific community is still limited in their understanding about precipitation amounts on the tops of mountains. Thus, it is essential that an improved climate station network is made available at a wider spatial and temporal scale. There are currently major limitations in soil data in the mountains. In the CRW some soil data are available, but only for a small portion (<10%), at the low lying mouth of the watershed. Currently, soil data in Alberta only extends to the adjacent foothills regions and very little, if any, actually penetrates the interior Rocky Mountain region. Improved land cover data are also needed. Current land cover is generalized to some extent, but an improved dataset would enhance the quality of research able to be performed. Snow data in the mountains are often very sparse, yet they are one of the most important types of data in hydrological studies. Currently there are only two sites in the entire CRW where SWE data are collected. In one location, a snow pillow and a snow course has been set up, while the other is solely a snow course site. Improvements to a snow network would provide an increased capacity to make quality predictions regarding snowmelt and streamflow runoff

peaks and volumes. Remote sensing has can be used to provide information on land cover, soils and snow extent, which if added, could enhance the quality of modelling and analysis.

It would be useful to make a comparison between currently used lapse rates and those delineated following methodology set forth by Pigeon and Jiskoot (2008) that focuses on the separation of inversion days, the categorization of wet and dry precipitation days, and applying the multi-year lapse rate mode.

Statistical results of the SWE verification and sensitivity analysis on snow interception reveal that ACRU's snow routines could be improved. It is assumed that current snow routines in ACRU are treated as very basic in terms of snow interception storage and evaporation and sublimation processes.

When the 10 km Grid was first obtained, the data were originally made available for the 1961-2003 period of record. Several months later, an updated dataset was made available for the 1951-2010 period. Data from the 10 km Grids and climate stations that overlaid each other were compared. Prairie-based stations compared well and those located in the mountains were slightly more variable as expected. The 2004-2010 period however, initially showed considerable variability for mountain-based grids. Since the dataset was obtained from the AAFC, these anomalies were brought to their attention and a newly updated gridded dataset was provided. Comparison between the gridded and observed datasets revealed improvement. Thus, to further improve this research, it would be of interest to remove the 2004-2010 period from all datasets to see an effect of change on the verification and simulation of hydrological processes in the CRW.

6.2.2 Future Research

Modelling the hydrological impacts of climate change on the CRW requires the application of future climate scenarios depicting a range of possible future climates. Due to time constraints on this research, only a single scenario depicting warmer and wetter conditions was made available. The four other scenarios representing a more complete range of climate projections were not completed in time to be included in the simulation of future climate change. Thus, to aid those in water resource management

and planning, the addition of the four absent climate scenarios is needed to make a more robust projection of future climate change in the CRW.

In recent years, there has been much concern from local residents that are located near and within the CRW opposing logging in the area. There has been interest from industry to log certain parts of the CRW and access has been granted as early as the 2020s. Of interest to local residents, nearby communities and government would be a hydrological impact assessment of logging the CRW. An objective such as this would be relatively easy to accomplish. The current model setup for the CRW would all remain the same with exception to the addition of a land cover file depicting projected land use change, and all ACRU variables either representing land cover dependent hydrological processes (such as interception rates or plant transpiration coefficients) would be adjusted accordingly. A simple model run would then provide a foundation on which an impact assessment could be made.

It has been stated that considerable snowpack spatial variability exists within small mountain ranges (Pigeon and Jiskoot, 2008). Some new research in the CRW is investigating snowpack at the West Castle Ski Resort using LiDAR (Light Detection And Ranging) technology. LiDAR provides sub-meter resolution which allows for an analysis of seasonal snow extent and depth. Current snowpack measurement techniques rely on the digging of snow pits, mapping out snow surveys, and the setup and maintenance of snow pillows. Although the LiDAR research is currently focused on the mapping of snow properties on a single mountain range, expanding this to a regional or watershed scale would provide supplementary data from which comparisons to present snow data could be made as well as estimations to un-monitored sites.

Hydrological modelling is a tool used to better understand the environment in its current condition and in the future. Although this research has provided a glimpse into the future hydrological behavior of the CRW under warmer and wetter conditions, there is a need to identify whether the variability of future climate and whether extreme events will continue to increase in frequency and intensity.

REFERENCES CITED

Ahrens, C.D. (2007). *Meteorology today: an introduction to weather, climate, and the environment*: Cengage Learning.

Agriculture and Agri-Food Canada. (2013). 10 km Gridded Dataset

Akinremi, O., McGinn, S., and Cutforth, H. (1999). Precipitation Trends on the Canadian Prairies*. *Journal of Climate, 12*(10), 2996-3003.

Al-Rawas, G.A., and Valeo, C. (2009). Characteristics of rainstorm temporal distributions in arid mountainous and coastal regions. *Journal of Hydrology, 376*(1), 318-326.

Alberta Agriculture and Rural Development. (2012a). Agricultural Regions of Alberta Soil Inventory Database (AGRASID), Available from: http://www1.agric.gov.ab.ca/$Department/deptdocs.nsf/All/sag14652

Alberta Agriculture and Rural Development. (2012b). Current and Historical Alberta Weather Station Data Viewer, Available from: http://agriculture.alberta.ca/acis/alberta-weather-data-viewer.jsp

Alberta Environment. (2009). *Monitoring and Managing Snow Data.* Paper presented at the Western Snow Conference, Canmore, Alberta.

Alberta Environment. (2013). What about Climate Change? Retrieved November 4, 2013, from http://environment.alberta.ca/02497.html

Alberta Environment. (2014). Water Allocation. Retrieved June 17, 2014, from http://esrd.alberta.ca/water/programs-and-services/water-allocation.aspx

Allen, R.G., Pereira, L.S., Raes, D., and Smith, M. (1998). Crop evapotranspiration-Guidelines for computing crop water requirements-FAO Irrigation and drainage paper 56. *FAO, Rome, 300*, 6541.

Arnell, N.W. (1992). Factors controlling the effects of climate change on river flow regimes in a humid temperate environment. *Journal of Hydrology, 132*(1), 321-342.

Axelson, J.N., Sauchyn, D.J., and Barichivich, J. (2009). New reconstructions of streamflow variability in the South Saskatchewan River Basin from a network of tree ring chronologies, Alberta, Canada. *Water Resources Research, 45*(9).

Balk, B., and Elder, K. (2000). Combining binary decision tree and geostatistical methods to estimate snow distribution in a mountain watershed. *Water Resources Research, 36*(1), 13-26.

Barnett, T.P., Adam, J.C., and Lettenmaier, D.P. (2005). Potential impacts of a warming climate on water availability in snow-dominated regions. *Nature, 438*(7066), 303-309.

Barrow, E., and Yu, G. (2005). Climate scenarios for Alberta. *Prairie Adaptation Research Collaborative*.

Barry, R.G. (2008). *Mountain Weather and Climate* (3 ed.). New York: Cambridge University Press.

Basist, A., Bell, G.D., and Meentemeyer, V. (1994). Statistical relationships between topography and precipitation patterns. *Journal of Climate, 7*(9), 1305-1315.

Bathurst, J., and O'Connell, P. (1992). Future of distributed modelling: the Système Hydrologique Européen. *Hydrological Processes, 6*(3), 265-277.

Beckers, J., Smerdon, B., and Wilson, M. (2009). Review of hydrologic models for forest management and climate change applications in British Columbia and Alberta. *FORREX Series*(25).

Beniston, M., Keller, F., and Goyette, S. (2003). Snow pack in the Swiss Alps under changing climatic conditions: an empirical approach for climate impacts studies. *Theoretical and Applied Climatology, 74*(1-2), 19-31.

Beniston, M., Stoffel, M., & Hill, M. (2011). Impacts of climatic change on water and natural hazards in the Alps: can current water governance cope with future challenges? Examples from the European "ACQWA" project. *Environmental Science & Policy, 14*(7), 734-743.

Beven, K. (1989). Changing ideas in hydrology—the case of physically-based models. *Journal of Hydrology, 105*(1), 157-172.

Beven, K. (2011). *Rainfall-runoff modelling: the primer*: John Wiley and Sons.

Beven, K. (1979). A sensitivity analysis of the Penman-Monteith actual evapotranspiration estimates. *Journal of Hydrology, 44*(3), 169-190.

Beven, K. (2001). Rainfall-Runoff Modelling: The Primer. (First ed.): New York: Wiley.

Blandford, T.R., Humes, K.S., Harshburger, B.J., Moore, B.C., Walden, V.P., and Ye, H. (2008). Seasonal and synoptic variations in near-surface air temperature lapse rates in a mountainous basin. *Journal of Applied Meteorology and Climatology, 47*(1), 249-261.

Boé, J., Terray, L., Habets, F., and Martin, E. (2007). Statistical and dynamical downscaling of the Seine basin climate for hydro-meteorological studies. *International Journal of Climatology, 27*(12), 1643-1655.

Bolstad, P.V., Swift, L., Collins, F., and Régnière, J. (1998). Measured and predicted air temperatures at basin to regional scales in the southern Appalachian mountains. *Agricultural and Forest Meteorology, 91*(3), 161-176.

Bormann, H., Breuer, L., Giertz, S., Huisman, J.A., and Viney, N.R. (2009). Spatially explicit versus lumped models in catchment hydrology–experiences from two case studies *Uncertainties in environmental modelling and consequences for policy making* (pp. 3-26): Springer.

Brierley, J.A., Martin, T.C., and Spiess, D.J. (2001). AGRASID Version 3.0: Soil Landscapes User's Manual Retrieved August 6, 2013, from http://www1.agric.gov.ab.ca/$department/deptdocs.nsf/all/sag3254/$file/AGRASID%20Users%20Manual.pdf?OpenElement

Brutsaert, W. (1988). *Evaporation into the atmosphere: theory, history, and applications*: Reidel Dordrecht.

Bunnell, F.L., McNay, R.S., and Shank, C.C. (1985). *Trees and Snow: The Deposition of Snow on the Ground: a Review and Quantitative Synthesis*: Research, Ministries of Environment and Forests.

Burn, D.H. (1994). Hydrologic effects of climatic change in west-central Canada. *Journal of Hydrology, 160*(1), 53-70.

Byrne, J.M., Barendregt, R., and Schaffer, D. (1989). Assessing potential climate change impacts on water supply and demand in southern Alberta. *Canadian Water Resources Journal, 14*(4), 5-15.

Byrne, J., Kienzle, S., Johnson, D., Duke, G., Gannon, V., Selinger, B., and Thomas, J. (2006). Current and future water issues in the Oldman River Basin of Alberta, Canada. *Water Science and Technology, 53*(10), 327.

Calder, I.R. (1982). *Forest evaporation.* Paper presented at the Proc. Can. Hydrol. Symp.

Canadell, J., Jackson, R., Ehleringer, J., Mooney, H., Sala, O., and Schulze, E.-D. (1996). Maximum rooting depth of vegetation types at the global scale. *Oecologia, 108*(4), 583-595.

Castle Mountain Resort. (2009). The Mountains - Environment Retrieved July 4, 2013, from http://www.skicastle.ca/environment.cfm

Cayan, D.R., Dettinger, M.D., Kammerdiener, S.A., Caprio, J.M., and Peterson, D.H. (2001). Changes in the onset of spring in the western United States. *Bulletin of the American Meteorological Society, 82*(3), 399-415.

Chen, D., Gao, G., Xu, C.-Y., Guo, J., and Ren, G. (2005). Comparison of the Thornthwaite method and pan data with the standard Penman-Monteith estimates of reference evapotranspiration in China. *Climate Research, 28*(2), 123-132.

Chow, V.T. (1964). Handbook of applied hydrology; a compendium of water-resources technology.

Christensen, N.S., Wood, A.W., Voisin, N., Lettenmaier, D. P., and Palmer, R. N. (2004). The effects of climate change on the hydrology and water resources of the Colorado River basin. *Climatic Change, 62*(1-3), 337-363.

Clow, D.W. (2010). Changes in the timing of snowmelt and streamflow in Colorado: a response to recent warming. *Journal of Climate, 23*(9), 2293-2306.

Daly, C. (2006). Guidelines for assessing the suitability of spatial climate data sets. *International Journal of Climatology, 26*(6), 707-721.

Daly, C., Gibson, W.P., Taylor, G.H., Johnson, G.L. and Pasteris, P (2002). A knowledge-based approach to the statistical mapping of climate. *Climate Research, 22*(2), 99-113.

Daly, C., Helmer, E.H., and Quiñones, M. (2003). Mapping the climate of Puerto Rico, Vieques and Culebra. *International Journal of Climatology, 23*(11), 1359-1381.

Daly, C., Neilson, R.P., and Phillips, D.L. (1994). A statistical-topographic model for mapping climatological precipitation over mountainous terrain. *Journal of Applied Meteorology, 33*(2), 140-158.

Daly, C., Smith, J.W., Smith, J.I., and McKane, R.B. (2007). High-resolution spatial modeling of daily weather elements for a catchment in the Oregon Cascade Mountains, United States. *Journal of Applied Meteorology and Climatology, 46*(10), 1565-1586.

Daly, C., Halbleib, M., Smith, J.I., Gibson, W.P., Doggett, M.K., Taylor, G.H., Curtis, J., Pasteris, P.P. (2008). Physiographically sensitive mapping of climatological temperature and precipitation across the conterminous United States. *International Journal of Climatology, 28*(15), 2031-2064.

Dawdy, D.R., and O'Donnell, T. (1965). Mathematical models of catchment behavior. *J. Hydraul. Div. Am. Soc. Civ. Eng, 91*, 123-137.

De Loë, R., Kreutzwiser, R., and Moraru, L. (2001). Adaptation options for the near term: climate change and the Canadian water sector. *Global Environmental Change, 11*(3), 231-245.

Dent, M.C., Schulze, R.E., and Angus, G.R. (1988). *Crop Water Requirements, Deficits and Water Yield for Irrigation Planning in Southern Africa: Report to the Water Research Commission on the Project" A Detailed Regional Soil Moisture Deficit Analysis for Irrigation Planning in Southern Africa"*: University of Natal, Department of Agricultural Engineering.

Dettinger, M.D., and Cayan, D.R. (1995). Large-scale atmospheric forcing of recent trends toward early snowmelt runoff in California. *Journal of Climate, 8*(3), 606-623.

Diaz-Nieto, J., and Wilby, R.L. (2005). A comparison of statistical downscaling and climate change factor methods: impacts on low flows in the River Thames, United Kingdom. *Climatic Change, 69*(2-3), 245-268.

Dingman, S.L. (2002). *Physical hydrology* (2nd ed.): Prentice Hall, Englewood Cliffs, NJ. Physical hydrology. 2nd ed. Prentice Hall, Englewood Cliffs, NJ.

Diskin, M.H. (1964). *A basic study of the linearity of the rainfall-runoff process in watersheds.* University of Illinois.

Dodson, R., and Marks, D. (1997). Daily air temperature interpolated at high spatial resolution over a large mountainous region. *Climate Research, 8*(1), 1-20.

Dooge, J.C. (1959). A general theory of the unit hydrograph. *Journal of Geophysical Research, 64*(2), 241-256.

Drost, F., Renwick, J., Bhaskaran, B., Oliver, H., and McGregor, J. (2007). Simulation of New Zealand's climate using a high-resolution nested regional climate model. *International Journal of Climatology, 27*(9), 1153-1169.

Durman, C., Gregory, J., Hassell, D., Jones, R., and Murphy, J. (2001). A comparison of extreme European daily precipitation simulated by a global and a regional climate model for present and future climates. *Quarterly Journal of the Royal Meteorological Society, 127*(573), 1005-1015.

Elder, K., Dozier, J., and Michaelsen, J. (1991). Snow accumulation and distribution in an alpine watershed. *Water Resources Research, 27*(7), 1541-1552.

Environment Canada. (2012a). Historic Climate Data, Available from: http://climate.weather.gc.ca/index_e.html#access

Environment Canada. (2012b). Canadian Climate Normals, Available from: http://climate.weather.gc.ca/climate_normals/index_e.html#1981

Environment Canada. (2012c). Hydrometric Database (HYDAT), Water Survey of Canada. Available from: http://wateroffice.ec.gc.ca/search/search_e.html?sType=h2oArc

Everson, C. (2001). The water balance of a first order catchment in the montane grasslands of South Africa. *Journal of Hydrology, 241*(1), 110-123.

Flato, G., Marotzke, J., Abiodun, B., Braconnot, P., Chou, S.C., Collins, W., Cox, P., Driouech, F., Emori, S., Eyring, V., Forest, C., Gleckler, P., Guilyardi, E., Jakob, C., Kattsov, V., Reas, C. and Rummukain, M. (2013). Evaluation of Climate Models. In: Climate Change 2013: The Physical Science Basis. Contribution of Working Group I to the Fifth Assessment Report of the Intergovernmental Panel on Climate Change. In Stocker, T. F., Qin, D., Plattner, G.-K., Tignor, M., Allen, S.K., Boschung, J., Nauels, A., Xia, Y., Bex, V. and Midgle, P. M. (Eds.). Cambridge, United Kingdom and New York, NY, USA: IPCC.

Forbes, K.A., Kienzle, S.W., Coburn, C.A., Byrne, J.M., and Rasmussen, J. (2011). Simulating the hydrological response to predicted climate change on a watershed in southern Alberta, Canada. *Climatic Change, 105*(3-4), 555-576.

Fowler, H., Blenkinsop, S., and Tebaldi, C. (2007). Linking climate change modelling to impacts studies: recent advances in downscaling techniques for hydrological modelling. *International Journal of Climatology, 27*(12), 1547-1578.

Gan, T.Y. (2000). Reducing vulnerability of water resources of Canadian prairies to potential droughts and possible climatic warming. *Water Resources Management, 14*(2), 111-135.

Gardner, A.S., Sharp, M.J., Koerner, R.M., Labine, C., Boon, S., Marshall, S.J., Burgess, D.O., Lewis, D. (2009). Near-surface temperature lapse rates over Arctic glaciers and their implications for temperature downscaling. *Journal of Climate, 22*(16), 4281-4298.

GeoBase. (2011). Land Cover, Circa 2000 - Vector, 2011, Available from: http://www.geobase.ca/geobase/en/data/land cover/csc2000v/description.html

Gerrard, J. (1990). *Mountain environments: an examination of the physical geography of mountains*: The MIT Press.

Gillan, B.J., Harper, J.T., and Moore, J.N. (2010). Timing of present and future snowmelt from high elevations in northwest Montana. *Water Resources Research, 46*(1), W01507.

Gleick, P.H. (1986). Methods for evaluating the regional hydrologic impacts of global climatic changes. *Journal of Hydrology, 88*(1), 97-116.

Gleick, P.H. (1999). Introduction: Studies from the water sector of the National Assessment. *JAWRA Journal of the American Water Resources Association, 35*(6), 1297-1300.

Gobena, A.K., and Gan, T.Y. (2013). Assessment of Trends and Possible Climate Change Impacts on Summer Moisture Availability in Western Canada based on Metrics of the Palmer Drought Severity Index. *Journal of Climate, 26*(13), 4583-4595. doi: 10.1175/jcli-d-12-00421.1

Grismer, M., Orang, M., Snyder, R., and Matyac, R. (2002). Pan evaporation to reference evapotranspiration conversion methods. *Journal of irrigation and drainage engineering, 128*(3), 180-184.

Groisman, P.Y., Karl, T.R., Easterling, D.R., Knight, R.W., Jamason, P.F., Hennessy, K.J., Suppiah, R., Page, C.M., Wibig, J., Fortuniak, K., Razuvaev, V.N., Douglas, A., Førland, E. and Zhai, P.-M. (1999). Changes in the probability of heavy precipitation: important indicators of climatic change. *Climatic Change, 42*(1), 243-283.

Gurtz, J., Baltensweiler, A., and Lang, H. (1999). Spatially distributed hydrotope-based modelling of evapotranspiration and runo in mountainous basins. *Hydrological Processes, 13*, 2751-2768.

Hamlet, A.F., and Lettenmaier, D.P. (1999). Effects of climate change on hydrology and water resources in the Columbia River Basin. *JAWRA Journal of the American Water Resources Association, 35*(6), 1597-1623.

Hamlet, A.F., and Lettenmaier, D.P. (2005). Production of Temporally Consistent Gridded Precipitation and Temperature Fields for the Continental United States*. *Journal of Hydrometeorology, 6*(3), 330-336.

Harrison, S.J., Winterbottom, S., Johnson, R., Britain, G., and Executive, S. (2001). *Climate change and changing snowfall patterns in Scotland*: Scottish Executive Central Research Unit Edinburgh.

Hedstrom, N., and Pomeroy, J. (1998). Accumulation of intercepted snow in the boreal forest: measurements and modelling. *Hydrol. Processes, 12*, 1611-1625.

Hevesi, J.A., Istok, J.D., and Flint, A.L. (1992). Precipitation estimation in mountainous terrain using multivariate geostatistics. Part I: structural analysis. *Journal of Applied Meteorology, 31*(7), 661-676.

Hobbs, E., and Krogman, K. (1983). *Scheduling irrigation to meet crop demands*. Lethbridge, Alberta: Research Branch, Agriculture Canada.

Holmes, J., and Wronski, E. (1981). The influence of plant communities upon the hydrology of catchments. *Agricultural Water Management, 4*(1), 19-34.

Hopkinson, R.F., McKenney, D.W., Milewska, E. J., Hutchinson, M.F., Papadopol, P., and Vincent, L.A. (2011). Impact of aligning climatological day on gridding daily maximum-minimum temperature and precipitation over Canada. *Journal of Applied Meteorology and Climatology, 50*(8), 1654-1665.

Hudson, D., and Jones, R. (2002). Regional climate model simulations of present-day and future climates of southern Africa. *Hadley Centre Technical Note, 39*, 41.

Hungerford, R.D., Nemani, R.R., Running, S.W., and Coughlan, J.C. (1989). *MTCLIM: a mountain microclimate simulation model*: US Department of Agriculture, Forest Service, Intermountain Research Station Ogden, Utah, USA.

Hutchinson, M.F., McKenney, D.W., Lawrence, K., Pedlar, J.H., Hopkinson, R.F., Milewska, E., and Papadopol, P. (2009). Development and testing of Canada-wide interpolated spatial models of daily minimum-maximum temperature and precipitation for 1961-2003. *Journal of Applied Meteorology and Climatology, 48*(4), 725-741.

IPCC-TGICA. (2007). General Guidelines on the Use of Scenario Data for Climate Impact and Adaptation Assessment. Version 2. Prepared by T.R. Carter on behalf of the Intergovernmental Panel on Climate Change, Task Group on Data and Scenario Support for Impact and Climate Assessment.

IPCC, (2013). Summary for Policymakers. In: Climate Change 2013: The Physical Science Basis. Contribution of Working Group I to the Fifth Assessment Report of the Intergovernmental Panel on Climate Change [Stocker, T.F., D. Qin, G.-K. Plattner, M. Tignor, S.K. Allen, J. Boschung, A. Nauels, Y. Xia, V. Bex and P.M. Midgley (eds.)]. Cambridge University Press, Cambridge, United Kingdom and New York, NY, USA

IPCC. (2007). Climate Change 2007: Synthesis Report. Contribution of Working Groups I, II and III to the Fourth Assessment Report of the Intergovernmental Panel on Climate Change (pp. 104). Geneva, Switzerland: IPCC.

Jackson, R., Canadell, J., Ehleringer, J., Mooney, H., Sala, O., and Schulze, E. (1996). A global analysis of root distributions for terrestrial biomes. *Oecologia, 108*(3), 389-411.

Jensen, M.E., Burman, R.D., and Allen, R.G. (1990). *Evapotranspiration and irrigation water requirements*. ASCE Manuals and Reports on Engineering Practices No. 70., American Society of Civil Engineers., New York, NY, 360 p.

Jewitt, G.P.W. and Schulze, R.E. (1999). Verification of the ACRU model for forest hydrology applications. *Water Sa, 25*(4), 483-489.

Jewitt, G.P.W., Garratt, J.A., Calder, I.R., and Fuller, L. (2004). Water resources planning and modelling tools for the assessment of land use change in the Luvuvhu Catchment, South Africa. *Physics and Chemistry of the Earth, Parts A/B/C, 29*(15–18), 1233-1241.

Jha, M., Pan, Z., Takle, E.S., and Gu, R. (2004). Impacts of climate change on streamflow in the Upper Mississippi River Basin: A regional climate model perspective. *Journal of Geophysical Research: Atmospheres (1984–2012), 109*(D9).

Johnson, G.L. and Hanson, C.L. (1995). Topographic and atmospheric influences on precipitation variability over a mountainous watershed. *Journal of Applied Meteorology, 34*(1), 68-87.

Johnson, J.B. and Marks, D. (2004). The detection and correction of snow water equivalent pressure sensor errors. *Hydrological Processes, 18*(18), 3513-3525.

Jones, R., Murphy, J., and Noguer, M. (1995). Simulation of climate change over europe using a nested regional-climate model. I: Assessment of control climate, including sensitivity to location of lateral boundaries. *Quarterly Journal of the Royal Meteorological Society, 121*(526), 1413-1449.

Kampf, S.K., and Burges, S.J. (2007). A framework for classifying and comparing distributed hillslope and catchment hydrologic models. *Water Resources Research, 43*(5), W05423.

Kershaw, R. (2008). *Exploring the Castle: Discovering the Backbone of the World in Southern Alberta*: Rocky Mountain Books Ltd.

Kienzle, S.W., Lorenz, S.A. and Schulze, R.E. (1997). Hydrology and Water Quality of the Mgeni Catchment (pp. 1-88). Pretoria: Water Research Commission.

Kienzle, S.W. and Mueller, M. (2013). Mapping Alberta's surface water resources for the period 1971–2000. *The Canadian Geographer/Le Géographe canadien*. 57(4): 506–518.

Kienzle, S.W., Nemeth, M.W., Byrne, J.M., and MacDonald, R.J. (2012). Simulating the hydrological impacts of climate change in the upper North Saskatchewan River basin, Alberta, Canada. *Journal of Hydrology, 412*, 76-89.

Kienzle, S.W. and Schmidt, J. (2008). Hydrological impacts of irrigated agriculture in the Manuherikia Catchment, Otago, New Zealand. *Journal of Hydrology (New Zealand), 47*(2), 67-84.

Kienzle, S.W. and Schulze, R.E. (1992). A simulation model to assess the effect of afforestation on ground-water resources in deep sandy soils. *Water S. A., 18*(4), 265-272.

Kienzle, S.W. (1993). *Application of a GIS for simulating hydrological responses in developing regions.* Paper presented at the HydroGIS 93: Application of Geographical Information Systems in Hydrology and Water Resources Management Vienna, Austria.

Kienzle, S.W. (1996). *Using DTMs and GIS to define input variables for hydrological and geomorphological analysis.* Paper presented at the HydroGIS 96: Application of Geographical Information Systems in Hydrology and Water Resources Management, Vienna, Austria.

Kienzle, S.W. (2008). A new temperature based method to separate rain and snow. *Hydrological Processes, 22*(26), 5067-5085.

Kienzle, S.W. (2011). Effects of area under-estimations of sloped mountain terrain on simulated hydrological behaviour: a case study using the ACRU model. *Hydrological Processes, 25*(8), 1212-1227. doi: 10.1002/hyp.7886

Kienzle, S.W. (2013). Parameterization of a Physical Hydrological Model for a Mountain Region in Alberta *Putting Prediction in Ungauged Basins into Practice*: Canadian Water Resources Association.

Kiker, G., Clark, D., Martinez, C., and Schulze, R. (2006). A Java-based, object-oriented modeling system for southern African hydrology. *Transactions of the ASABE, 49*(5), 1419-1433.

Kitahara, H. and Saito, T. (1994). Snow interception by forest cano-pies: Weighing a conifer tree, meteorological observa-tion and analysis by the Penman-Monteith formula: Snow and Ice Covers: Interactions withthe Atmosphere and Ecosystem, Wallingford, UK: IAHS Press.

Kleijnen, J.P. (1995). Verification and validation of simulation models. *European Journal of Operational Research, 82*(1), 145-162.

Klemeš, V. (1986). Operational testing of hydrological simulation models. *Hydrological Sciences Journal, 31*(1), 13-24.

Knowles, N., Dettinger, M.D., and Cayan, D.R. (2006). Trends in snowfall versus rainfall in the western United States. *Journal of Climate, 19*(18), 4545-4559.

Lapp, S., Byrne, J., Townshend, I., and Kienzle, S. (2005). Climate warming impacts on snowpack accumulation in an alpine watershed. *International Journal of Climatology, 25*(4), 521-536.

Laurenson, E.M. (1964). A catchment storage model for runoff routing. *Journal of Hydrology, 2*(2), 141-163.

Leavesley, G.H. (1994). Modeling the effects of climate change on water resources-a review. *Climatic Change, 28*(1-2), 159-177.

Legates, D.R., and McCabe, G.J. (1999). Evaluating the use of "goodness-of-fit" measures in hydrologic and hydroclimatic model validation. *Water Resources Research, 35*(1), 233-241.

Lemmen, D.S., Warren, F. J., Lacroix, J., and Bush, E. (2008). *From Impacts to Adaptation: Canada in a Changing Climate 2007*. Ottawa, ON.

Lettenmaier, D.P., Wood, A.W., Palmer, R.N., Wood, E.F., and Stakhiv, E.Z. (1999). Water resources implications of global warming: A US regional perspective. *Climatic Change, 43*(3), 537-579.

Leung, L., and Ghan, S. (1999). Pacific Northwest climate sensitivity simulated by a regional climate model driven by a GCM. Part II: 2× CO2 simulations. *Journal of Climate, 12*(7), 2031-2053.

Loaiciga, H.A., Valdes, J.B., Vogel, R., Garvey, J., and Schwarz, H. (1996). Global warming and the hydrologic cycle. *Journal of Hydrology, 174*(1), 83-127.

Loukas, A., Vasiliades, L., and Dalezios, N.R. (2002). Potential climate change impacts on flood producing mechanisms in southern British Columbia, Canada using the CGCMA1 simulation results. *Journal of Hydrology, 259*(1), 163-188.

Luce, C.H., Tarboton, D.G., and Cooley, K.R. (1998). The influence of the spatial distribution of snow on basin-averaged snowmelt. *Hydrological Processes, 12*(1011), 1671-1683.

Luckman, B., and Wilson, R. (2005). Summer temperatures in the Canadian Rockies during the last millennium: a revised record. *Climate Dynamics, 24*(2-3), 131-144.

Lundberg, A., and Halldin, S. (2001). Snow interception evaporation. Review of measurementtechniques, processes, and models. *Theoretical and Applied Climatology, 70*(1-4), 117-133.

MacDonald, R.J., Byrne, J.M., Boon, S., and Kienzle, S.W. (2012). Modelling the potential impacts of climate change on snowpack in the North Saskatchewan River Watershed, Alberta. *Water Resources Management, 26*(11), 3053-3076.

MacDonald, R.J., Byrne, J.M., Kienzle, S.W. and Larson, R.P. (2011). Assessing the potential impacts of climate change on mountain snowpack in the St. Mary River watershed, Montana. *Journal of Hydrometeorology, 12*(2), 262-273.

Mahat, V., and Anderson, A. (2013). Impacts of climate and forest changes on streamflow and water balance in a mountainous headwater stream in Southern Alberta. *Hydrol. Earth Syst. Sci. Discuss., 10*(7), 8503-8536. doi: 10.5194/hessd-10-8503-2013

Martinez, C.J., Campbell, K.L., Annable, M.D., and Kiker, G.A. (2008). An object-oriented hydrologic model for humid, shallow water-table environments. *Journal of Hydrology, 351*(3), 368-381.

McDonnell, J., Sivapalan, M., Vaché, K., Dunn, S., Grant, G., Haggerty, R., Hinz, C., Hooper, R., Kirchner, J., Roderick, M., Selker, J. and Weiler, M. (2007). Moving beyond heterogeneity and process complexity: A new vision for watershed hydrology. *Water Resources Research, 43*(7).

Merritt, W.S., Alila, Y., Barton, M., Taylor, B., Cohen, S., and Neilsen, D. (2006). Hydrologic response to scenarios of climate change in sub watersheds of the Okanagan basin, British Columbia. *Journal of Hydrology, 326*(1), 79-108.

Middelkoop, H., Daamen, K., Gellens, D., Grabs, W., Kwadijk, J.C., Lang, H., Parmet, B.W.A.H, Shädler, B., Schulla, J. and Wilke, K. (2001). Impact of climate change on hydrological regimes and water resources management in the Rhine basin. *Climatic Change, 49*(1-2), 105-128.

Minder, J.R., Mote, P.W., and Lundquist, J.D. (2010). Surface temperature lapse rates over complex terrain: Lessons from the Cascade Mountains. *Journal of Geophysical Research, 115*(D14), D14122.

Montesi, J., Elder, K., Schmidt, R., and Davis, R.E. (2004). Sublimation of intercepted snow within a subalpine forest canopy at two elevations. *Journal of Hydrometeorology, 5*(5).

Moriasi, D., Arnold, J., Van Liew, M., Bingner, R., Harmel, R., and Veith, T. (2007). Model evaluation guidelines for systematic quantification of accuracy in watershed simulations. *Trans. ASABE, 50*(3), 885-900.

Mote, P.W. (2003). Trends in snow water equivalent in the Pacific Northwest and their climatic causes. *Geophysical Research Letters, 30*(12).

Mote, P.W., Hamlet, A.F., Clark, M.P. and Lettenmaier, D.P. (2005). Declining mountain snowpack in western North America.

Mote, P., Hamlet, A., and Salathé, E. (2008). Has spring snowpack declined in the Washington Cascades? *Hydrology and Earth System Sciences, 12*(1), 193-206.

Mtetwa, S., Kusangaya, S., and Schutte, C. (2003). The application of geographic information systems (GIS) in the analysis of nutrient loadings from an agro-rural catchment. *Water Sa, 29*(2), 189-194.

Nash, J., and Sutcliffe, J. (1970). River flow forecasting through conceptual models part I—A discussion of principles. *Journal of Hydrology, 10*(3), 282-290.

National Land and Water Information Service. (2009) *Data.*

Natural Resources Canada. (2014). Regional, national and international climate modelling Retrieved February 5, 2014, from http://cfs.nrcan.gc.ca/projects/3/4

Nemeth, M.W. (2010). *Climate Change Impacts on Streamflow in the Upper North Saskatchewan River Basin, Alberta.* M.Sc., Univeristy of Lethbridge, Lethbridge, Alberta.

Nemeth, M.W., Kienzle, S.W., and Byrne, J.M. (2012). Multi-variable verification of hydrological processes in the upper North Saskatchewan River basin, Alberta, Canada. *Hydrological Sciences Journal, 57*(1), 84-102.

New, M. (2002). Climate change and water resources in the southwestern Cape, South Africa. [Article]. *South African Journal of Science, 98*(7/8), 369-376.

New, M., Hulme, M. and Jones, P. (2000). Representing twentieth-century space-time climate variability. Part II: Development of 1901-96 monthly grids of terrestrial surface climate. *Journal of Climate, 13*(13), 2217-2238.

New, M., Lister, D., Hulme, M. and Makin, I. (2002). A high-resolution data set of surface climate over global land areas. *Climate Research, 21*(1), 1-25.

New, M. and Schulze, R.E. (1996). Hydrologic sensitivity to climate change in the Langrivier catchment, Stellenbosch, South Africa and some implications for geomorphic processes. *Zeitschrift fur Geomorphologie, Supplementband, 107*, 11-34.

Nijssen, B., O'Donnell, G.M., Hamlet, A.F., and Lettenmaier, D.P. (2001). Hydrologic sensitivity of global rivers to climate change. *Climatic Change, 50*(1-2), 143-175.

Nkemdirim, L.C., and Purves, H. (1994). Comparison of recorded temperature and precipitation in the Oldman Basin with scenarios projected in general circulation models. *Canadian Water Resources Journal, 19*(2), 157-164.

Northwest Alliance for Computational Science and Engineering. (2014). PRISM Climate Data (Vol. 2014). Corvallis, OR.

Perry, M., and Hollis, D. (2005). The generation of monthly gridded datasets for a range of climatic variables over the UK. *International Journal of Climatology, 25*(8), 1041-1054.

Pettapiece, W. (1971). Land classification and soils in the Rocky Mountains of Alberta along the North Saskatchewan River Valley.

Pielke, R.A., and Mehring, P. (1977). Use of mesoscale climatology in mountainous terrain to improve the spatial representation of mean monthly temperatures. *Monthly Weather Review, 105*(1), 108-112.

Pigeon, K.E., and Jiskoot, H. (2008). Meteorological controls on snowpack formation and dynamics in the southern Canadian Rocky Mountains. *Arctic, Antarctic, and Alpine Research, 40*(4), 716-730.

Plummer, D., Caya, D., Frigon, A., Côté, H., Giguère, M., Paquin, D., Biner, S., Harvey, R. and De Elia, R. (2006). Climate and climate change over North America as simulated by the Canadian RCM. *Journal of Climate, 19*(13), 3112-3132.

Pomeroy, J., and Dion, K. (1996). Winter radiation extinction and reflection in a boreal pine canopy: measurements and modelling. *Hydrological Processes, 10*(12), 1591-1608.

Pomeroy, J., and Gray, D. (1995). Snowcover accumulation, relocation and management. *Bulletin of the International Society of Soil Science no, 88*(2).

Pomeroy, J., Gray, D., Shook, K., Toth, B., Essery, R., Pietroniro, A., and Hedstrom, N. (1998a). An evaluation of snow accumulation and ablation processes for land surface modelling. *Hydrological Processes, 12*(15), 2339-2367.

Pomeroy, J., Parviainen, J., Hedstrom, N., and Gray, D. (1998b). Coupled modelling of forest snow interception and sublimation. *Hydrological Processes, 12*(15), 2317-2337.

Pomeroy, J., and Schmidt, R. (1993). *The use of fractal geometry in modeling intercepted snow accumulation and sublimation.* Paper presented at the Proceedings of the Eastern Snow Conference.

Poyck, S., Hendrikx, J., McMillan, H., Örn Hreinsson, E., and Woods, R. (2011). Combined snow and streamflow modelling to estimate impacts of climate change on water resources in the Clutha River, New Zealand. *Journal of Hydrology (00221708), 50*(2).

Praskievicz, S., and Chang, H. (2009). A review of hydrological modelling of basin-scale climate change and urban development impacts. *Progress in Physical Geography, 33*(5), 650-671.

Public Safety Canada. (2013). The Canadian Disaster Database (Vol. 2013). Ottawa, ON: Government of Canada.

Read, K.E., Hedges, P.D., and Fermor, P.M. (2008). Monthly Evapotranspiration Coefficients of Large Reed Bed Habitats in the United Kingdom *Wastewater Treatment, Plant Dynamics and Management in Constructed and Natural Wetlands* (pp. 99-109): Springer.

Refsgaard, J. (1996). Terminology, modelling protocol and classification of hydrological model codes *Distributed hydrological modelling* (pp. 17-39): Springer.

Regonda, S.K., Rajagopalan, B., Clark, M., and Pitlick, J. (2005). Seasonal cycle shifts in hydroclimatology over the western United States. *Journal of Climate, 18*(2), 372-384.

Reinelt, E. (1970). On the role of orography in the precipitation regime of Alberta. *Albertan Geographer, 6*, 45-58.

Robinson, S. (1997). *Simulation model verification and validation: increasing the users' confidence.* Paper presented at the Proceedings of the 29th conference on Winter simulation.

Rolland, C. (2003). Spatial and seasonal variations of air temperature lapse rates in Alpine regions. *Journal of Climate, 16*(7), 1032-1046.

Rood, S.B., Pan, J., Gill, K.M., Franks, C.G., Samuelson, G.M., and Shepherd, A. (2008). Declining summer flows of Rocky Mountain rivers: Changing seasonal hydrology and probable impacts on floodplain forests. *Journal of Hydrology, 349*(3), 397-410.

Rood, S.B., Samuelson, G., Weber, J., and Wywrot, K. (2005). Twentieth-century decline in streamflows from the hydrographic apex of North America. *Journal of Hydrology, 306*(1), 215-233.

Rowe, C.M. (1991). Modeling land-surface albedos from vegetation canopy architecture. *Physical Geography, 12*(2), 93-114.

Running, S.W., Nemani, R.R., and Hungerford, R.D. (1987). Extrapolation of synoptic meteorological data in mountainous terrain and its use for simulating forest evapotranspiration and photosynthesis. *Canadian Journal of Forest Research, 17*(6), 472-483.

Rutter, A. (1967). *An analysis of evaporation from a stand of Scots pine.* Paper presented at the International symposium on forest hydrology.

Sargent, R.G. (2005). *Verification and validation of simulation models.* Paper presented at the Proceedings of the 37th conference on Winter simulation.

Sauchyn, D., and Kulshreshtha, S. (2008). Prairies; *in* From Impacts to Adaptation: Canada in a Changing Climate 2007 (pp. 275-328). Ottawa, ON: Government of Canada.

Sauchyn, D. and St. Jacques, J. (2009) Security of Western Water Supplies under a Changing Climate. *Proceedings of the 18th Convocation of the International Council of Academies of Engineering and Technological Sciences,* July 13-17: Calgary, Alberta.

Schindler, D.W., and Donahue, W.F. (2006). An impending water crisis in Canada's western prairie provinces. *Proceedings of the National Academy of Sciences, 103*(19), 7210-7216.

Schmidt, J., Kienzle, S.W. and Srinivasan, M.S. (2009). Estimating increased evapotranspiration losses caused by irrigated agriculture as part of the water balance of the Orari catchment, Canterbury, New Zealand. *Journal of Hydrology (New Zealand), 48*(2), 73.

Schmidt, E.J. and Schulze, R.E. (1987). Flood Volume and Peak Discharge from Small Catchments in Southern Africa, based on the SCS Technique (pp. 164). Pretoria: Water Research Commission.

Schmidt, R., and Gluns, D.R. (1991). Snowfall interception on branches of three conifer species. *Canadian Journal of Forest Research, 21*(8), 1262-1269.

Schulze, R.E., Lorentz, S., Kienzle, S.W. and Perks, L. (2004). Case study 3: Modelling the impacts of land-use and climate change on hydrological responses in the mixed underdeveloped/developed Mgeni catchment, South Africa *Vegetation, Water, Humans and the Climate* (pp. 441-453): Springer.

Schulze, R.E. and Perks, L. (2003). The Potential Threat of Significant Changes to Hydrological Responses in Southern Africa as a Result of Climate Change: A Threshold Analysis on When These Could Occur, and Where the Vulnerable Areas Are (pp. 250-258). Pretoria, RSA.

Schulze, R.E., Schäfer, N.W. and Lynch, S.D. (1989). *An assessment of regional runoff production in Qwa Qwa: A G. I. S. application of the" ACRU" modelling system.* Paper presented at the 1989 Southern Africa Geographic Information Systems Conference.

Schulze, R.E. (1995). Hydrology and Agrohydrology: *A Text to Accompany the ACRU 3.00 Agrohydrological Modelling System*. Pretoria, RSA: Water Research Commission.

Schulze, R.E. (2000). Modelling Hydrological Responses to Land Use and Climate Change: A Southern African Perspective. *Ambio, 29*(1), 12-22. doi: 10.2307/4314988

Schulze, R.E. (2005). Selection of a suitable agrohydrological model for climate change impact studies over southern Africa. *Climate Change and Water Resources in Southern Africa: Studies on Scenarios, Impacts, Vulnerabilities and Adaptation. Water Research Commission, Pretoria, RSA, WRC Report, 1430*(1), 05.

Schumann, A. (1993). Development of conceptual semi-distributed hydrological models and estimation of their parameters with the aid of GIS. *Hydrological Sciences Journal, 38*(6), 519-528.

Sentelhas, P.C., Gillespie, T.J., and Santos, E.A. (2010). Evaluation of FAO Penman–Monteith and alternative methods for estimating reference evapotranspiration with missing data in Southern Ontario, Canada. *Agricultural Water Management, 97*(5), 635-644.

Shaw, E.M., Beven, K.J., Chappell, N.A., and Lamb, R. (2010). *Hydrology in practice*: Taylor and Francis US.

Shea, J.M., Marshall, S.J., and Livingston, J.M. (2004). Glacier distributions and climate in the Canadian Rockies. *Arctic, Antarctic, and Alpine Research, 36*(2), 272-279.

Shen, S., Yin, H., Cannon, K., Howard, A., Chetner, S., and Karl, T. (2005). Temporal and spatial changes of the agroclimate in Alberta, Canada, from 1901 to 2002. *Journal of Applied Meteorology, 44*(7), 1090-1105.

Shenbin, C., Yunfeng, L., and Thomas, A. (2006). Climatic change on the Tibetan Plateau: potential evapotranspiration trends from 1961–2000. *Climatic Change, 76*(3-4), 291-319.

Singh, V.P., and Frevert, D.K. (2002). *Mathematical models of large watershed hydrology*: Water Resources Publications.

Smithers, J.C. Schulze, R.E. and Kienzle, S.W. (1997). Design flood estimation using a modelling approach: A case study using the ACRU model. *IAHS Publications-Series of Proceedings and Reports-Intern Assoc Hydrological Sciences, 240*, 365-376.

Smithers, J.C., Schulze, R.E., Pike, A. and Jewitt, G.P.W. (2001). A hydrological perspective of the February 2000 floods: A case study in the Sabie River Catchment. *Water Sa, 27*(3), 325-332.

Smithers, J.C. and Schulze, R.E. (1995). ACRU Agrohydrological Modelling System User Manual. Pretoria, Republic of South Africa: Water Research Commission.

Steenburgh, W.J., Mass, C.F., and Ferguson, S.A. (1997). The influence of terrain-induced circulations on wintertime temperature and snow level in the Washington Cascades. *Weather and forecasting, 12*(2), 208-227.

Stewart, I.T. (2009). Changes in snowpack and snowmelt runoff for key mountain regions. *Hydrological Processes, 23*(1), 78-94.

Stewart, I.T., Cayan, D.R., and Dettinger, M.D. (2005). Changes toward earlier streamflow timing across western North America. *Journal of Climate, 18*(8), 1136-1155.

Stewart, I.T., Cayan, D.R., and Dettinger, M.D. (2004). Changes in snowmelt runoff timing in western North America under abusiness as usual'climate change scenario. *Climatic Change, 62*(1-3), 217-232.

Storck, P., Lettenmaier, D.P., and Bolton, S.M. (2002). Measurement of snow interception and canopy effects on snow accumulation and melt in a mountainous maritime climate, Oregon, United States. *Water Resources Research, 38*(11), 5-1-5-16.

Strong, W., and Roi, G.L. (1983). Root-system morphology of common boreal forest trees in Alberta, Canada. *Canadian Journal of Forest Research, 13*(6), 1164-1173.

Tang, Z., and Fang, J. (2006). Temperature variation along the northern and southern slopes of Mt. Taibai, China. *Agricultural and Forest Meteorology, 139*(3), 200-207.

Tarboton, K., and Schulze, R. (1993). *Hydrological consequences of development scenarios for the Mgeni catchment.* Paper presented at the Proceedings of the Sixth South African National Hydrological Symposium, University of Natal, Pietermaritzburg, Department of Agricultural Engineering.

Te Chow, V., Maidment, D.R., and Mays, L.W. (1988). *Applied hydrology*: Tata McGraw-Hill Education.

Teutschbein, C., and Seibert, J. (2012). Bias correction of regional climate model simulations for hydrological climate-change impact studies: Review and evaluation of different methods. *Journal of Hydrology, 456*, 12-29.

Thornton, P.E., Running, S.W., and White, M.A. (1997). Generating surfaces of daily meteorological variables over large regions of complex terrain. *Journal of Hydrology, 190*(3), 214-251.

Todini, E. (1988). Rainfall-runoff modeling—Past, present and future. *Journal of Hydrology, 100*(1), 341-352.

Trenberth, K.E., Dai, A., Rasmussen, R.M., and Parsons, D.B. (2003). The changing character of precipitation. *Bulletin of the American Meteorological Society, 84*(9), 1205-1217.

Troendle, C.A., and Meiman, J. (1986). *The effect of patch clearcutting on the water balance of a subalpine forest slope.* Paper presented at the Proceedings-Western Snow Conference.

Varhola, A., Coops, N.C., Weiler, M., and Moore, R.D. (2010). Forest canopy effects on snow accumulation and ablation: An integrative review of empirical results. *Journal of Hydrology, 392*(3), 219-233.

Wang, T., Hamann, A., Spittlehouse, D.L., and Murdock, T.Q. (2012). ClimateWNA-High-resolution spatial climate data for western North America. *Journal of Applied Meteorology and Climatology, 51*(1), 16-29.

Warburton, M., Schulze, R., and Jewitt, G. (2010). Confirmation of ACRU model results for applications in land use and climate change studies. *Hydrology and Earth System Sciences Discussions, 7*, 4591-4634.

Winkler, R., Spittlehouse, D., and Golding, D. (2005). Measured differences in snow accumulation and melt among clearcut, juvenile, and mature forests in southern British Columbia. *Hydrological Processes, 19*(1), 51-62.

Winstral, A., Elder, K., and Davis, R.E. (2002). Spatial snow modeling of wind-redistributed snow using terrain-based parameters. *Journal of Hydrometeorology, 3*(5), 524-538.

Xu, C.-Y. and Halldin, S. (1997). The effect of climate change on river flow and snow cover in the NOPEX area simulated by a simple water balance model. *Nordic Hydrology, 28*(4), 273-282.

Xu, C.-Y. and Singh, V.P. (1998). A review on monthly water balance models for water resources investigations. *Water Resources Management, 12*(1), 20-50.

Xu, C.-Y. (1999a). Climate change and hydrologic models: A review of existing gaps and recent research developments. *Water Resources Management, 13*(5), 369-382.

Xu, C.-Y. (1999b). Operational testing of a water balance model for predicting climate change impacts. *Agricultural and Forest Meteorology, 98*, 295-304.

Zhang, X., Vincent, L.A., Hogg, W., and Niitsoo, A. (2000). Temperature and precipitation trends in Canada during the 20th century. *Atmosphere-ocean, 38*(3), 395-429.